

**Seasonal Shoreline Changes along the North Coast of  
Puerto Rico,  
from Isla de Cabras to Aguadilla**

By

Joanna Cepeda Díaz

A thesis submitted in partial fulfillment of the requirements for the degree of

MASTER OF SCIENCE

in  
Geology

UNIVERSITY OF PUERTO RICO

MAYAGÜEZ CAMPUS

2007

Approved by:

\_\_\_\_\_  
Fernando Gilbes, Ph. D.  
Member, Graduate Committee

\_\_\_\_\_  
Date

\_\_\_\_\_  
Wilson R. Ramírez, Ph. D.  
President, Graduate Committee

\_\_\_\_\_  
Date

\_\_\_\_\_  
Hernán Santos, Ph. D.  
Member, Graduate Committee

\_\_\_\_\_  
Date

\_\_\_\_\_  
Clark Sherman, Ph. D.  
Representative of Graduate Studies

\_\_\_\_\_  
Date

\_\_\_\_\_  
Johannes H. Schellekens, Ph. D.  
Director of the Department

\_\_\_\_\_  
Date

## ABSTRACT

Seven beaches were studied along the north coast of Puerto Rico in order to qualitatively compare seasonal changes for each system. These are Punta Borinquen, Aguadilla, Jobos, Isabela, Camuy, Arecibo port, Mameyal, Vega Baja, Palmas Atlas, Barceloneta, and Isla de Cabras, Cataño. Field data was collected during two sampling periods: March (dry season) and September (wet season) of 2003. Satellite images processing, beach profiling, sediment composition and sediment texture (grain size) were studied in each site.

The beach systems studied were classified as reflective or dissipative systems according to topographical survey data. As for sand movement, it is noticeable in the beach profiles that there is movement to the west side of each system. There does not seem to be a significant change in sediment texture and composition between seasons, probably influenced by the presence of major river systems discharging near most systems and to the dynamic conditions in the north coast all year round.

Landsat-7 satellite images were used in a prior study to discriminate bottom sediment types in the nearshore areas. Higher spatial resolution was recommended (Barreto et al, 1998). In this study, IKONOS images were chosen because of better spatial resolution (1 meter). After several pre-processing methods and due to missing image acquisition information, no valid classifications were made. It became evident that not only is spatial resolution important, but spectral resolution is important as well. A better assessment might have been possible if reflectance values would have been calculated, but due to the fact that the exact date and time of image acquisition were not available this could not be accomplished. Radiance values were used instead but the varying range among these did not prove useful.

## RESUMEN

Siete playas en la costa norte de Puerto Rico se estudiaron para comparar cualitativamente los cambios estacionales en cada sistema. Estos son Punta Borinquen, Aguadilla, Jobos, Isabela, Camuy, el puerto de Arecibo, Mameyal, Vega Baja, Atlas de Palmas, Barceloneta, e Isla de Cabras, Cataño. Los datos de campo se recopilaron durante dos períodos de muestreo: Marzo (temporada seca) y Septiembre (temporada húmeda) del 2003. Imágenes de satélite, perfiles de playa, composición y textura (tamaño de grano) de sedimento fueron estudiados para cada sistema.

Los sistemas de la playa estudiados se clasificaron como reflectivas o disipativas, según los datos de los perfiles. En cuanto al movimiento de la arena, es evidente en los perfiles de la playa que hay movimiento hacia el oeste de cada sistema. No aparenta haber ningún cambio significativo en la textura de sedimento y composición entre temporadas, probablemente influido por la presencia de sistemas mayores de río que descargan cerca de la mayoría de los sistemas y a las condiciones dinámicas en la costa norte durante todo el año.

Imágenes del satélite Landsat-7 se utilizaron en un estudio previo para discriminar los tipos de sedimento en las áreas llanas de la costa. Se recomendó una resolución espacial más alta (Barreto et al, 1998). En este estudio, las imágenes de IKONOS se escogieron por su mayor resolución espacial (1 metro). Después de varios métodos de procesamiento y debido a falta de información sobre la adquisición de las imágenes, ningunas clasificaciones válidas se hicieron. Es evidente que no sólo es la resolución espacial importante, sino que la espectral es importante también. Una mejor evaluación pudo haber sido posible si los valores de reflectancia se hubiesen calculado, pero debido al hecho que la fecha y tiempo exactos de la adquisición de la imagen no estaban disponibles, esto no se pudo alcanzar. Los valores de radianza se utilizaron en su lugar pero la diferencia entre estos no demostró ser útil.

.DEDICATION

*To knowing that you can  
and learning to not let go...*

*I'll be forever grateful,*

*Joanna*

## ACKNOWLEDGEMENTS

I would like to thank all the people who helped me through this learning experience:

- Ivy, Pillin, Yaya, Felipe, Gary and Fritz for helping me in the field
- My advisor Dr. Wilson Ramírez for helping me grow professionally, as well as personally, through the good and the bad
- My committee members, Dr. Fernando Gilbes and Dr. Hernán Santos for their support during frustrating times
- Dr. Johannes Schellekens for his unconditional guidance and support
- To all the geology faculty members, administration, students and colleagues for keeping it real
- My family, especially to my mother for understanding and believing

# Table of Contents

<b>ABSTRACT</b> .....	<b>ii</b>
<b>RESUMEN</b> .....	<b>iii</b>
<b>ACKNOWLEDGEMENTS</b> .....	<b>v</b>
<b>TABLE OF CONTENTS</b> .....	<b>vi</b>
<b>TABLE LIST AND EQUATIONS</b> .....	<b>vii</b>
<b>FIGURE LIST</b> .....	<b>viii</b>
<b>1 INTRODUCTION</b> .....	<b>2</b>
1.1 GEOGRAPHICAL SETTING .....	5
1.2 GEOLOGY OF THE AREA .....	7
<b>2 PREVIOUS WORKS</b> .....	<b>9</b>
<b>3 METHODS</b> .....	<b>13</b>
3.1 TOPOGRAPHICAL SURVEY .....	13
3.1.1 BEACH CLASSIFICATION .....	14
3.2 SEDIMENT ANALYSIS.....	15
3.3 REMOTE SENSING .....	15
3.3.1 IMAGES PREPROCESSING.....	16
3.3.2 IMAGES CLASSIFICATION .....	17
<b>4 RESULTS</b> .....	<b>19</b>
4.1 STATION SB1 .....	19
4.2 STATION SB2 .....	29
4.3 STATION SB3 .....	39
4.4 STATION SB4 .....	49
4.5 STATION SB5 .....	59
4.6 STATION SB6 .....	69
4.7 STATION SB7 .....	80
<b>5 DISCUSSION</b> .....	<b>90</b>
5.1 BEACH PROFILE INTERPRETATION .....	90
5.2 SEDIMENT TEXTURE AND COMPOSITION ANALYSIS .....	91
5.3 IMAGE ANALYSIS .....	94
5.4 NORTH COAST SYNTHESIS .....	96
<b>6 CONCLUSIONS</b> .....	<b>99</b>
<b>7 RECOMMENDATIONS FOR FUTURE STUDIES</b> .....	<b>101</b>
<b>REFERENCES</b> .....	<b>103</b>

## Table List

TABLE	PAGE
TABLE 1: Geographical Coordinates of Study Sites .....	6
TABLE 2: Radiance Values SB1 .....	27
TABLE 3: Radiance Values SB2 .....	37
TABLE 4: Radiance Values SB3 .....	47
TABLE 5: Radiance Values SB4 .....	57
TABLE 6: Radiance Values SB5 .....	67
TABLE 7: Radiance Values SB6 .....	78
TABLE 8: Radiance Values SB7 .....	88

## Equations

EQUATIONS	PAGE
EQUATION 3.1: IKONOS Radiometric Calibration equation .....	15
EQUATION 3.2: IKONOS calibration coefficient .....	15

# Figure List

FIGURES	PAGE
Figure 1.1: Site Locality Map .....	6
Figure 4.1: Beach Profile for SB1 (March) .....	20
Figure 3.1: Topographical Survey.....	13
Figure 3.2: Beach profiles for dissipative and reflective beaches.....	14
Figure 4.2: Beach Profile for SB1 (September) .....	21
Figure 4.3: Grain Size SB1-1 .....	22
Figure 4.4: Grain Size SB1-2 .....	22
Figure 4.5: Grain Size SB1-3 .....	23
Figure 4.6: Cumulative Curve SB1 .....	24
Figure 4.7: Composition Comparison SB1 .....	25
Figure 4.8: IKONOS Satellite Images SB1 .....	26
Figure 4.9: Band Ratio SB1 .....	28
Figure 4.10: Beach Profile for SB2 (March) .....	30
Figure 4.11: Beach Profile for SB2 (September) .....	31
Figure 4.12: Grain Size SB2-1 .....	32
Figure 4.13: Grain Size SB2-2 .....	32
Figure 4.14: Cumulative Curve SB2 .....	34
Figure 4.15: Composition Comparison SB2 .....	35
Figure 4.16: IKONOS Satellite Images SB3 .....	36
Figure 4.17: Band Ratios SB2 .....	38
Figure 4.18: Beach Profile for SB3 (March) .....	40
Figure 4.19: Beach Profile for SB3 (September) .....	41
Figure 4.20: Grain Size SB3-1 .....	42
Figure 4.21: Grain Size SB3-2 .....	42
Figure 4.22: Grain Size SB3-3 .....	43
Figure 4.23: Cumulative Curve SB3 .....	44
Figure 4.24: Composition Comparison SB3 .....	45
Figure 4.25: IKONOS Satellite Images SB3 .....	46
Figure 4.26: Band Ratios SB3 .....	48
Figure 4.27: Beach Profile for SB4 (March) .....	50
Figure 4.28: Beach Profile for SB4 (September) .....	51
Figure 4.29: Grain Size SB41 and SB4-2 .....	52
Figure 4.30: Cumulative Curve SB4 .....	54
Figure 4.31: Composition Comparison SB4 .....	55
Figure 4.32: IKONOS Satellite Images SB4 .....	56
Figure 4.33: Band Ratios SB4.....	58
Figure 4.34: Beach Profile for SB5 (March) .....	60
Figure 4.35: Beach Profile for SB5 (September) .....	61
Figure 4.36: Grain Size SB5-1 .....	62
Figure 4.37: Grain Size SB5-2 .....	62
Figure 4.38: Grain Size SB5-3 .....	63
Figure 4.39: Cumulative Curve SB5 .....	64
Figure 4.40: Composition Comparison SB5 .....	65
Figure 4.41: IKONOS Satellite Images SB5 .....	66
Figure 4.42: Band Ratios SB5 .....	68
Figure 4.43: Beach Profile for SB6 (March) .....	70
Figure 4.44: Beach Profile for SB6 (September) .....	71

## Figure List (cont.)

FIGURES	PAGE
Figure 4.45: Grain Size SB6-1 .....	72
Figure 4.46: Grain Size SB6-2 .....	72
Figure 4.47: Grain Size SB6-3 .....	73
Figure 4.48: Grain Size SB6-4 .....	73
Figure 4.49: Cumulative Curve SB6 .....	75
Figure 4.50: Composition Comparison SB6 .....	76
Figure 4.51: IKONOS Satellite Images SB6 .....	77
Figure 4.52: Band Ratios SB6 .....	79
Figure 4.53: Beach Profile for SB7 (March) .....	81
Figure 4.54: Beach Profile for SB7 (September) .....	82
Figure 4.55: Grain Size SB7-1 .....	83
Figure 4.56: Grain Size SB7-2 .....	83
Figure 4.57: Grain Size SB7-3 .....	84
Figure 4.58: Cumulative Curve SB7 .....	85
Figure 4.59: Composition Comparison SB7 .....	86
Figure 4.60: IKONOS Satellite Images SB7 .....	87
Figure 4.61: Band Ratios SB7 .....	89
Figure 5.1: Sediment Composition and Texture and Beach Classification Variations.....	96

## CHAPTER 1: INTRODUCTION

In order to fully understand the dynamic beach system, all the interacting processes that affect its sediment budget must be taken into account. A sediment budget depends on the sediment movement within the beach system, the dynamic variables causing shoreline gain or loss, and the availability of sediment from which the system is replenished (Morelock, 1987). It includes sediment input sources (also known as credits) such as river systems, offshore sand deposits, up-current beach transport, and transport from sand dunes (Morelock, 1987). It also includes sediment losses (also known as debits) such as offshore transport, down-current beach transport, and transport into sand dunes (Morelock, 1987).

In order to develop an appropriate sediment budget, there should be qualitative as well as quantitative evaluations of the incoming sediment supply, its sources, sediment loss to nearshore features, and comparisons of beach system rate of change through time (Morelock et al., 2002). An imbalance in the budget is reflected in the erosion or accretion of the shoreline. Erosion occurs where debits exceed credits in the sediment transport. Accretion results from the opposite. Oceanographic, meteorological and geomorphologic events are variables that may also be involved in the alteration of the beach system. (Morelock et al., 2002).

Other factors that cause changes in the beach system include the morphology of the coast, its location and orientation, the availability of sand deposits in the nearshore area, and geological features, such as marine valleys or submarine canyons, gullies and hardgrounds (Morelock et al., 2002). These features trap the sand offshore, thus contributing to sediment

loss and causing a deficit in the budget. The type of rock forming the shoreline can also contribute to the sediment budget.

Wind transport plays an important role in sand dune formation, which contributes to beach loss as well as serving as a sediment source in the beach system (Morelock et al., 2002). Dunes contribute to the sediment gain in the budget, especially during storms. This will always depend on other physical variables interacting within the system, which may or may not allow dune formation.

Beach systems are usually categorized by the texture of their sediments, the composition of these sediments, and the beach slope. These in turn allow the classification of beach systems into dissipative and reflective (Wright and Short, 1983). Dissipative beaches develop under high wave conditions and have an abundant supply of sand. They have a wide beach face and its slope is less than five degrees. They usually do not have a developed berm (Short, 1984; Smith, 1990).

Reflective beaches are developed under low to moderate wave conditions. The beach face is usually higher than 10 degrees and transitions with lower slope offshore. In higher-energy reflective beaches, there is a berm crest, upper and lower beach face, step and deeper nearshore. Low-energy reflective beaches have only a beach face, and a step nearshore zone. In the transition from higher to lower wave energy, the berm remains but becomes wider and with less slope. Beaches may have seasonal shifts from reflective to dissipative in response to storm and swell conditions.

All the variables needed to obtain the ideal beach budget may be difficult to measure in the system. However, an estimate of non-measured variables may be produced from the

integration of field data and remote sensing techniques. Many factors affecting the sediment budget have been identified, but more work is needed for more accurate determinations. Quantifying the magnitude of these variables will help restore the natural processes affected for so long and help preserve these dynamic and important environments.

The integration of field data and remote sensing techniques to study shoreline changes and beach sand potential sources may prove useful, especially in areas where sample collection may not be viable (Barreto, 1997). Remote sensing is the use of the earth's surface images acquired from satellites using electromagnetic radiation, which are then processed and interpreted using different techniques depending on the objective (Campbell, 1996). It is a method of obtaining data from a specific object without being in direct contact with it and using this data to make assumptions after processing. This method is a valuable tool that can provide information about coastal lithology and structure, and it can help identify sea level and shoreline changes and better define these dynamic environments. If it is applied correctly, it may aid in protecting such areas when it comes to management.

A sand budget is important for Puerto Rico because beach environments surround the island and its balance should be of great concern not only geologically, but economically as well. Tourism is a major industry in the island, and beaches are one of its major attractions. In Puerto Rico, human activity has produced major changes on the coasts, especially due to the construction of housing and other structures and sand dune extraction. Sand is used for construction materials, especially cement, leading companies to extract sand from beach and river environments without taking into account the catastrophic effect it may have. Sand dunes are important because they protect beaches during storms and serve as potential

sources for beach replenishment. Finding potential near-shore and off-shore sand sources may lead the way to a solution to control beach erosion by using beach replenishment

## **1.1 Geographical Setting**

On the north coast of the island of Puerto Rico, sediment movement is mostly dominated by erosion caused by physical factors (Morelock et al., 2002). These include wave action, wind transport (dunes), tides, long-shore currents, storms, and the construction of structures that affect the dynamic processes of sediment erosion and deposition by altering and reducing the incoming sediment supply to the beach system. In this area the major sediment sources are river systems (e.g. Río Grande de Manatí) with a lesser contribution of marine biogenic production (not many reefs along the north coast of the island) (Morelock et al., 2002). The incoming sediment supply provided by a river depends on its catchment area size, water volume, land cover, and sediment movement within the river (especially at the river mouth). River dams also have an effect on the sediment supply because as the water flow is held back, so is the sediment it carries. In beaches near coral reefs and with high biogenic productivity in the nearshore area, the carbonate sediment production and deposition contribute to the sediment supply of such systems (Morelock et al., 2002).

The study area is along the north coast of Puerto Rico, extending from Isla de Cabras to Aguadilla (Fig. 1). Seven sites were chosen: (SB1) Isla de Cabras, Cataño, (SB2) Palmas Altas, Barcelonesa, (SB3) Mameyal, Vega Baja, (SB4) Arecibo port, (SB5) Camuy, (SB6) Jobos, Isabela, and (SB7) Punta Borinquen, Aguadilla. These specific sites were selected based on accessibility and availability of data from previous studies (i.e. Barreto,

unpublished Ph. D. Thesis, 1997). Exact coordinates of the points and/or lines measured were lost, benchmarks are not available, however qualitative comparisons can be made for each beach system between older studies (Barreto, 1997) and this study.



**Figure 1.1: Site locality map -**

- 1. SB7-Aguadilla (Punta Borinquen), 2. SB6- Isabela, 3. SB5-Camuy,**
- 4. SB4-Arecibo, 5. SB3-Barceloneta (Palmas Altas),**
- 6. SB2-Levitown (Mameyal), 7. SB1- Cataño (Isla de Cabras)**

**Table 1: Geographical Coordinates of study sites.**

<i>Site</i>	<i>Latitude</i>	<i>Longitude</i>
<b>SB1 – Isla de Cabras</b>	N 18° 27.837’	W 66° 08.479’
<b>SB2 – Mameyal</b>	N 18° 27.938’	W 66° 13.102’
<b>SB3 – Palmas Altas, Barceloneta</b>	N 18° 29.222’	W 66° 33.193’
<b>SB4 – Arecibo Port</b>	N 18° 28.332’	W 66° 42.356’
<b>SB5 – Camuy</b>	N 18° 29.427’	W 66° 51.758’
<b>SB6 – Jobos, Isabela</b>	N 18° 30.859’	W 67° 05.067’
<b>SB7 – Punta Borinquen, Aguadilla</b>	N 18° 29.410’	W 67° 09.382’

## **1.2 Geology Of The Area**

The north coast of Puerto Rico is composed mostly of middle Tertiary (Oligocene and Miocene) to younger sedimentary rocks overlain by recent deposits. The middle Tertiary sequence begins with clastics from the San Sebastián formation overlain by limestone from the San Sebastián Formation overlain and sometimes inter-bedded with the Lares Limestone (Krushensky and Schellekens, 2001).

The Cibao Formation overlies these units and grades into the sand and gravel of the Mucarabones sand (Krushensky and Schellekens, 2001). The Aguada Limestone overlies the upper member of the Cibao Formation. Above, the lower and upper members of the Aymamón Limestone are presently overlain by the Camuy Formation, which is the youngest of the middle Tertiary rock of the north coast (Krushensky and Schellekens, 2001).

The recent deposits (Holocene) along the north coast include: beach deposits, beach sand, sand dune deposits, swamp deposits, alluvium (especially along rivers), alluvial fan deposits (Moca and Isabela), beachrock and reef deposits (Punta Salinas and Punta Corazon, Bayamón) (Krushensky and Schellekens, 2001)

Recent deposits from the Pleistocene include: ancient beach rock (Aguadilla to Quebradillas and Vega Alta), eolianite, cemented dunes, silica sand (Camuy, Manatí to Bayamón), lagoonal deposits (Arecibo to Barceloneta), marine terrace deposits (around Laguna Tortuguero, Manatí), river terrace deposits (Río de la Plata, Vega Alta), and ancient deltaic and mud flat deposits (Río de la Plata, Vega Alta). There are some miscellaneous superficial deposits in Quebradillas. Blanket sand deposits from the Miocene to Recent (mostly Pliocene-Pleistocene) lie above the unconformity between the Tertiary and the Quaternary (Krushensky and Schellekens, 2001)

In the Bayamón Quadrangle (Monroe, 1973), a geological unit classified as artificial landfill is composed of sand, limestone and volcanic rocks that were used to fill valleys, swamps and areas of the San Juan Bay. Isla de Cabras is connected to the main island by this artificial fill.

## CHAPTER 2: PREVIOUS WORKS

Barreto (1991) conducted sediment budget analyses for a period of two years in Esperanza, Vieques, Puerto Rico. The purpose of the project was to identify the causes for high erosion rates by analyzing tides, winds, waves, storms, and physical variables (shoreline position, beach profiles, sediments, and nearshore submarine topography). She concluded that the major sand losses resulted from the interaction of waves, tides, swell, storms, and geomorphic features (dunes, coral reefs and sedimentary characteristics), as well as human activities.

Later in 1997, Barreto extended the project to the entire island of Puerto Rico in her doctoral thesis “Shoreline changes in Puerto Rico (1936-1993)”. The purpose was to document the changes in shoreline position and describe the possible causes that produced those changes with the use of aerial photographs. Twenty-nine sites were chosen around the island. Barreto concluded that the factors affecting shoreline position were: 1) human activity; 2) lack of sand deposits in the nearshore area; 3) variability of wave regime; 4) flood events; 5) presence of submarine canyons; and 6) rise in tropical storm occurrence.

Morelock has published several papers on the coastal areas of Puerto Rico (Morelock, 1978, 1984, 1985, 1987). In 1978, “Shorelines of Puerto Rico”, he studied the island coastal types, beach systems, composition, erosional and shoreline changes. The coast was classified under three divisions: rocky cliff and headlands, mangrove coast and sand or gavel beaches. From San Juan to Arecibo, beach sand, cemented dunes, beach rock, and mangrove swamps dominate. From Arecibo to Aguadilla, there are a series of rocky cliffs, with sand beaches and dunes between them. The north is a high energy coast with rugged shoreline and active beach

systems, which are short and separated from each other. The sources of sand for the island include offshore sands, land erosion and biogenic material. The causes for erosion on the island were identified as changes in sea level, erosion of barrier reefs and eolianites, human activities and maturation of the coastal system.

In 1984, Morelock used aerial photographs of ten sites to analyze the severe coastal erosion problems along these areas. The photographs used covered a time span of 40 years. The analyses showed that the erosion rates were variable but the trends of shoreline gain or loss seemed consistent. Morelock and Trumbull (1985) studied the island shores, classifying and describing different beach systems. They stated that the beach systems are relatively short and have little interaction with each other. These were separated mostly based in sediment composition, which is a combination of input from offshore biogenic and sand bodies, rivers, and coastal erosion. The north coast of the island has greater river discharge, rainfall and vegetation cover. The offshore sediments of the north coast are dominated by terrigenous sediments. Part of the beach sand in the north coast is being incorporated into dunes by means of wind action.

Morelock (1987) analyzed fifty sand samples for composition, texture and grain size for the west coast of the island. The composition was divided into carbonate (from reef biogenic material), quartz and feldspar grains (from inland sedimentary rocks and alluvial deposits), and rock fragments and dark minerals (from basalts and serpentines of the central mountain range). A beach budget analysis was conducted using variables such as beach composition, river input sources, and coastal erosion. It was concluded that longshore transport is from north to south. The beaches in the north of the west coast are a mixture of carbonate, quartz and feldspar, rock

fragments, and dark minerals. The Mayaguez beaches are dominantly rock fragments, and the southern beaches are mostly carbonate in composition.

Barreto et al. (1998) studied bottom sediment distribution on the nearshore area of Puerto Rico. Thematic Mapper (TM) images were used to characterize the sediment sources in the coast. The sediment bottom types were identified based on composition and texture. Radiance distribution was used to discriminate among them. They found that terrigenous sand has lower radiance than carbonate sand. They stated that it was difficult to identify bottom types using TM images because they have poor spatial and spectral resolution. Satellite images with a resolution of 10 meters or less were recommended for future studies.

Morelock et al. (2002a) made qualitative and quantitative evaluations of sediment input and loss to the nearshore. TM images from the Landsat-5 satellite were used to identify sediment facies and used to compare with the rate of beach changes overall. With the use of aerial photographs, sand loss was observed in all north coast beaches from 1964 to 1999. This could be a result of storms (causing high amplitude waves), as well as human activities, such as sand extraction and construction.

Morelock et al. (2002b) show that in many parts of the island, a rapid erosion episode starts after a period of little or no erosion. After this, underlying rock is exposed (beach rock and eolianite) and the erosional rate is reduced, thus protecting the beach system. In some parts, the shoreline has adjusted to the wave and current patterns and the reduction in the incoming sediment supply, leading to equilibrium. No erosion or shoreline accretion was evident in shorelines with mangrove forests or offshore reef systems.

On December 2004, as part of research project in a remote sensing course, I worked on an IKONOS image to determine the best image processing procedure to study beach erosion. The image was preprocessed and several supervised and unsupervised classifications were conducted. That previous work helped establish the procedure used in this investigation.

Chiques (2005) applied remote sensing techniques to 15 beach systems in western Puerto Rico. She collected radiometric data using the GER-1500 spectroradiometer to calculate the reflectance. Sediment texture analyses (grain size and composition) were used to compare with reflectance curves in order to establish a relationship between them. Field data analyses were compared to IKONOS images in an attempt to create a spectral library for the studied beaches.

## CHAPTER 3: METHODS

### 3.1 Topographical Survey – Beach Profiling

Survey was done in March (dry season) and September (wet season) of 2003.

Benchmarks were placed in the sites chosen. These were referenced to GPS coordinates.

Initially, U.S.G.S. benchmarks were to be used but this proved difficult because they could not be located due to erosion or human tampering. A profile line (vegetation line to the swash zone) was made perpendicular to the benchmark. The sampling distances and heights were measured at two feet intervals along the profile taking note of important features, such as high tide and low tide. Two additional profiles were measured 20 meters to the left and right of the benchmark.

The data was then used to make graphs to compare the differences in sand accumulation along each beach.

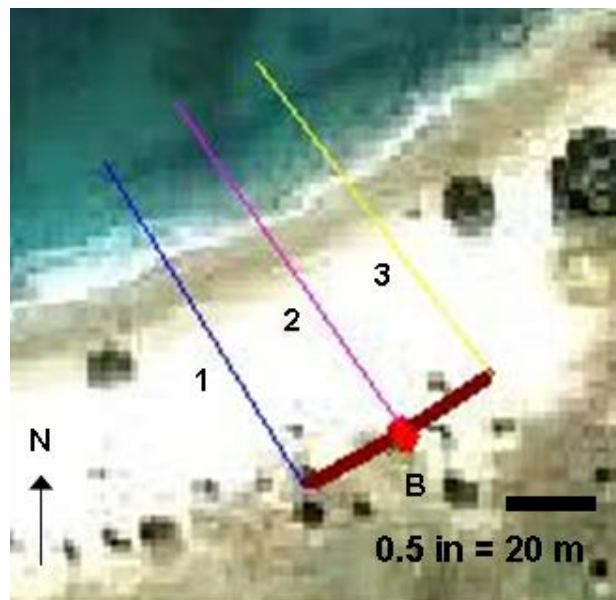


**Figure 3.1: Topographical survey. Three beach profiles were measured in each beach as shown (B = benchmark).**

### 3.1.1 Beach Classification

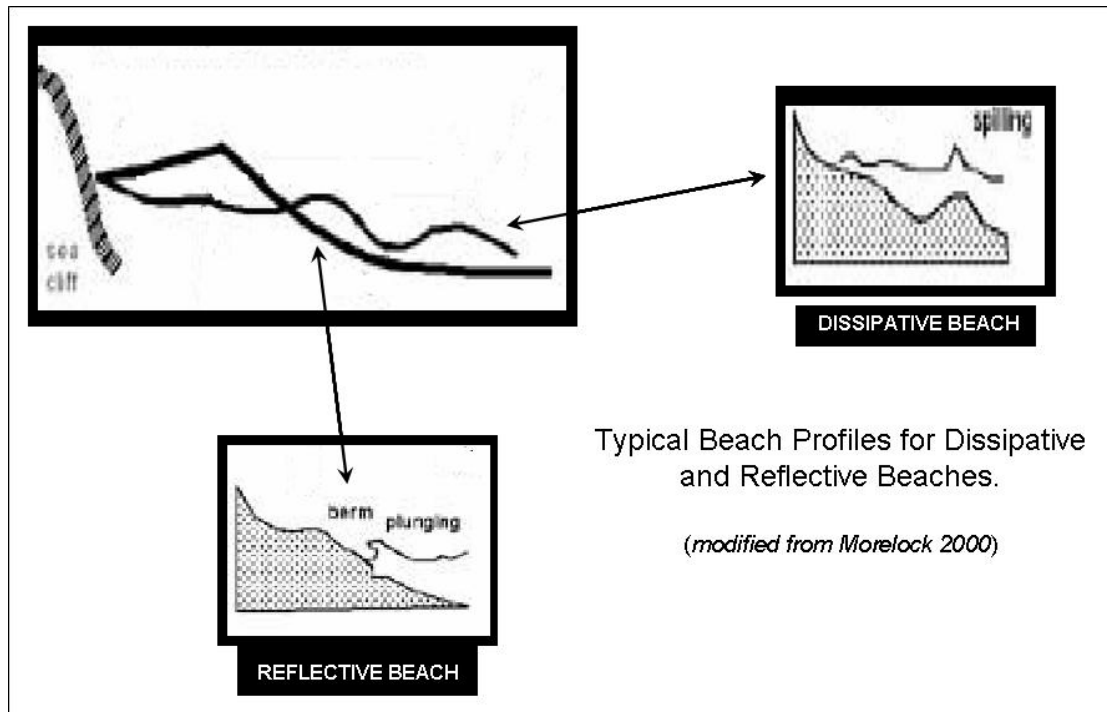


**Figure 3.2: Beach profiles for dissipative and reflective beaches.**

Beach profiles from the beach systems were classified into dissipative or reflective during both sampling periods (March and September 2003). Factors such as wave conditions, berm development and beach slope were used to make a qualitative classification. As seen in figure 3.2, a dissipative beach develops under high wave conditions, has a wide beach face and it usually lacks berm development (Short, 1984; Smith, 1990). A reflective beach develops under low to moderate wave conditions, has a higher beach slope and has berm development. Beaches may have seasonal shifts from reflective to dissipative in response to storm and swell conditions.

## **3.2 Sediment Analyses – Granulometry and Composition**

Sand samples from the beach systems were collected in March and September of 2003. Samples were collected in each site from the dune, berm, swash zone and nearshore. Due to the high energy of the area, nearshore sand samples were not taken from all sites.

Grain size analyses were conducted using net sieves ranging in size from  $-4\Phi$  to  $4\Phi$ . The samples were dried prior to analysis and 100 grams were used. The distribution of sediments (mean and sorting) was reported as histograms and cumulative curves. The Udden-Wentworth grain size scale was used to classify sand samples. Composition analyses were conducted using hydrochloric acid (10 %) to determine carbonate to terrigenous ratio. The samples were dried and weighed and HCl was added. After the HCl dissolved all the carbonate material, the samples were washed with distilled water several times, dried and weighed. The difference in weight was used to determine the sediment ratios.

## **3.3 Remote Sensing**

The original objective of this research was to identify hard grounds and sand types in the nearshore by using reflectance from IKONOS satellite images. Since reflectance values were not able to be calculated due to missing information for atmospheric correction, radiance values were used to determine sediment composition in sand bodies in the nearshore area. The program used to process the images was ENVI (Environment for Visualizing Images) version 4.0. These images were provided by the Pascor lab in UPRM.

### 3.3.1 Images Pre-Processing

The images were preprocessed before multispectral analysis. The initial step included rectification (georeferencing), masking, calibration and atmospheric correction. The rectification procedure was already performed prior to image acquisition. Masking was performed to cover the land and ocean boundary. This was done by creating a shape file in ESRI ArcGIS version 8.2. The shape file was then imported to ENVI as a vector file. A mask was built and then applied to the IKONOS images. Radiometric calibration was performed using an algorithm to change raw digital values to radiance values. The equation used was (Space Imaging, 2003):

$$L_{i,j,k} = \frac{DN_{i,j,k}}{CalCoef_k} \tag{3.1}$$

where,

$i,j,k$  = IKONOS image pixel  $i,j$  in spectral band  $k$

$L_{i,j,k}$  = in-band radiance at the sensor aperture (mW/cm<sup>2</sup>\*sr )

$DN_{i,j,k}$  = image product digital value (DN)

$CalCoef_k$  = In-Band Radiance Calibration Coefficient (DN\*cm<sup>2</sup>\*sr/mW)

(Space Imaging, 2003).

The calibration coefficients for IKONOS are determined by the equation:

$$L_k = \int L(\lambda)R_k'(\lambda) d\lambda \tag{3.2}$$

where,

$L_k$  = in-band radiance at the sensor aperture for IKONOS band  $k$  ( $\text{mW}/\text{cm}^2\text{-sr}$ )

$L(\lambda)$  = spectral radiance at the sensor aperture ( $\text{mW}/\text{cm}^2\text{-sr-mm}$ )

$R_k'(\lambda)$  = peak-normalized spectral response for IKONOS band  $k$

$\lambda$  = wavelength (mm)

The exact date of collection of the image is unknown, but it is known that it was after February 2001. Therefore, the IKONOS radiometric calibration coefficients for 11 bit products [ $\text{mW}/(\text{cm}^2\text{-sr}\cdot\text{DN})$ ] post 2/22/01 are 728 (blue), 727 (green), 949 (red) and 843 (near infrared) (Space Imaging, 2003).

The corrections for local atmospheric conditions were performed using the dark subtract function in ENVI. This function subtracts the minimum band value to all the other bands assuming that the minimum value is the atmospheric contribution to the digital values in the image. Normally, the infrared band is used for this correction.

### 3.3.2 Images Classification

Multispectral analyses of IKONOS satellite images were used to describe bottom sediment facies in the nearshore area. IKONOS has four spectral bands (blue, green, red, and near-infrared) with a spatial resolution of 4m and one panchromatic band (black and white) with a spatial resolution of 1m. The images I used had a spatial resolution of 1m due to a merge of the multispectral bands with the panchromatic band. Radiometric resolution was 11 bits (Space Imaging 2003).

Band 1 (blue) was used to analyze bathymetry, bottom sediment facies and sediment distribution. This wavelength is designed for water body penetration (Barreto et al., 1998). Radiance value distribution was used to distinguish among sediment types. Radiance is the brightness of reflected radiation measured in physical units (brightness –watts \* wavelength – micrometer \* angular unit – steradian) (Campbell, 1996). A prior study determined that carbonate sands tend to have a higher radiance value, mixed sands have a lower value, and no-radiance values could be associated with possible hard grounds (Morelock et al 2002).

Unsupervised classifications were made first to have an idea of the possible classifications. Isodata and K-means classifications were used. In this case the isodata classification proved to be more useful. After taking into consideration the isodata classification, regions of interest (ROI's) were established to make a supervised classification. In this case, a minimum distance supervised classification was used. Radiance values for the blue band were determined for each class and compared to determine sand type. Usually reflectance is used to do this, but since I did not have it, radiance values were used to find a relationship between value and sediment composition. The ROI classes 2, 3 and 6 were the radiance values used. A method of band ratios was also used as an alternate method for classification. This consisted of band 1 (blue) over band 2 (green).

## CHAPTER 4: RESULTS

### 4.1 Station SB1 – Isla de Cabras

Based on the comparison of the beach profiles (Fig. 4.1 and 4.2), Isla de Cabras (SB1) was categorized as a reflective beach system. There was berm development on both seasons, but more deposition is evident in September. There seems to be sand movement to the west side of the beach. In the nearshore area, there seems to be more sand deposited to the east side during March. The wet line is located higher during the wet season.

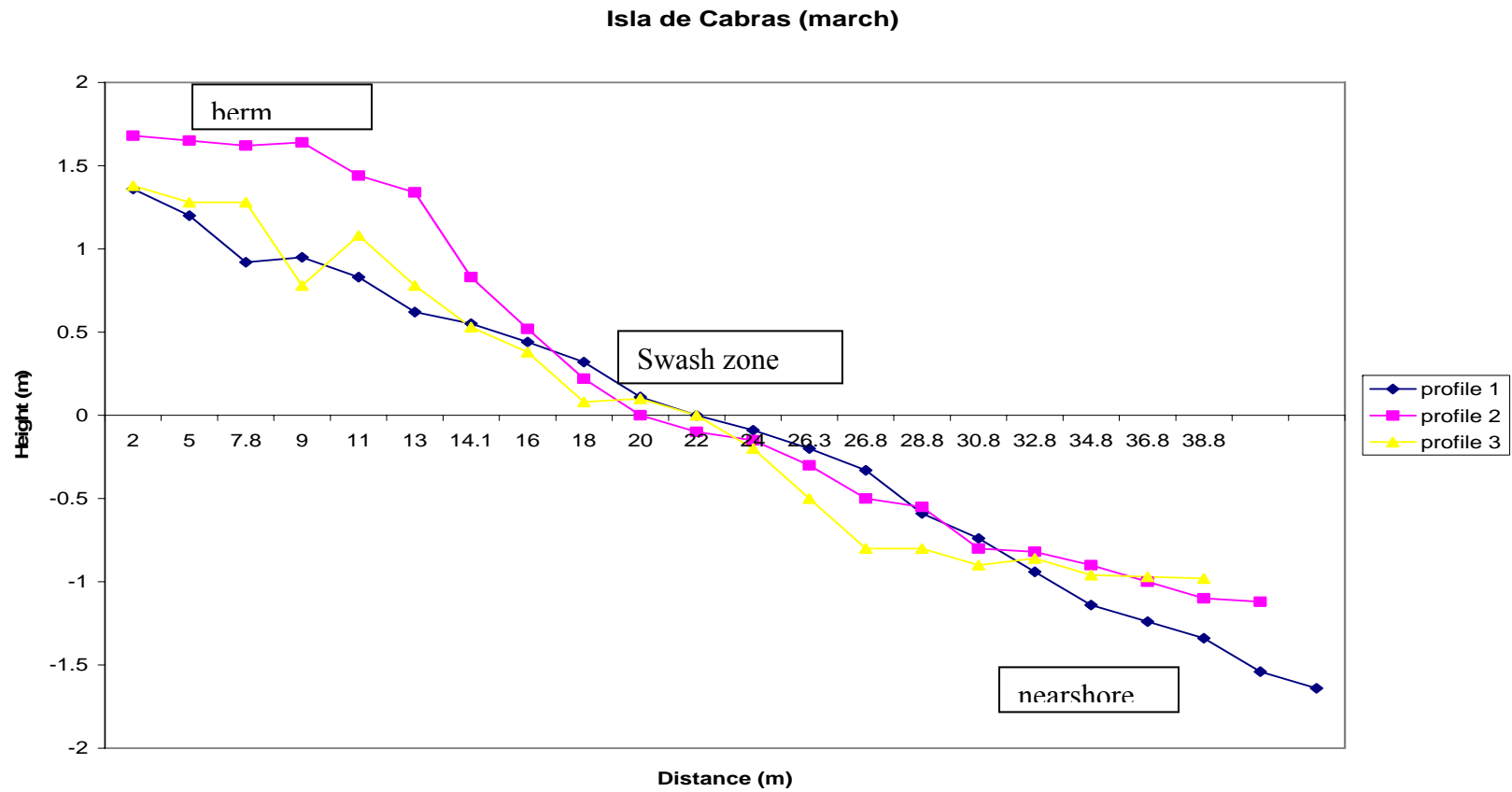


**Figure 4.1: Beach profiles for station SB1 during March 2003, classified as a reflective beach.**

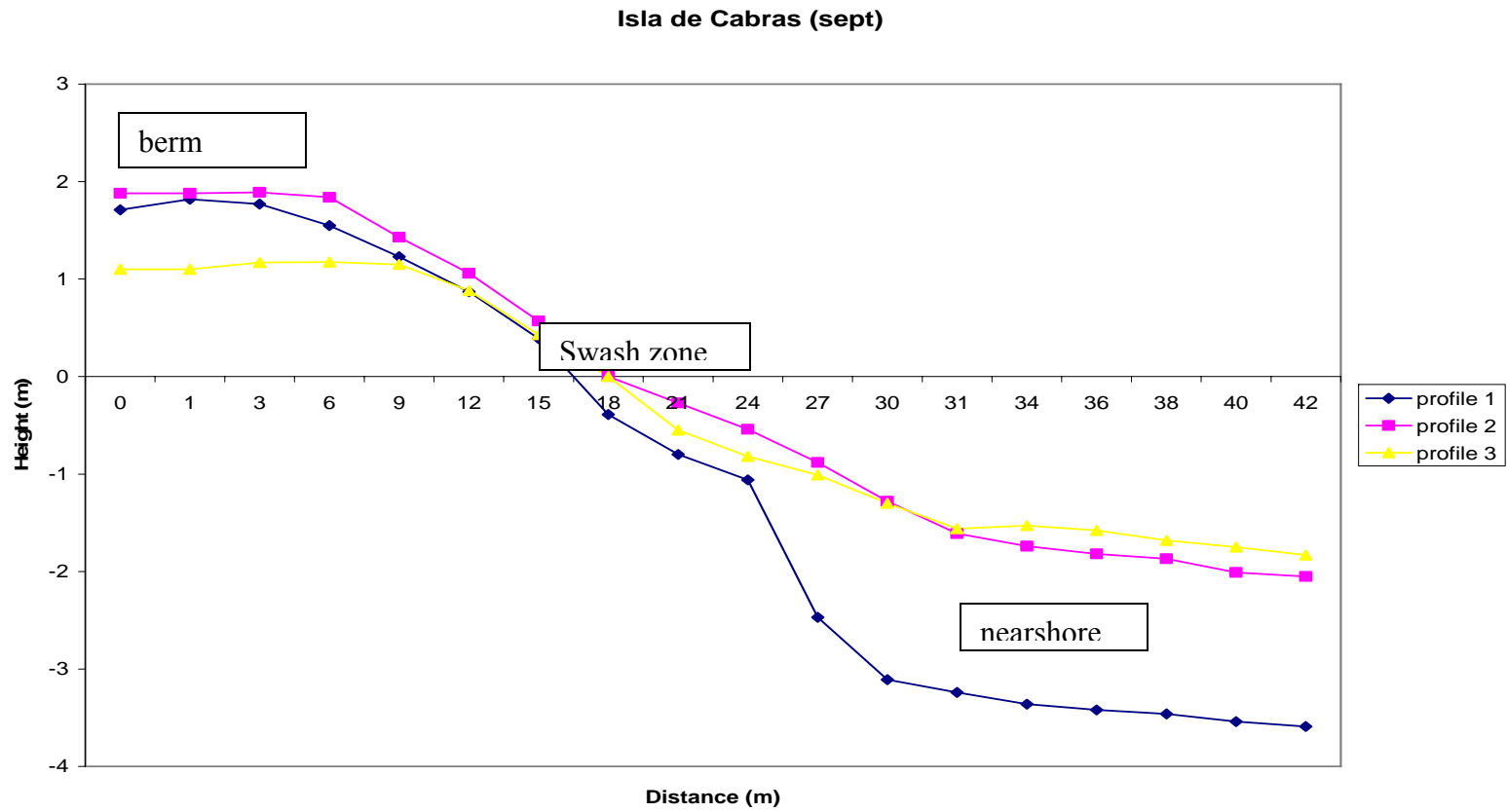


**Figure 4.2: Beach profiles for station SB1 during September 2003, classified as a reflective beach.**

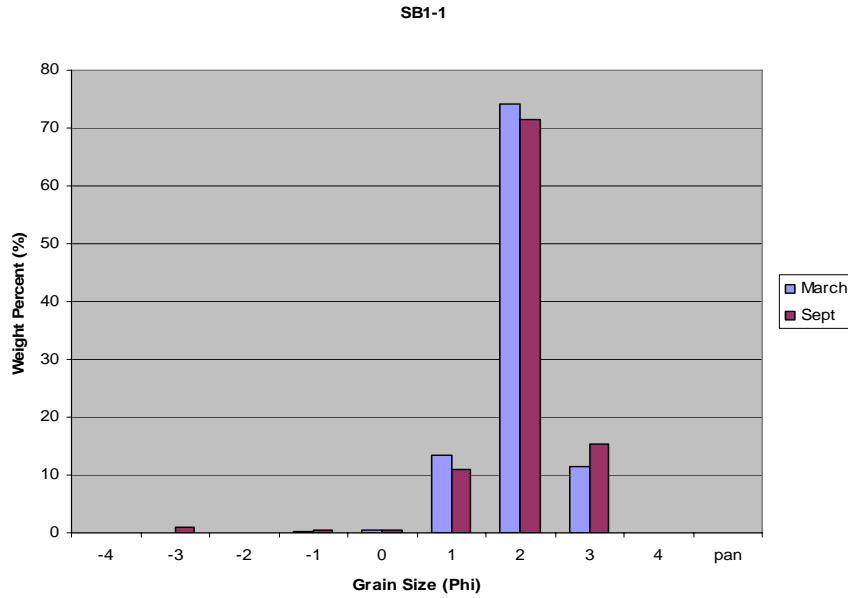


**Figure 4.3: Grain size comparison for station SB1-1 – Isla de Cabras, P.R. berm.**

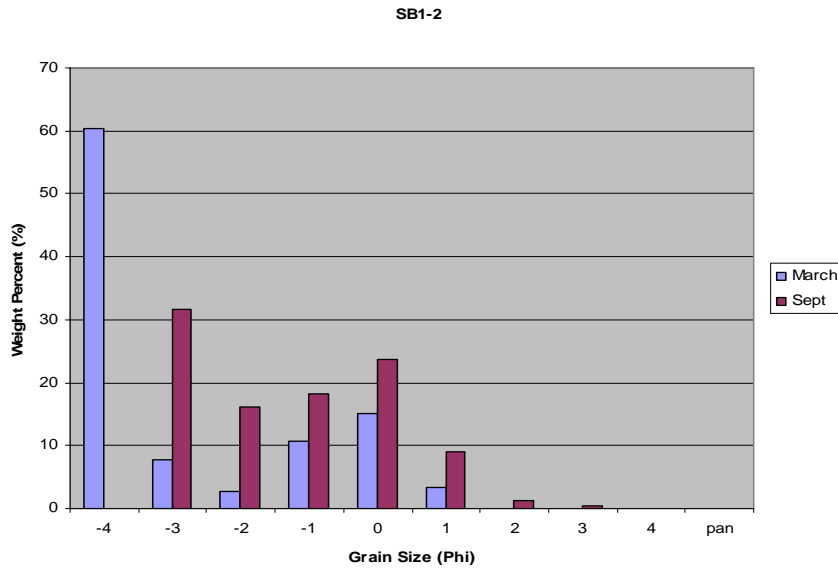


**Figure 4.4: Grain size comparison for station SB1-2 – Isla de Cabras, P.R. swash zone.**

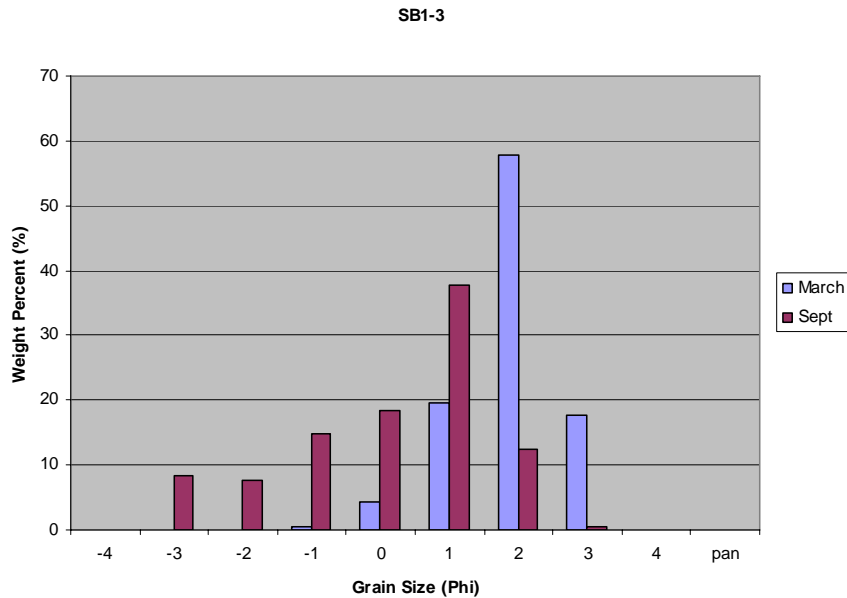


**Figure 4.5: Grain Size Comparison for station SB1-3 – Isla de Cabras, P.R. nearshore.**

The granulometry showed sediment distribution ranging from pebbles to very fine sand. In the berm, grain size ranged from fine to very fine sand (Fig. 4.3). In the swash zone, sediments were mostly pebble size (Fig. 4.4). In the surf zone very coarse sand to very fine sand was found (Fig. 4.5). A comparison of cumulative curves for both seasons for the three areas of the beach studied show that the sediments are moderately sorted (Fig. 4.6). This was concluded by looking at the slanting of the curves, which is more towards the right of the graph. The compositional percentages of sediments indicate that more terrigenous material and less carbonates were present during the month of March, with the exception of the swash zone, where carbonate material was higher (Fig. 4.7). During the month of September the percentage of carbonates increased by 20% in the nearshore and 3% in the swash zone.

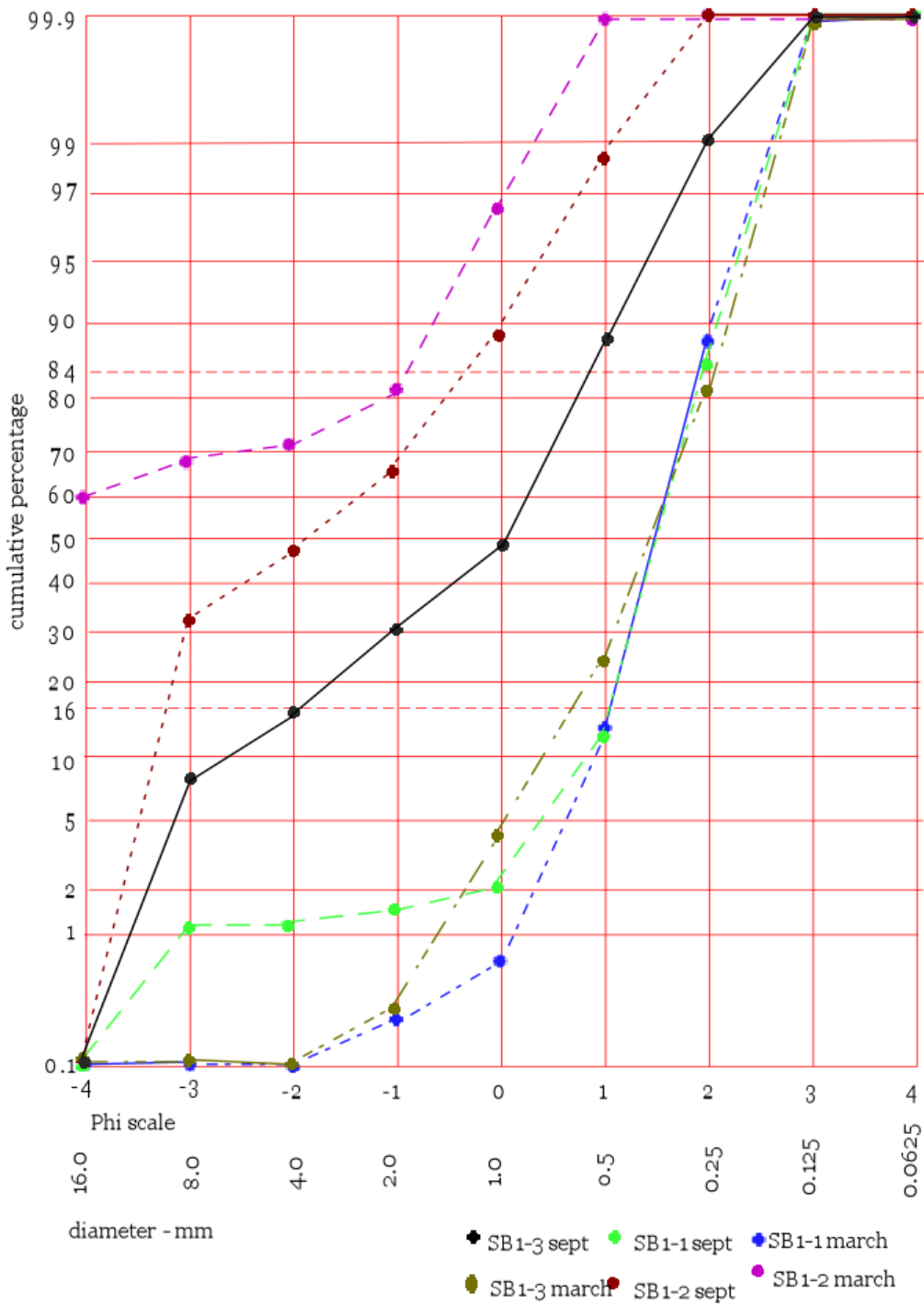


**Figure 4.6: Cumulative curves for station SB1 (Isla de Cabras, P.R.), showing moderately sorted grain distribution.**

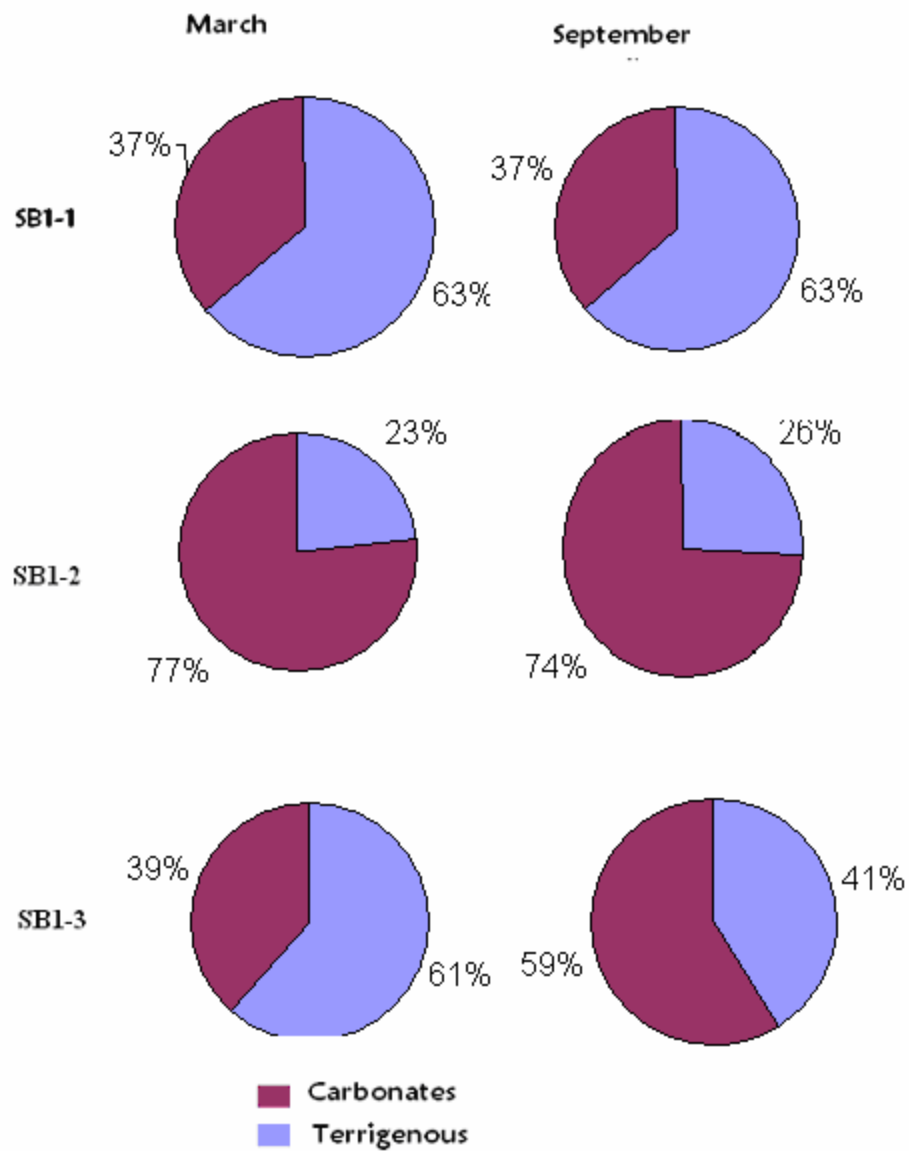
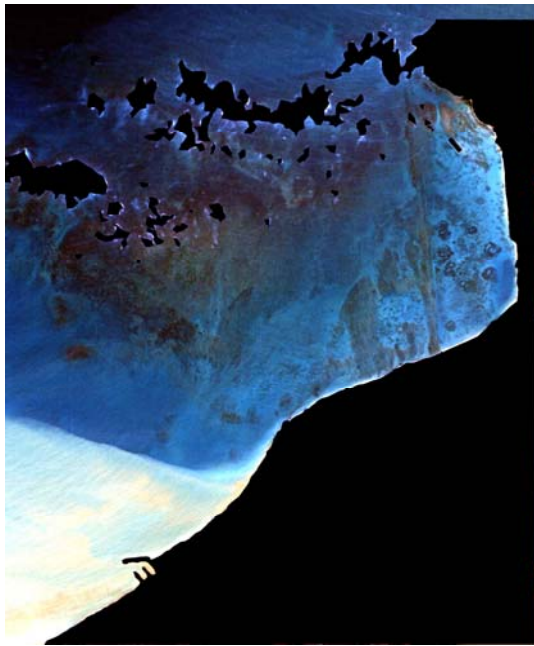


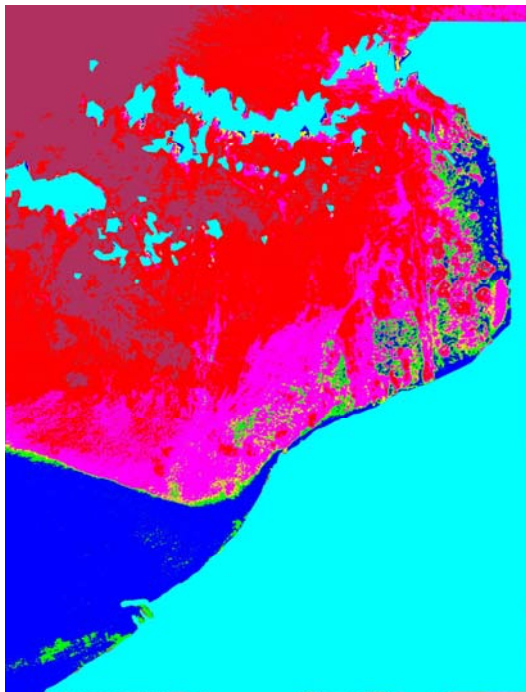
**Figure 4.7: Compositional comparison for station SB1 – Isla de Cabras, P.R.**

**(SB1-1: berm, SB1-2: swash zone and SB1-3: nearshore).**



(a)

**Figure 4.8: IKONOS Satellite Images for station SB1 – Isla de Cabras, PR. (a) Pre-processed image with mask, (b) Minimum Distance Supervised Classification, and (c) ROI's Legend.**



(b)

**Legend:**

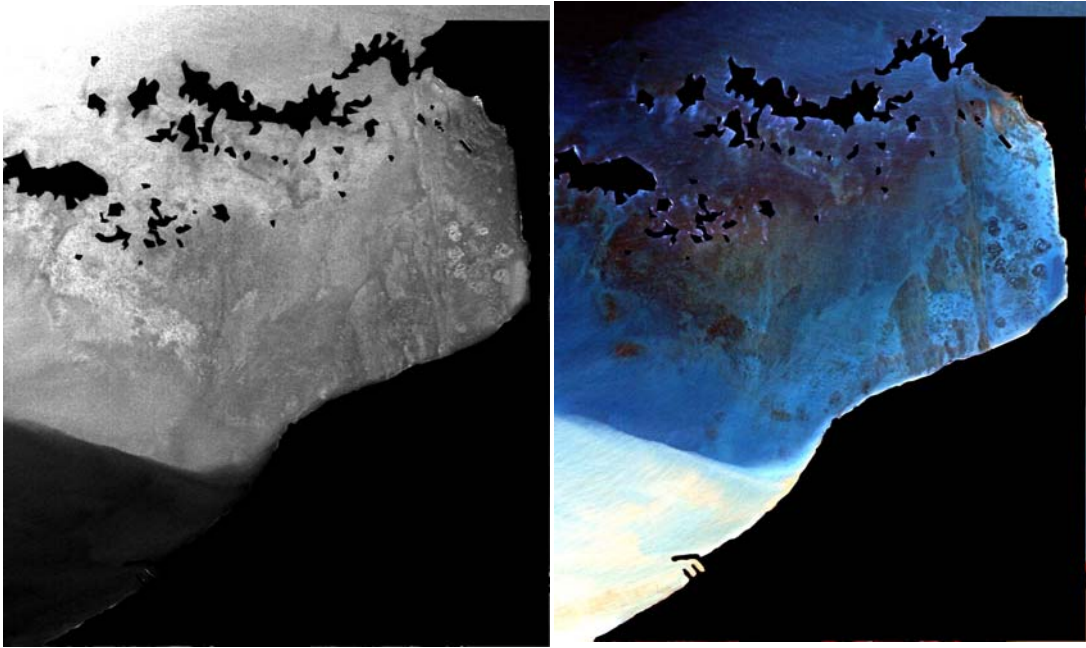
- Class 1: Cays
- Class 2: Sediment bottom (in between cays)
- Class 3: Sediment bottom
- Class 4: Clouds
- Class 5: Mask
- Class 6: Sediment bottom (deeper water)
- Class 7: Deep water

(c)

**Table 2: Radiance values for supervised classification image for station SB1.**

<b>Class Name</b>	<b>Radiance Value (Red Band)</b>	<b>Radiance Value (Green Band)</b>	<b>Radiance Value (Blue Band)</b>
Class 1	0.134879	0.403026	0.662088
Class 2	0.143309	0.609353	0.800824
Class 3	0.170706	0.678129	0.907967
Class 4	0.580468	0.820055	1.296703
Class 5	0	0	0
Class 6	0.127503	0.486933	0.717033
Class 7	0.109589	0.250344	0.524725

In figure 4.8a, the presence of sand bodies is noticeable, but when a supervised classification was attempted (Fig. 4.8b), the classes did not correlate as good as wanted. The radiance values for the satellite image ranged from 0.71 to 0.90 (Table 2). When comparing the original rgb satellite image with the band ratio blue over green image (Fig. 4.9), it can be seen that the water column component and sun glare affect the result. The lighter areas in the band ratio image appear in the deeper water area. There are grayish areas apparent in the nearshore area of the band ratio image that correlate to sand bodies in the rgb image.



(a)

(b)

**Figure 4.9: (a) Blue over green band ratio compared to (b) rgb IKONOS satellite image for SB1.**

## **4.2 Station SB2 – Mameyal**

In station SB2 (Mameyal) the comparison of the beach profiles shows that it is a dissipative beach (Fig. 4.10 and 4.11). In both seasons, there was no berm development, but a high slope in the beach face. There seems to be no relative change among the profiles between both seasons. The sand movement can be seen to the west of the beach system. Profile 1 shows higher sand deposition in both seasons.

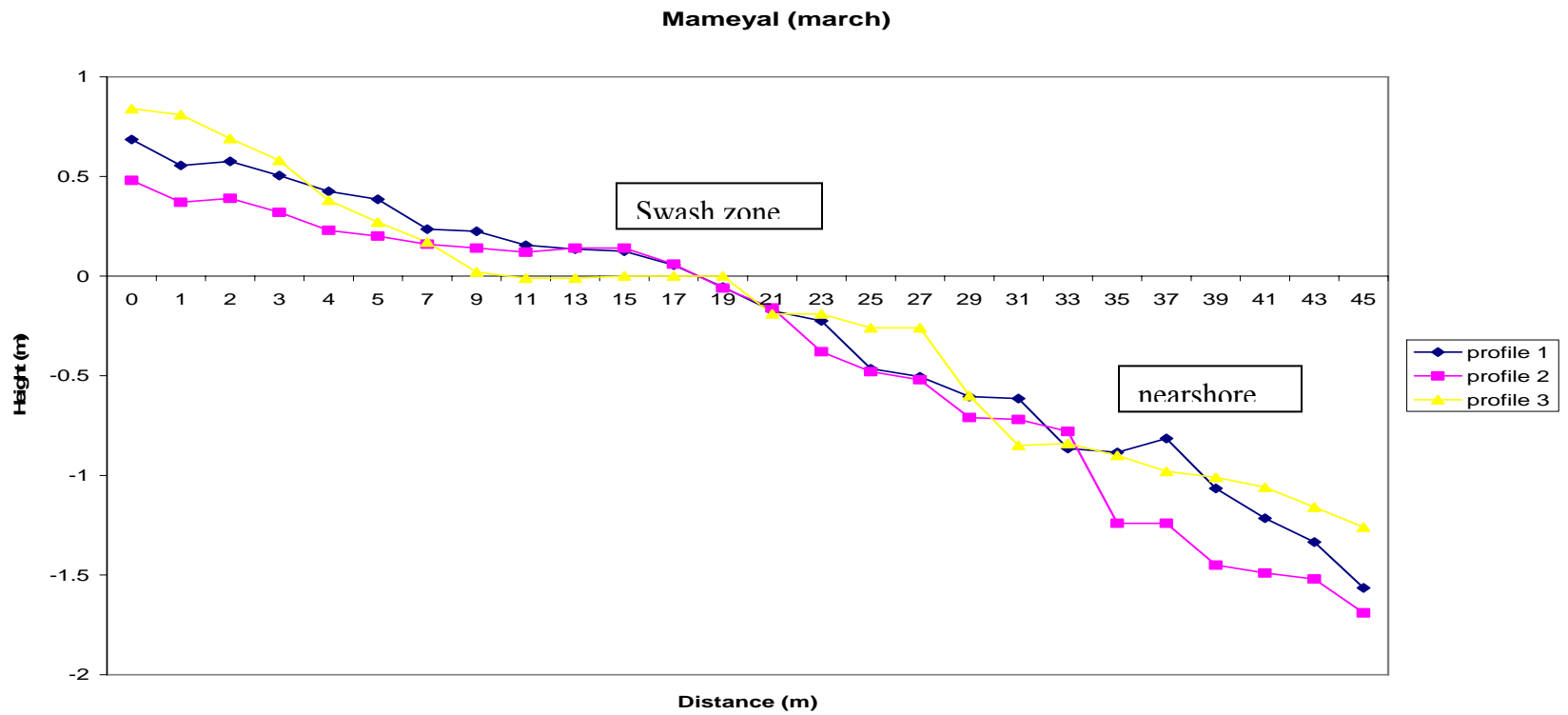


**Figure 4.10: Beach profiles for station SB2 during March 2003, classified as a dissipative beach.**

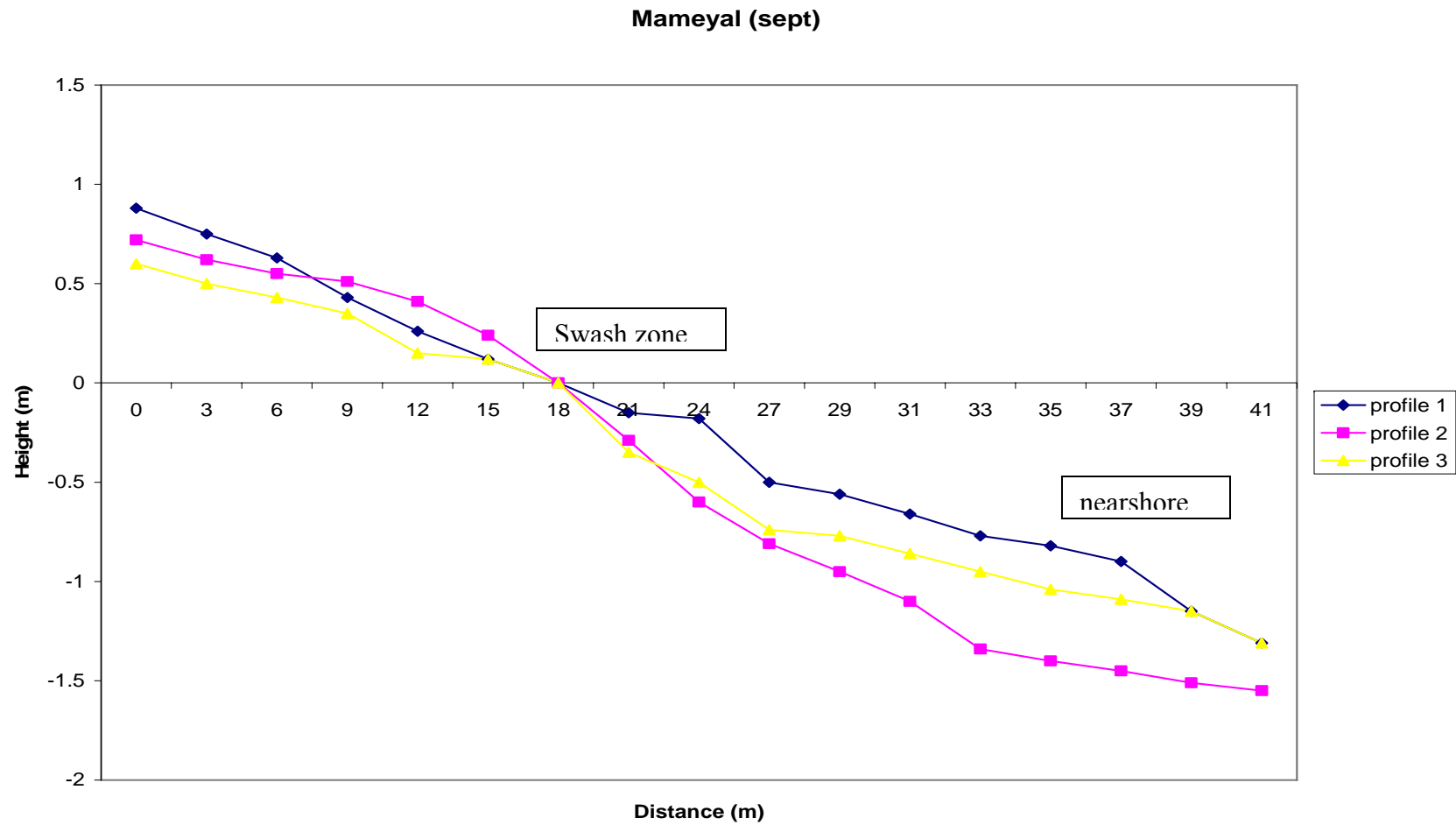


**Figure 4.11: Beach profiles for station SB2 during September 2003, classified as a dissipative beach.**

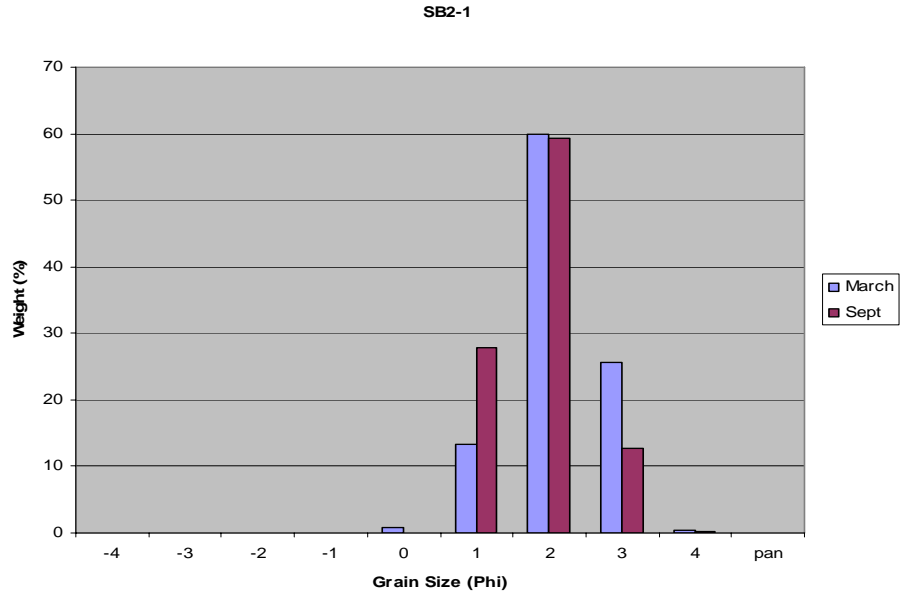


**Figure 4.12: Grain size comparison for station SB2-1 – Mameyal, P.R. swash zone.**

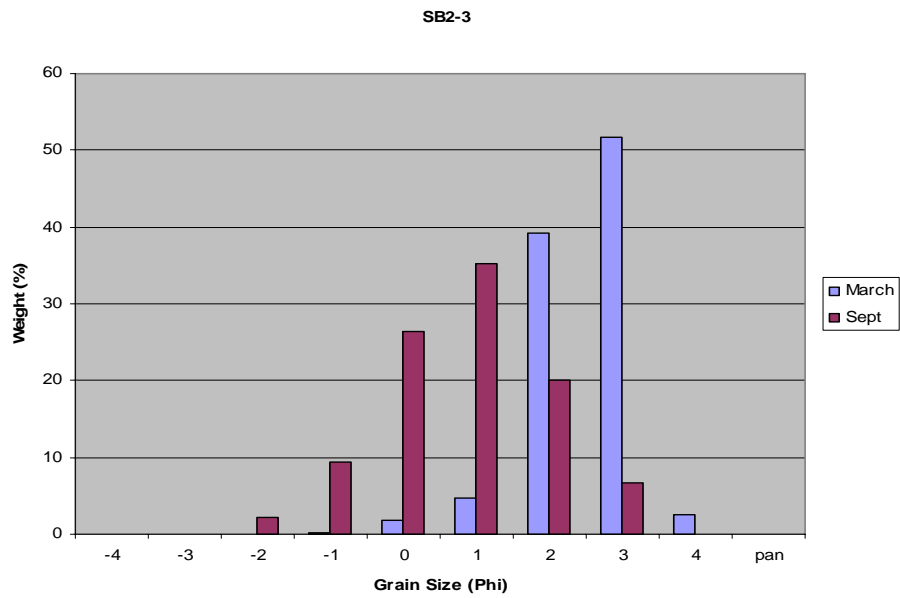


**Figure 4.13: Grain Size Comparison for station SB2-2 – Mameyal (Dorado), P.R. nearshore.**

The granulometry was similar at the two points (swash zone and nearshore) of the system where sand was collected. The grain size ranged from very coarse sand to very fine sand (Fig. 4.12 and 4.13). The cumulative percentages show that the sediments are moderately well sorted (Fig. 4.14). This can be concluded by the slopes that slightly slant to the right in the cumulative curves. The compositional percentage showed higher terrigenous material than carbonate sediments. There was no significant difference between percentages in both seasons.

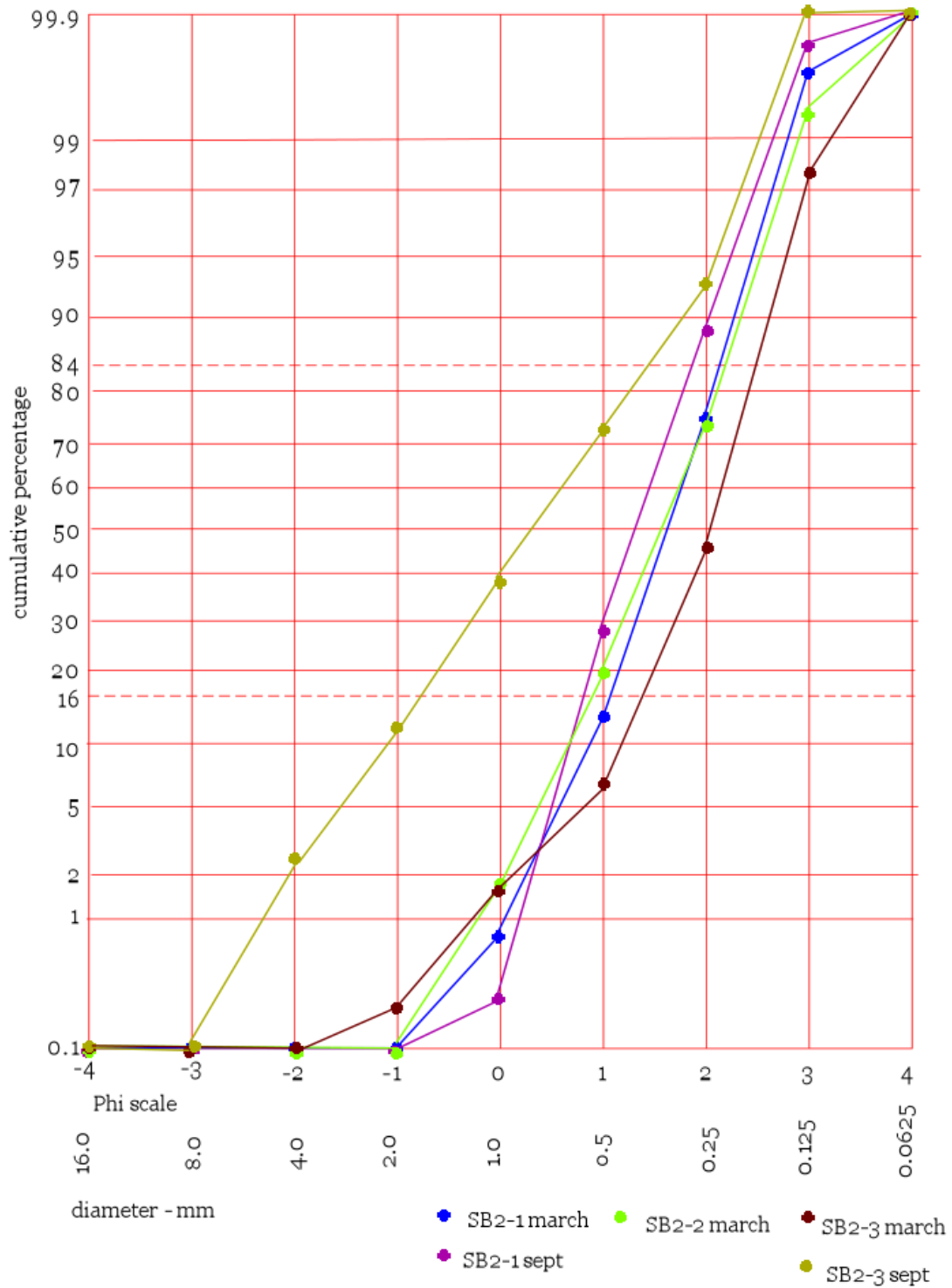


**Figure 4.14: Cumulative Curves for station SB2 (Mameyal Dorado, P.R.), showing moderately well sorted grain distribution.**

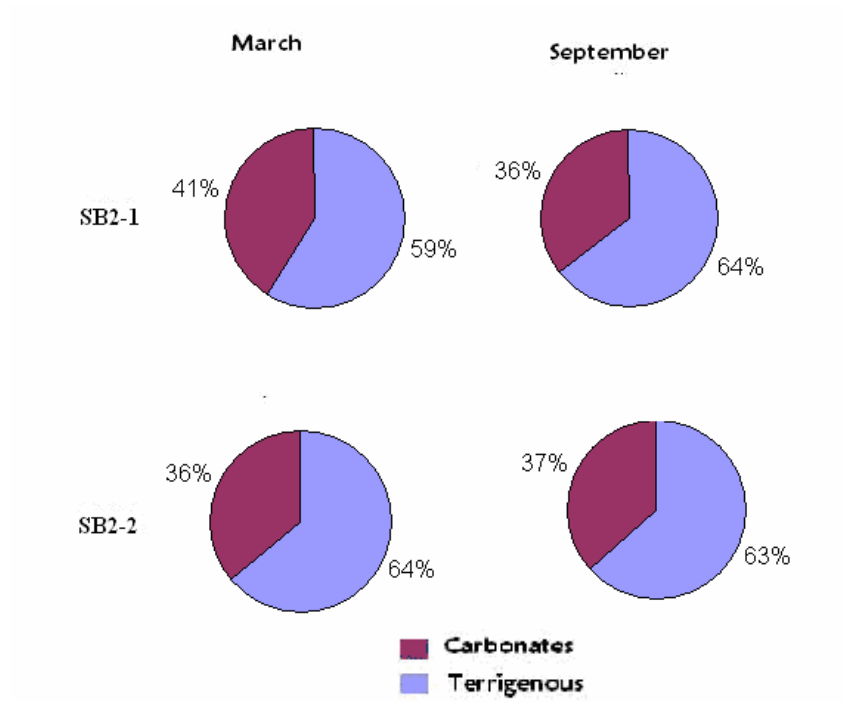
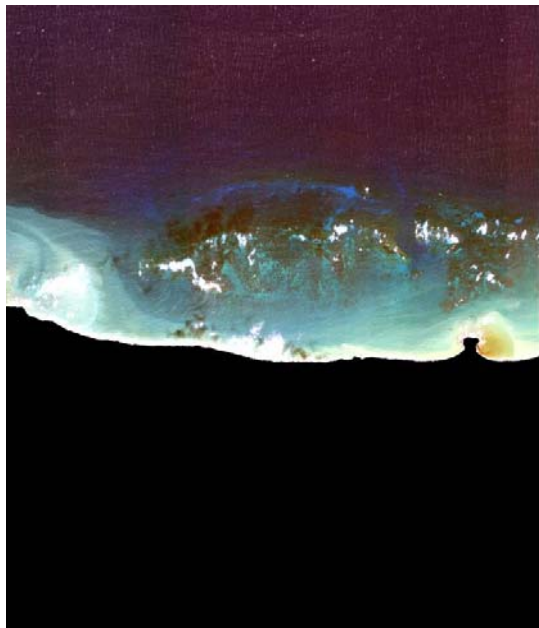


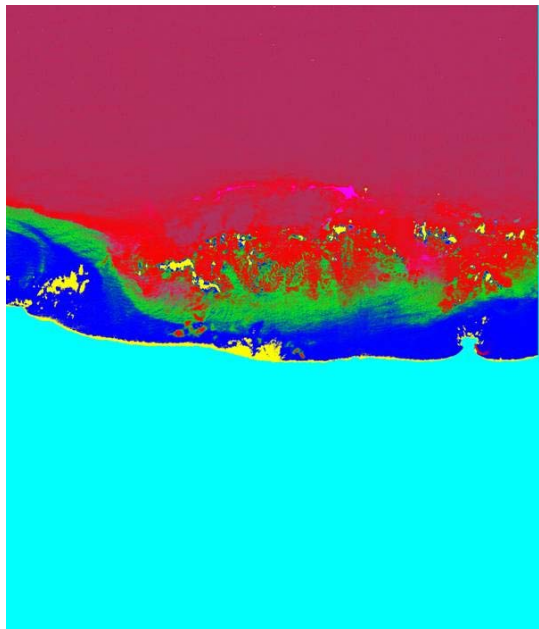
**Figure 4.15: Compositional Comparison for station SB2 – Mameyal (Dorado), P.R.**

**(SB2-1: swash zone and SB2-2: nearshore).**



(a)

**Figure 4.16: IKONOS Satellite Images for station SB2 – Mameyal, Dorado PR. (a) Pre-processed image with mask, (b) Minimum Distance Supervised Classification, and (c) ROI's Legend.**



(b)

Legend:

- Class 1: Cays
- Class 2: Sediment bottom (in between cays)
- Class 3: Sediment bottom
- Class 4: Clouds
- Class 5: Mask
- Class 6: Sediment bottom (deeper water)
- Class 7: Deep water

(c)

**Table 3: Radiance Values for supervised classification image for station SB2.**

<b>Class Name</b>	<b>Radiance Value (Red Band)</b>	<b>Radiance Value (Green Band)</b>	<b>Radiance Value (Blue Band)</b>
Class 1	0.110643	0.338377	0.575549
Class 2	0.067439	0.433288	0.60989
Class 3	0.119073	0.496561	0.68956
Class 4	0.508957	1.100413	1.296703
Class 5	0	0	0
Class 6	0.045311	0.305365	0.703297
Class 7	0.059009	0.180193	0.440934

In figure 4.16a, the presence of sand bodies is noticeable, but when classifications were attempted (Fig. 4.16b and 4.16c), the classes do not correlate as good as wanted. The radiance values for the satellite image ranged from 0.60 to 0.70 (Table 3). When comparing the original rgb satellite image with the band ratio blue over green image (Fig. 4.17), it can be seen that the water column component and sun glare affect the result. The lighter areas in the band ratio image appear in the deeper water area. There are grayish areas apparent in the nearshore area of the band ratio image that correlate to sand bodies in the rgb image. It appears that the darker gray areas might be related to a lighter sand composition.

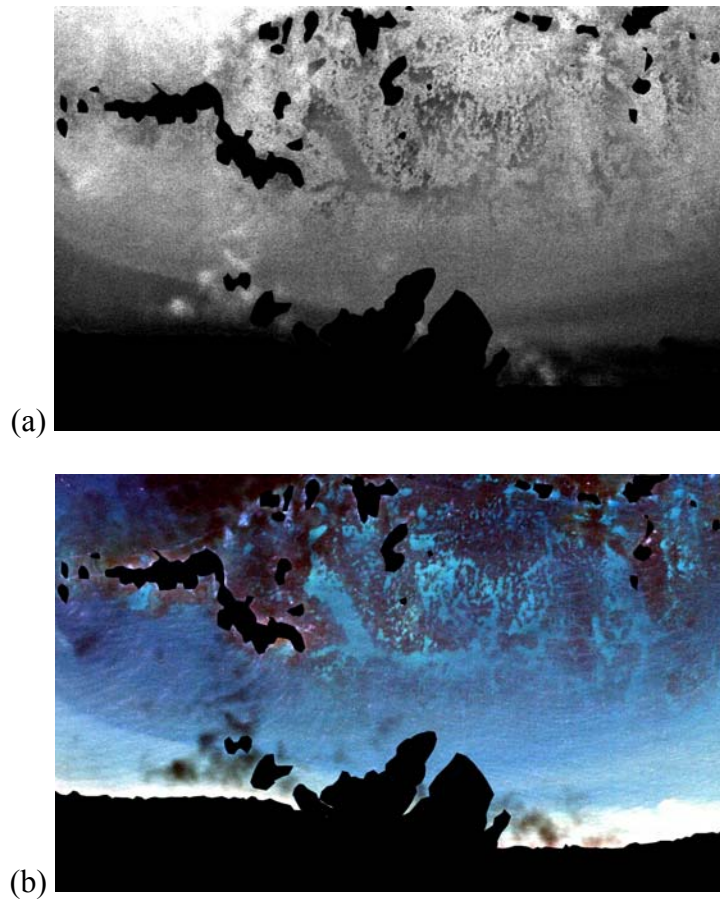


**Figure 4.17: (a) Blue over green band ratio compared to (b) rgb IKONOS satellite image for station SB2.**

### **4.3 Station SB3 – Palmas Altas, Barceloneta**

In station SB3 the beach profiles show the system to be dissipative to reflective (Fig. 4.18 and 4.19). It had no berm development in March, but later in September it was present. There was more sand deposition in September along the beach face and the water line was higher. Sand movement seems to be to the west of the system when comparing profile 1 with profile 3.

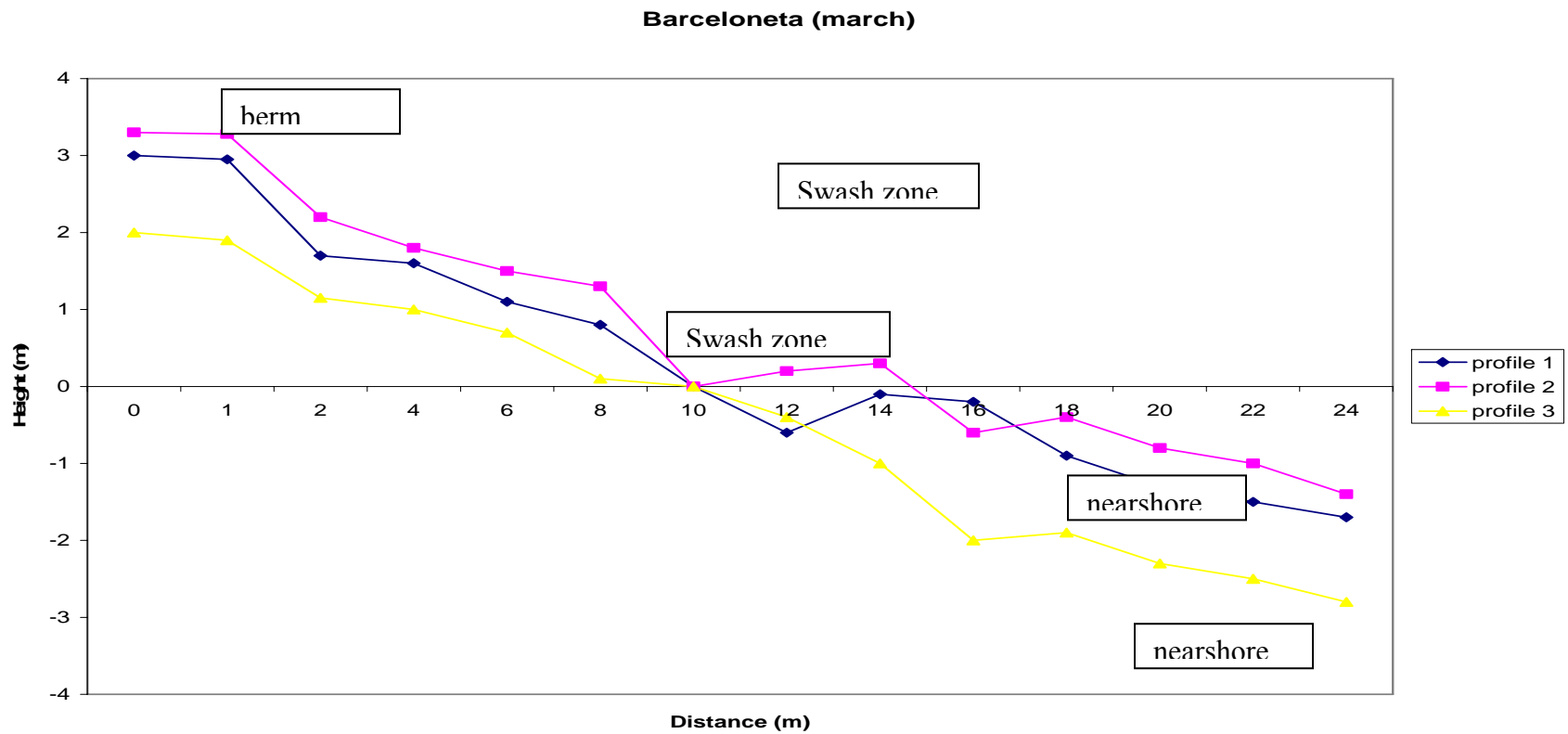


**Figure 4.18: Beach profiles for station SB3 during March 2003, classified as a dissipative beach.**

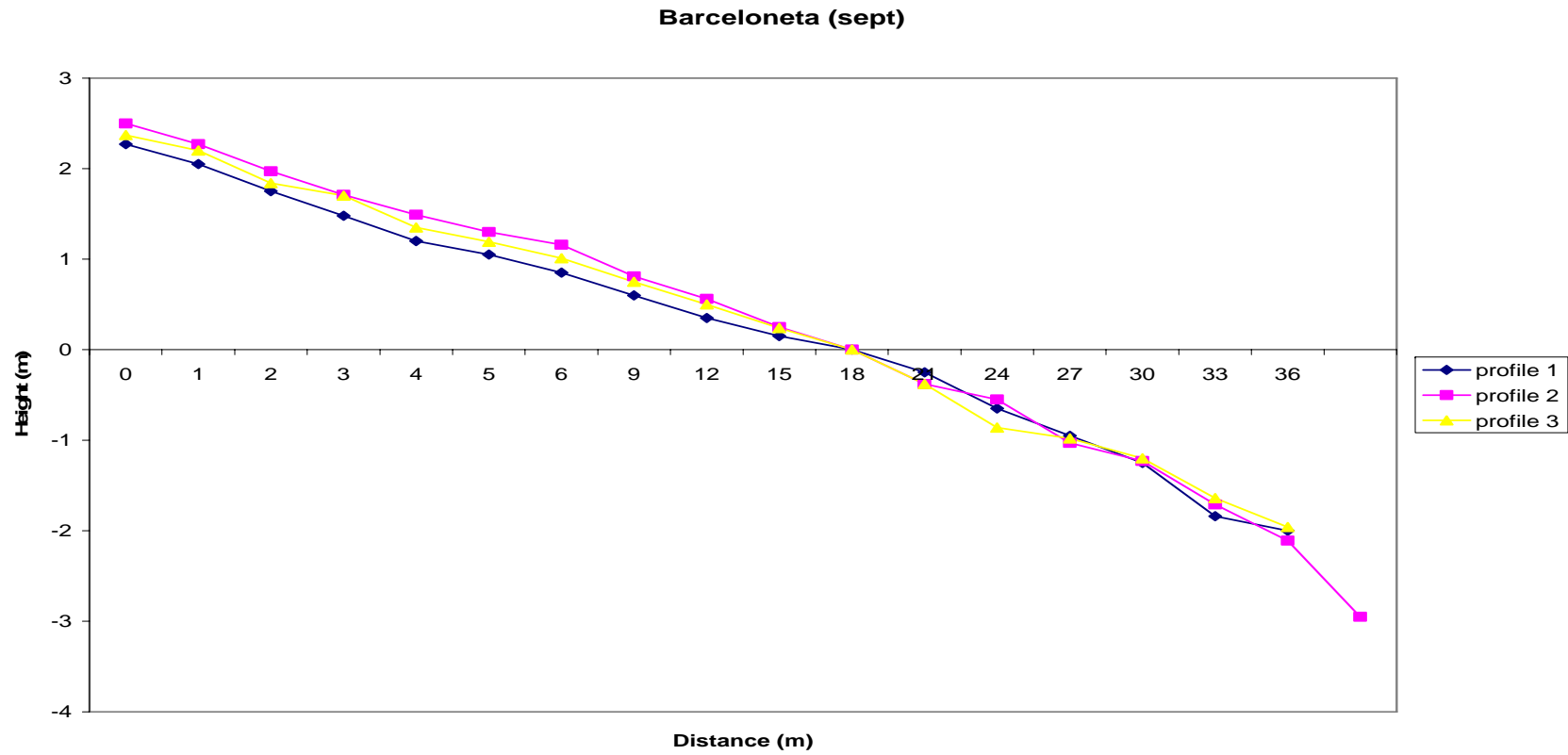


**Figure 4.19: Beach profiles for station SB3 during September 2003, classified as a reflective beach.**

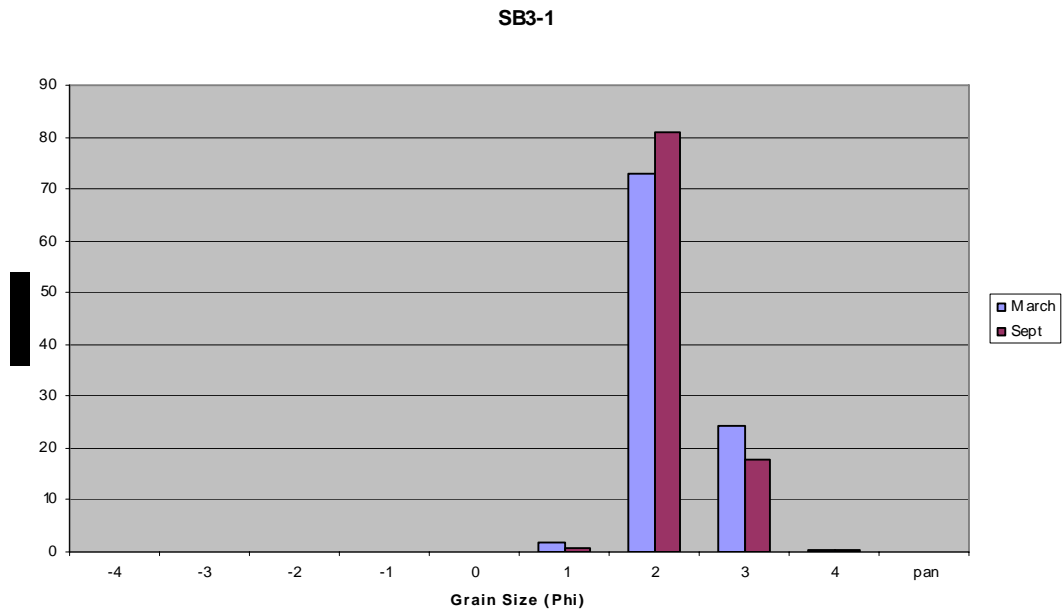


**Figure 4.20: Grain size comparison for station SB3-1 – Barceloneta, P.R. dune.**

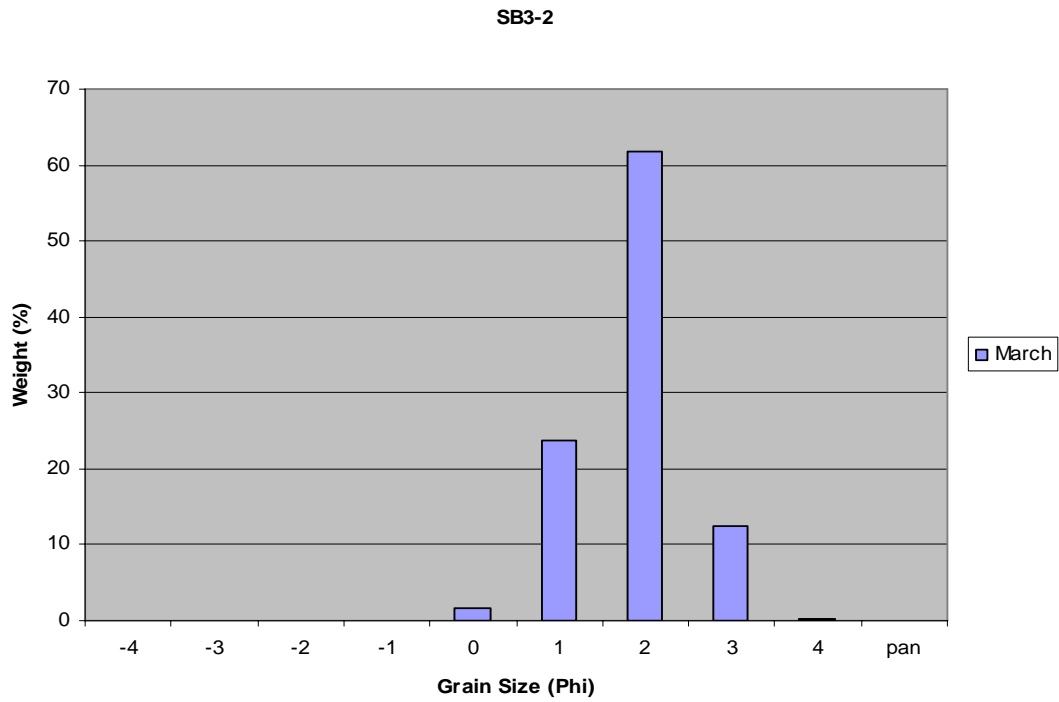


**Figure 4.21: Grain size comparison for station SB3-2 – Palmas Altas (Barceloneta), P.R. berm.**

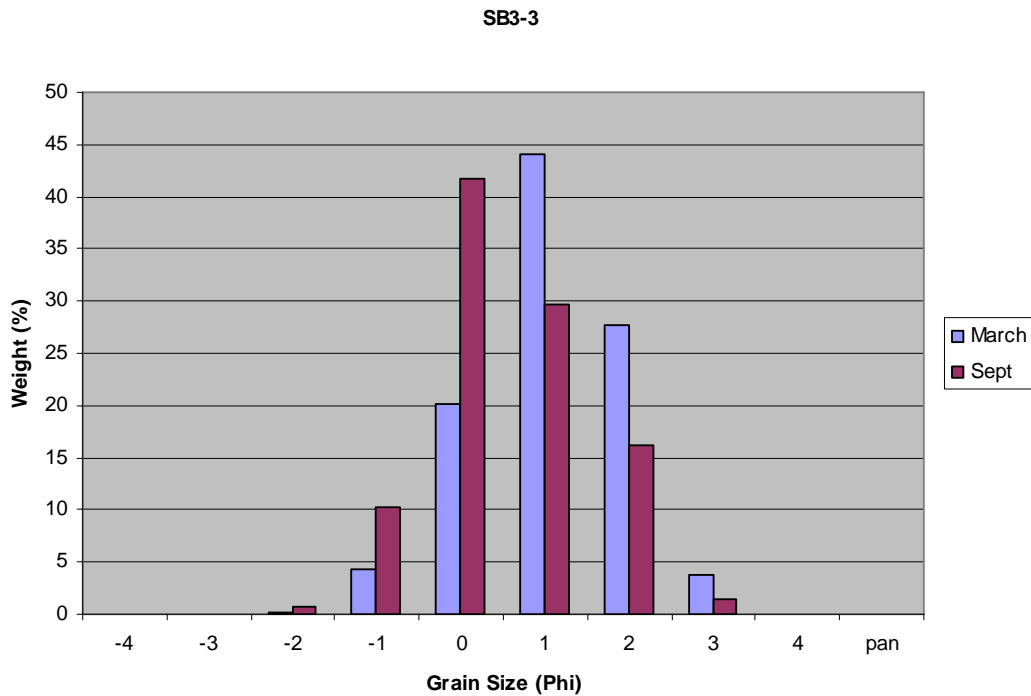


**Figure 4.22: Grain size comparison for station SB3-3 – Palmas Altas (Barceloneta), P.R. swash zone.**

Sand samples were collected only from the dune, berm and swash zone, because the surf zone was completely covered by beachrock. The sediment grain size ranged from very coarse sand to very fine sand (Fig. 4.20, 4.21 and 4.22). The cumulative curves show that the sediments are moderately well sorted (Fig. 4.23). The grain composition percentage showed higher terrigenous material than carbonate grain material during both seasons, showing no significant difference between them (figure 4.24).

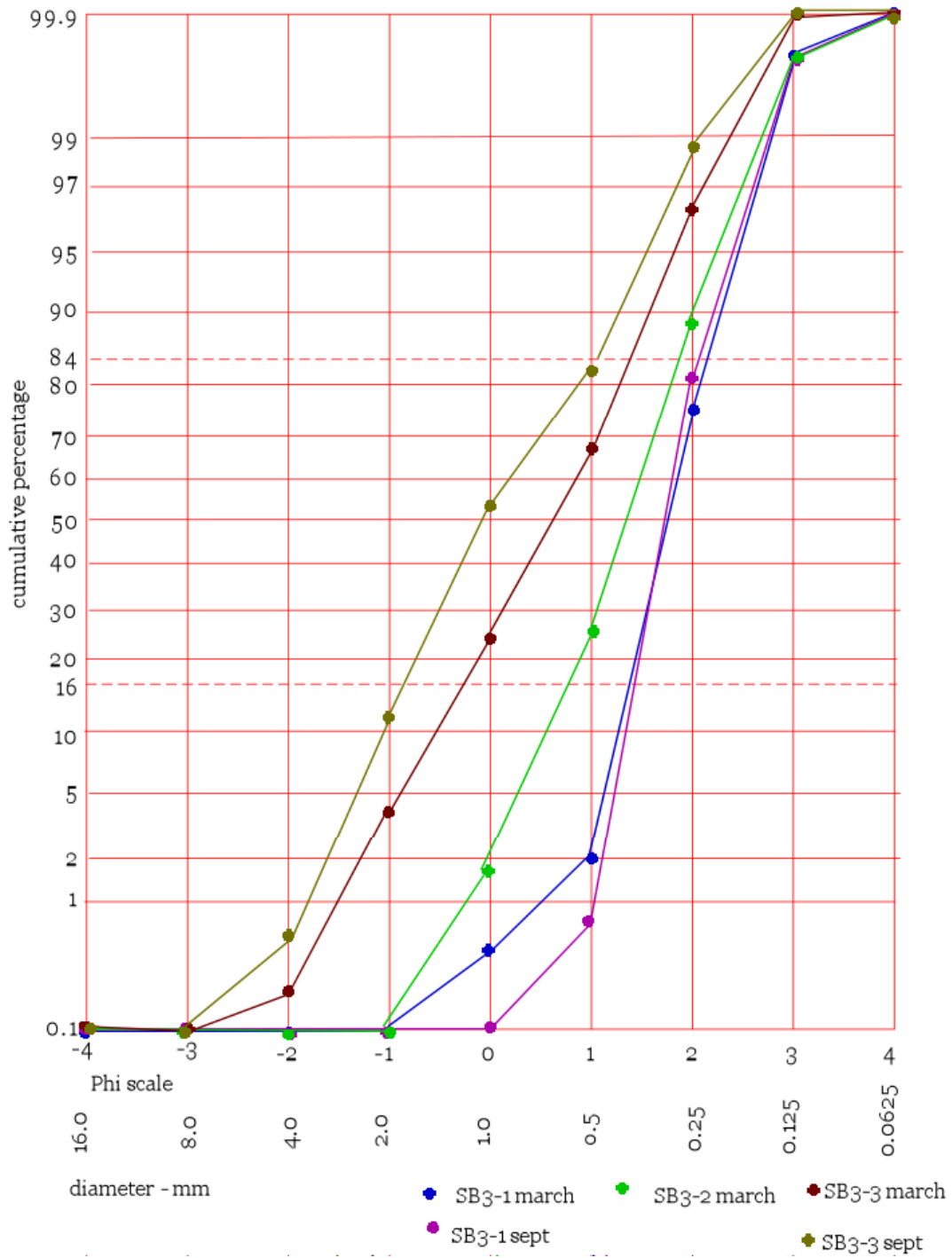


**Figure 4.23: Cumulative Curves for station SB3 (Palmas Altas - Barceloneta, P.R.), showing moderately well sorted grain distribution.**

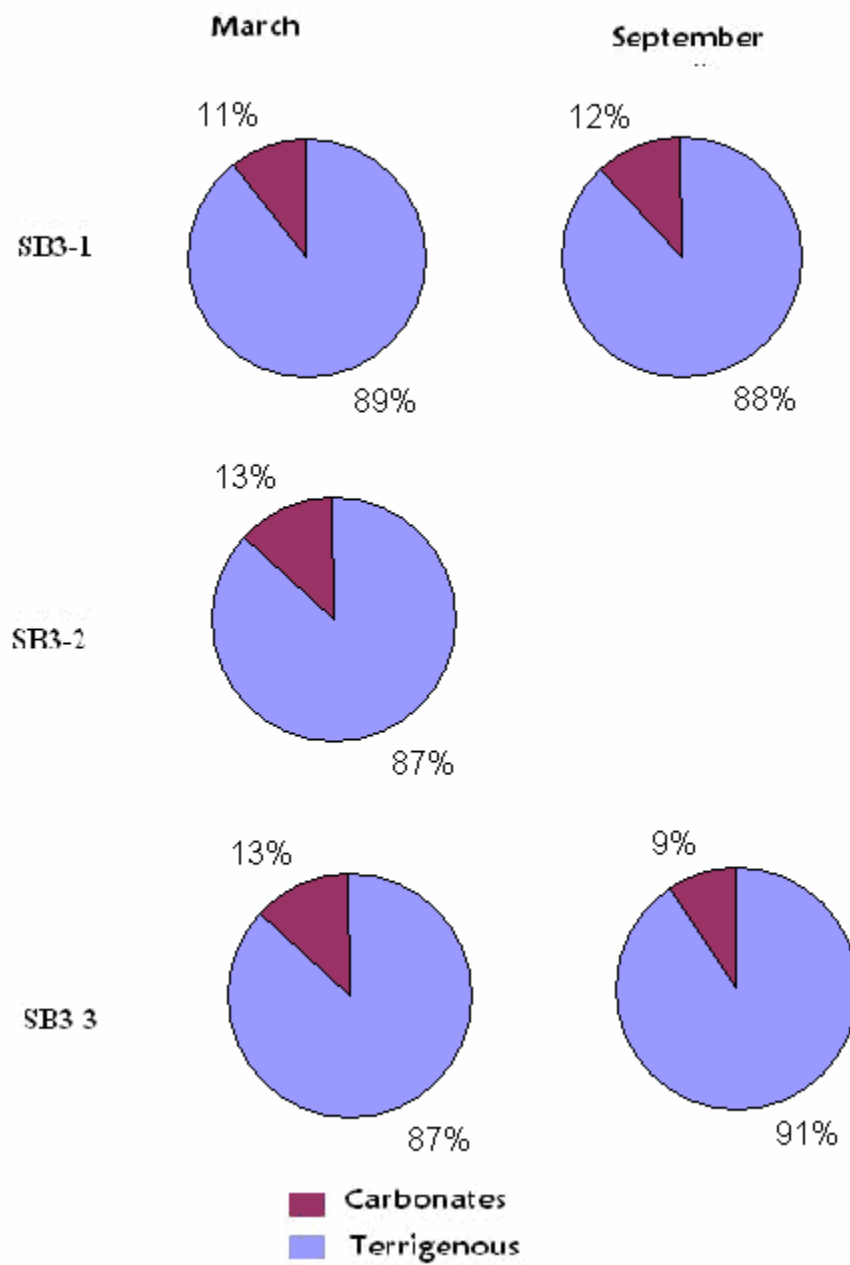
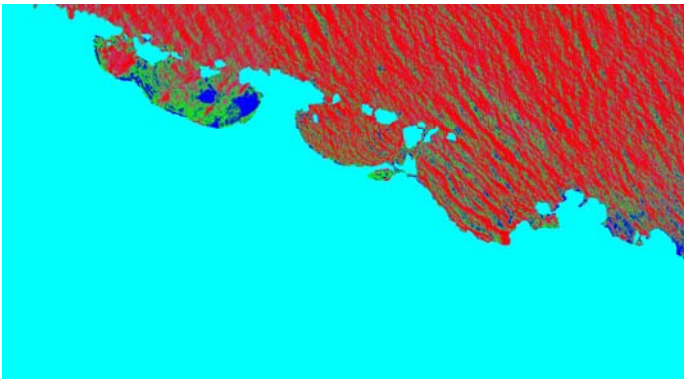


**Figure 4.24: Compositional comparison for station SB3 – Palmas Altas (Barceloneta), P.R.**

**(SB3-1: dune, SB3-2: berm and SB3-3: swash zone).**



(a)



(b)

**Figure 4.25: IKONOS Satellite Images for station SB3 –Palmas Altas, Barceloneta PR. (a) Pre-processed image with mask (b) Minimum Distance Supervised Classification, and (c) ROI's Legend.**

- Legend:
- Class 1: Cays
  - Class 2: Sediment bottom (in between cays)
  - Class 3: Sediment bottom
  - Class 4: Clouds
  - Class 5: Mask
  - Class 6: Sediment bottom (deeper water)
  - Class 7: Deep water

(c)

**Table 4: Radiance Values for supervised image for station SB3.**

<b>Class Name</b>	<b>Radiance Value (Red Band)</b>	<b>Radiance Value (Green Band)</b>	<b>Radiance Value (Blue Band)</b>
Class 1	0.015806	0.303989	0.708791
Class 2	0.261328	0.807428	1.141489
Class 3	0.289779	1.038514	1.364011
Class 4	0	0	0
Class 5	0	0	0
Class 6	0.195996	0.701513	0.932692
Class 7	0	0	0

In figure 4.25a, the presence of sand bodies is noticeable, but when classifications were attempted (Fig. 4.25b and 4.25c), the classes do not correlate as good as wanted. The radiance values for the satellite image ranged from 0.90 to 1.36 (Table 4). When comparing the original rgb satellite image with the band ratio blue over green image (Fig. 4.26), no assessment could be made because it gave a result with poor resolution. The water column and waves present interfere noticeably in this image.

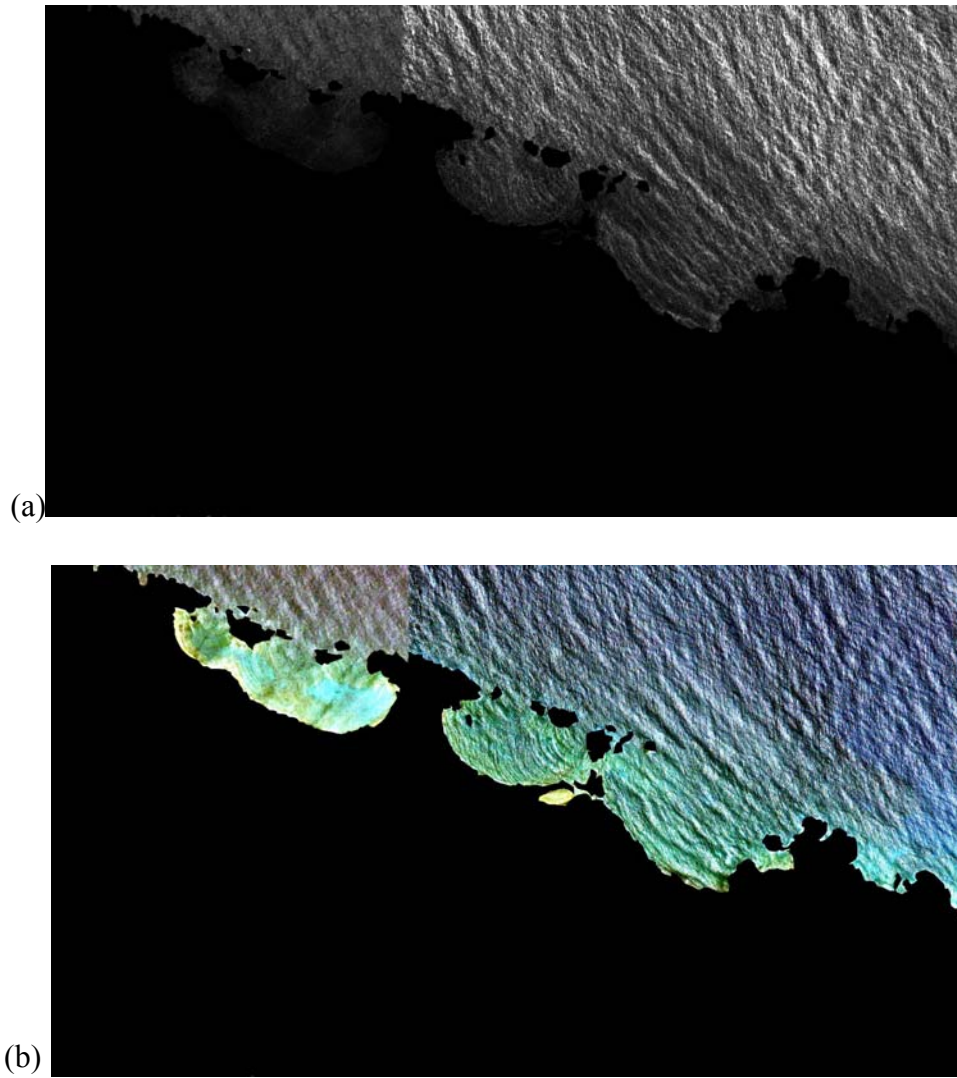


**Figure 4.26: (a) Blue over green band ratio compared to (b) rgb IKONOS satellite image for station SB3.**

#### **4.4 Station SB4 – Arecibo**

In station SB4 the profiles show this beach classification varies from reflective to dissipative (Fig. 4.27 and 4.28). It was classified as dissipative because there was no berm development both times measured. The water line was higher in September. It shows that sand deposition was higher to the west side of the system during September in all areas of the beach. In March, deposition was higher to the west in the nearshore area, but not in the beach face.

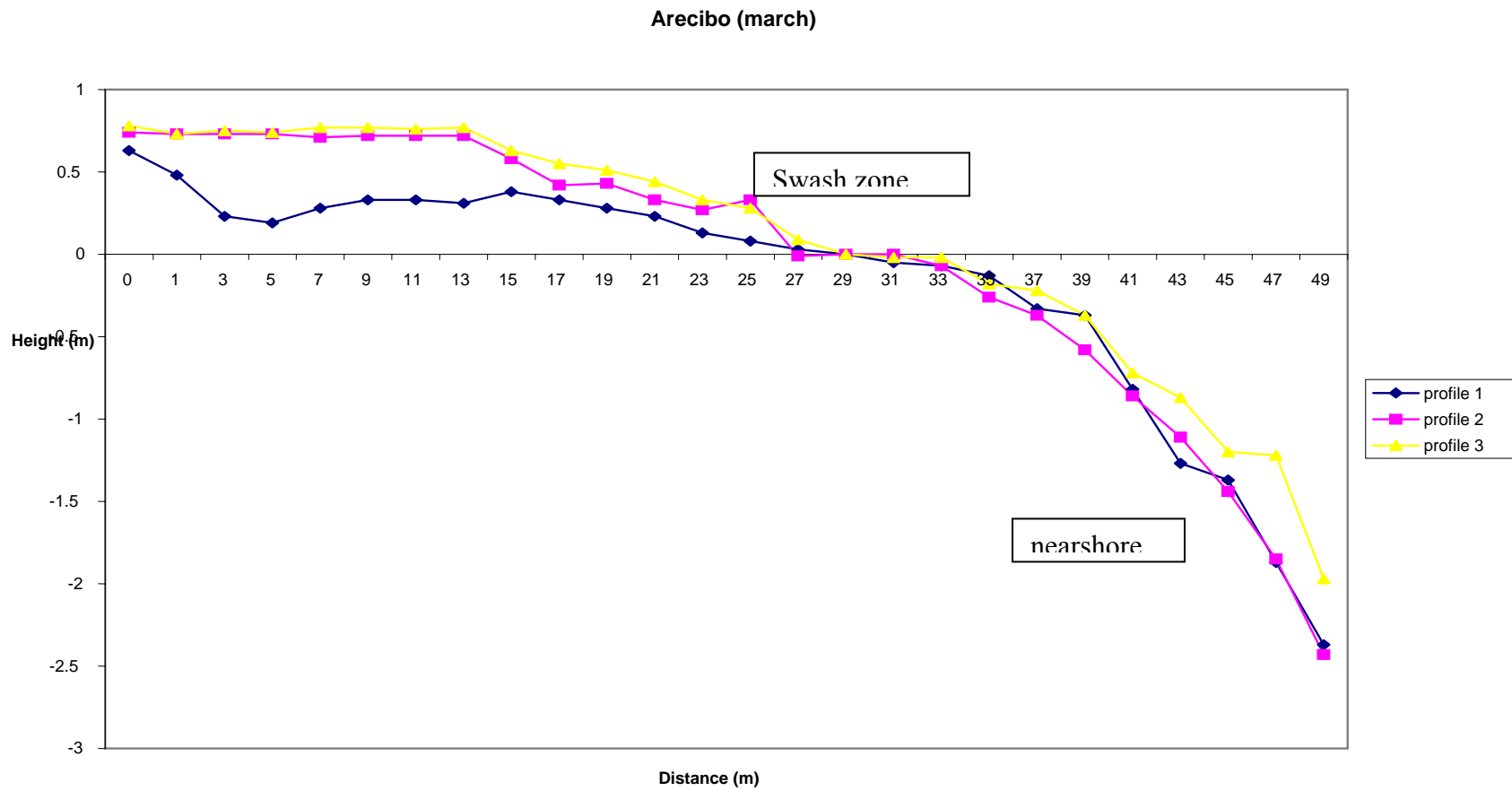


**Figure 4.27: Beach profiles for station SB4 during March 2003, classified as a dissipative beach.**

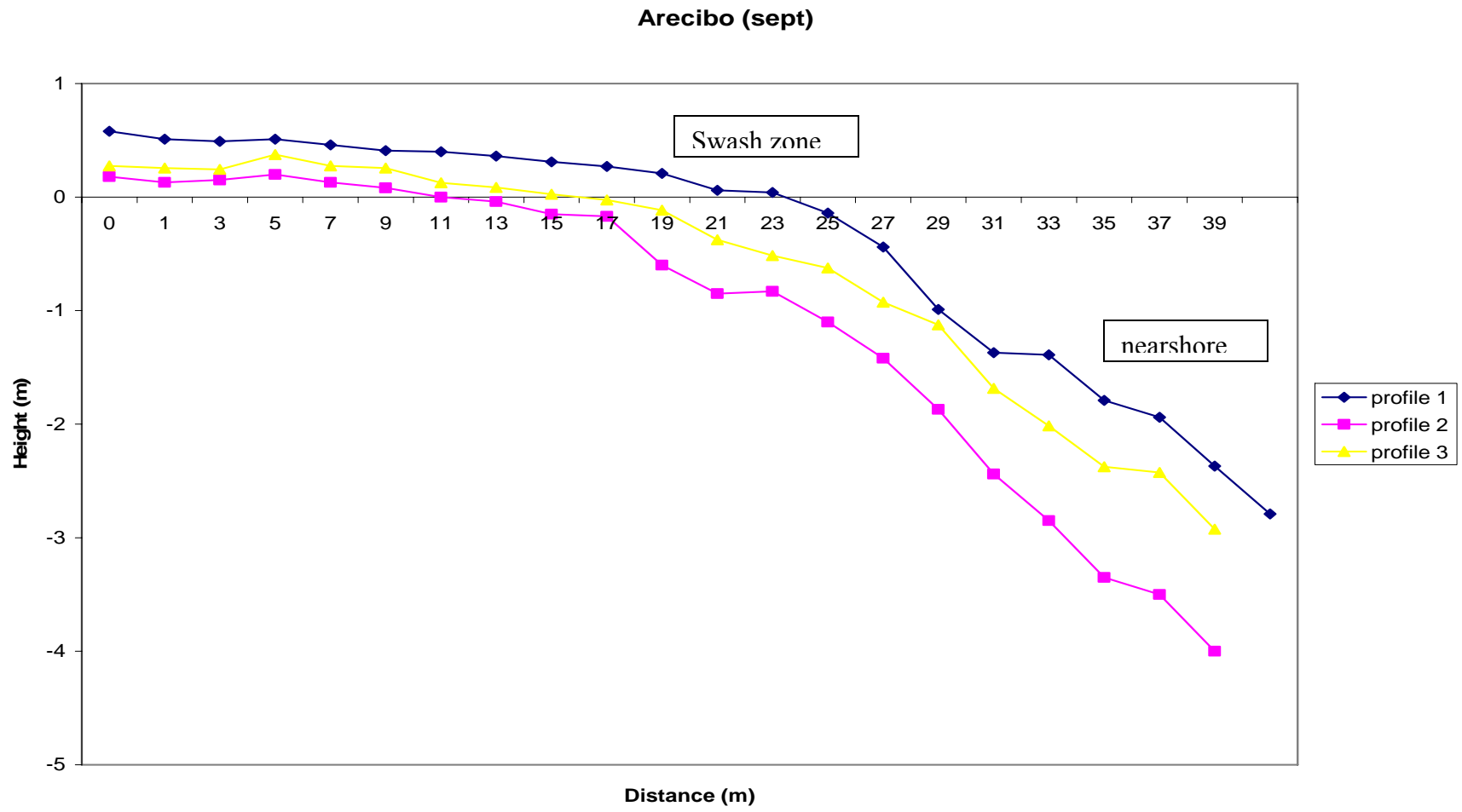


**Figure 4.28: Beach profiles for station SB4 during September 2003, classified as a dissipative beach.**

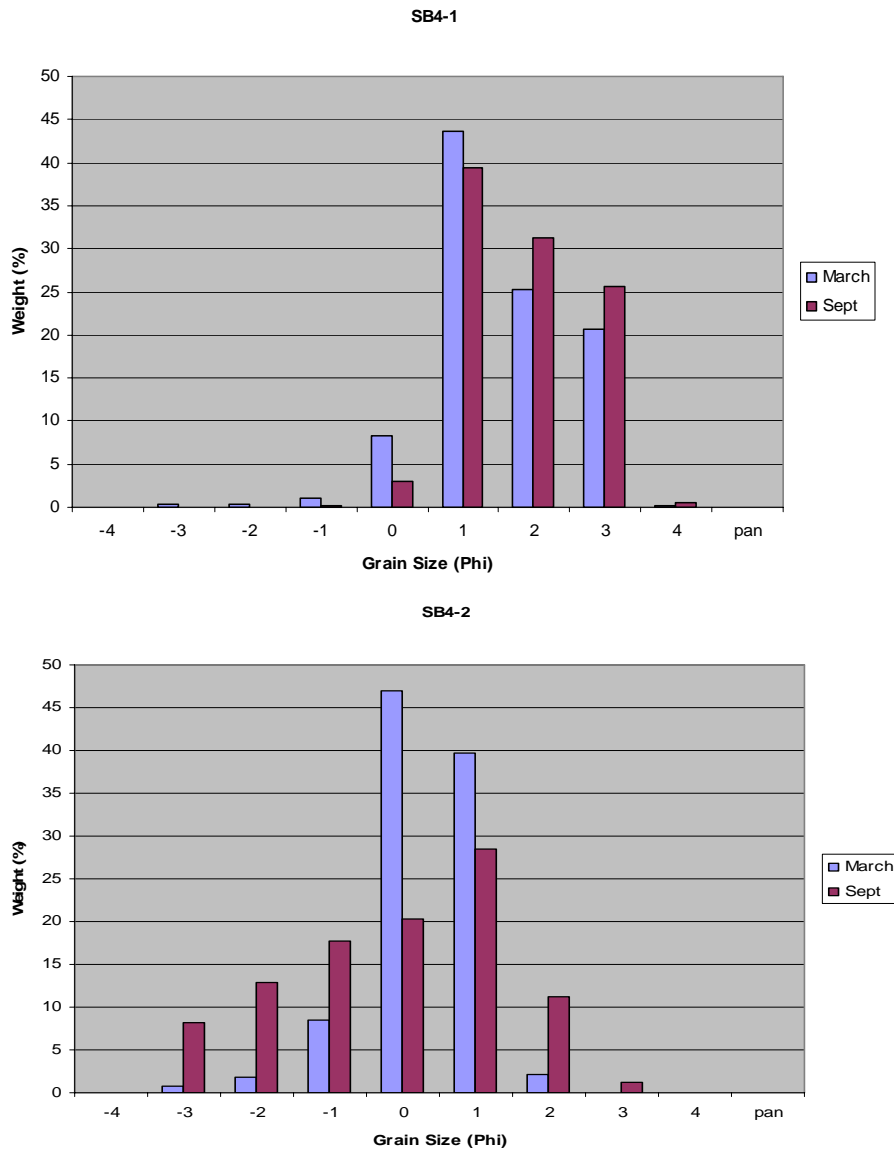


**Figure 4.29: Grain size comparison for station SB4 – Arecibo Port, P.R. (SB4-1: swash zone and SB4-2: nearshore)**

Sand samples were collected from the swash zone and nearshore. During September 2003, there was not much sand in the nearshore because beachrock was exposed. The granulometry of the area suggests that the wave energy is higher because the grain size ranges from coarse sand to medium sand (Fig. 4.29). This grain size distribution could be the result of high energy waves present in the surf zone. The cumulative curves show that the sediments are moderately sorted (Fig. 4.30). The grain composition of the beach was dominantly terrigenous, showing a slightly higher carbonate material percentage in September in the swash zone (figure 4.31).

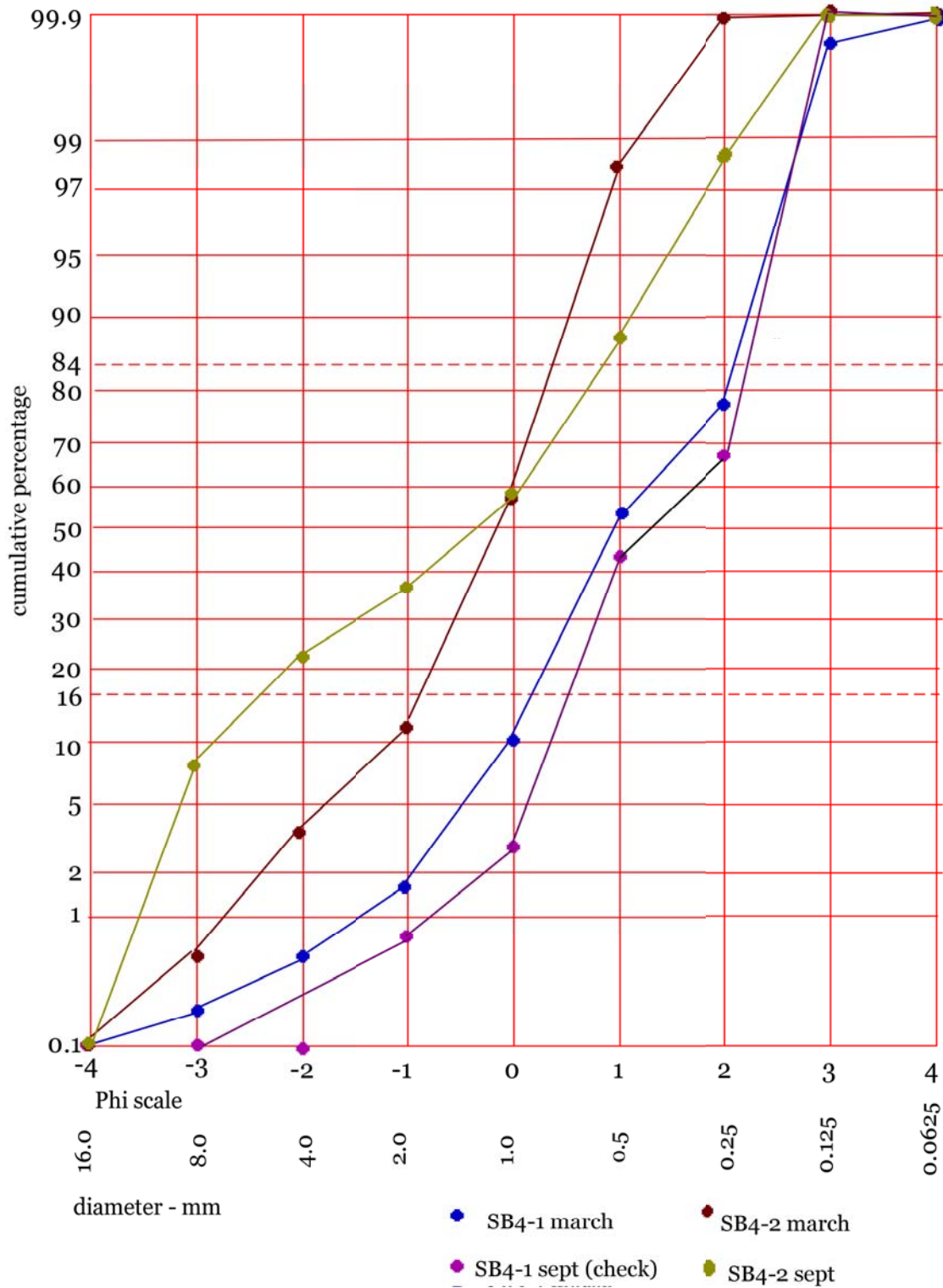


**Figure 4.30: Cumulative Curves for station SB4 (Arecibo Port, P.R.), showing moderately sorted grain distribution.**

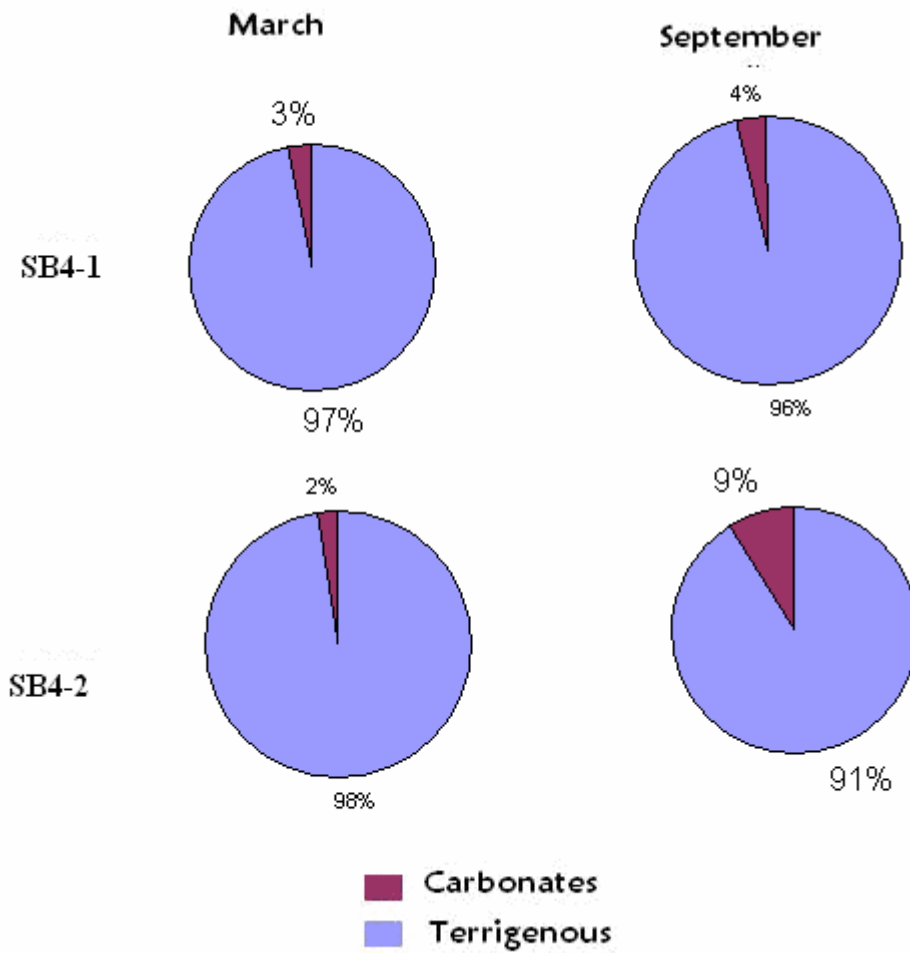
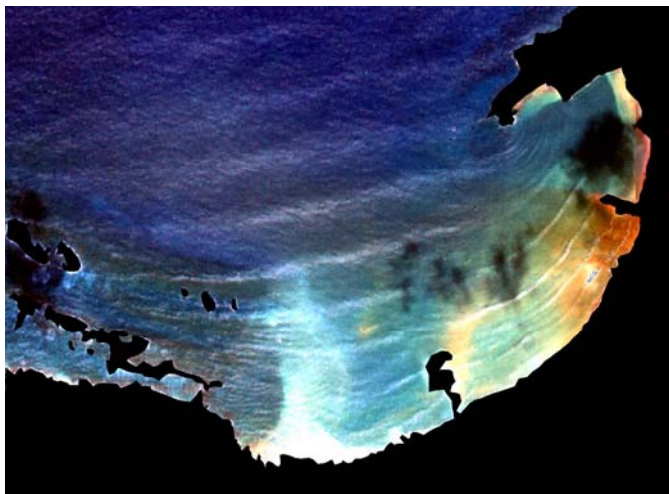
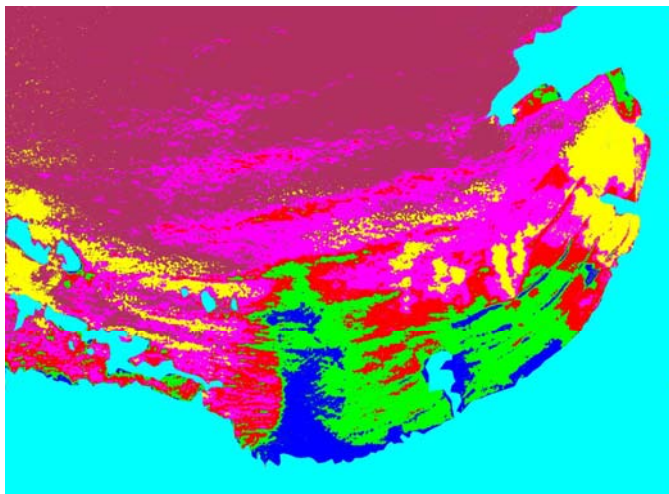


**Figure 4.31: Compositional Comparison for station SB4 – Arecibo Port, P.R.**

**(SB4-1: swash zone and SB4-2: nearshore).**



(a)



(b)

**Figure 4.32: IKONOS Satellite Images for station SB4 – Arecibo Port, PR. (a) Pre-processed image with mask (b) Minimum Distance Supervised Classification, and (c) ROI's Legend.**

**Legend:**

- Class 1: Cays
- Class 2: Sediment bottom (in between cays)
- Class 3: Sediment bottom
- Class 4: Clouds
- Class 5: Mask
- Class 6: Sediment bottom (deeper water)
- Class 7: Deep water

(c)

**Table 5: Radiance Values for supervised classification for station SB4.**

<b>Class Name</b>	<b>Radiance Value (Red Band)</b>	<b>Radiance Value (Green Band)</b>	<b>Radiance Value (Blue Band)</b>
Class 1	0.301370	0.833563	0.741258
Class 2	0.201264	0.949106	0.913462
Class 3	0.321391	1.119670	1.082747
Class 4	0.138040	0.499012	0.487637
Class 5	0	0	0
Class 6	0.105374	0.361761	0.250000
Class 7	0	0	0

In figure 4.32a, the presence of sand bodies is noticeable, but when classifications were attempted (Fig. 4.32b and 4.32c), the classes do not correlate as good as wanted. The radiance values for the satellite image ranged from 0.25 to 1.08 (Table 5). When comparing the original rgb satellite image with the band ratio blue over green image (Fig. 4.33), no assessment could be made because it gave a result with poor resolution. The water column and waves present interfere noticeably in this image.

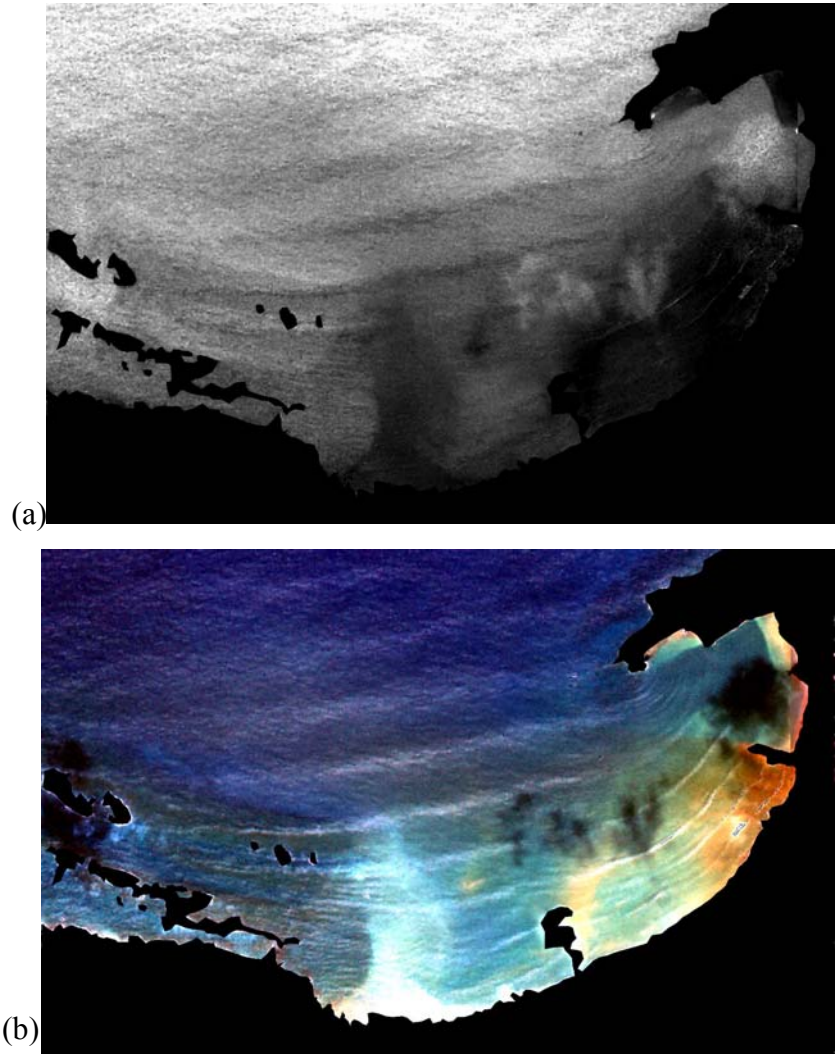


**Figure 4.33: (a) Blue over green band ratio compared to (b) rgb IKONOS satellite image for station SB4.**

## **4.5 Station SB5 – Camuy**

In station SB5, the profiles show this beach classification is dissipative (Fig. 4.34 and 4.35). There was no berm present in both seasons. Profile 2 was measured starting from a dune. This is why in both profiles that one is higher at the top of the beach face. Comparing profile 1 and 3 it is noticeable that sand deposition was higher in March. Sand movement seems to be to the west.

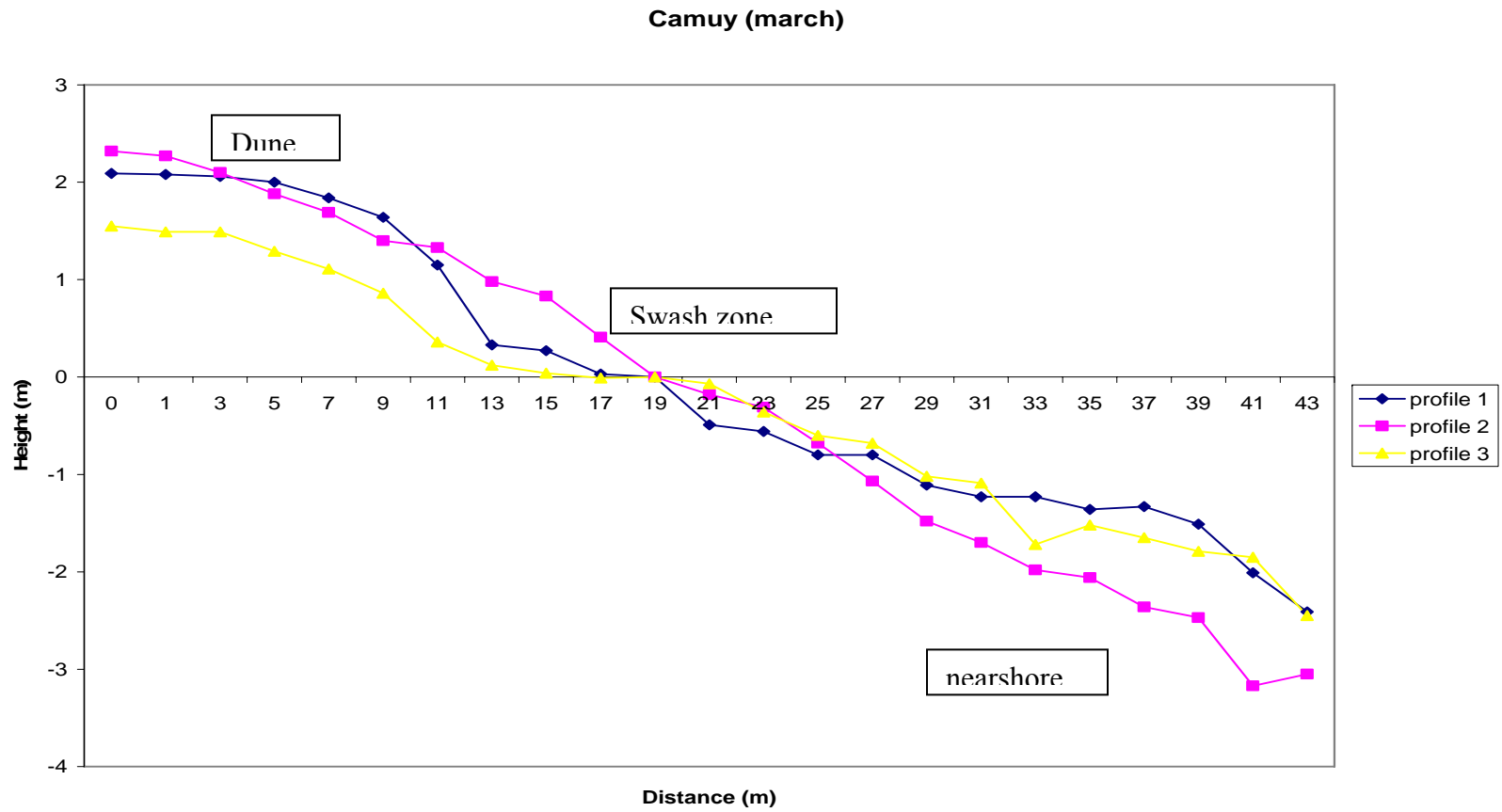


**Figure 4.34: Beach profiles for station SB5 during March 2003, classified as a dissipative beach.**

Camuy (sept)

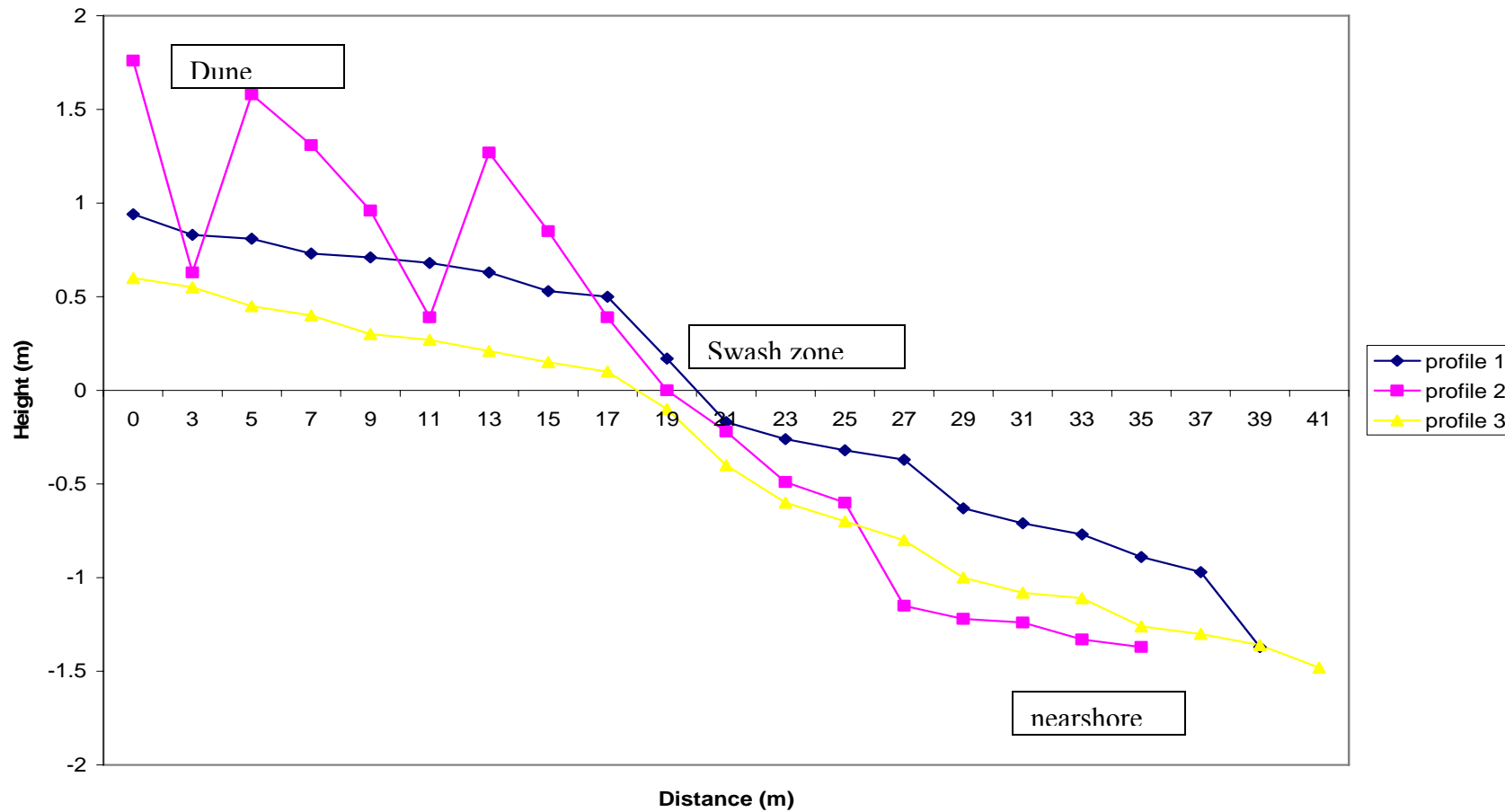
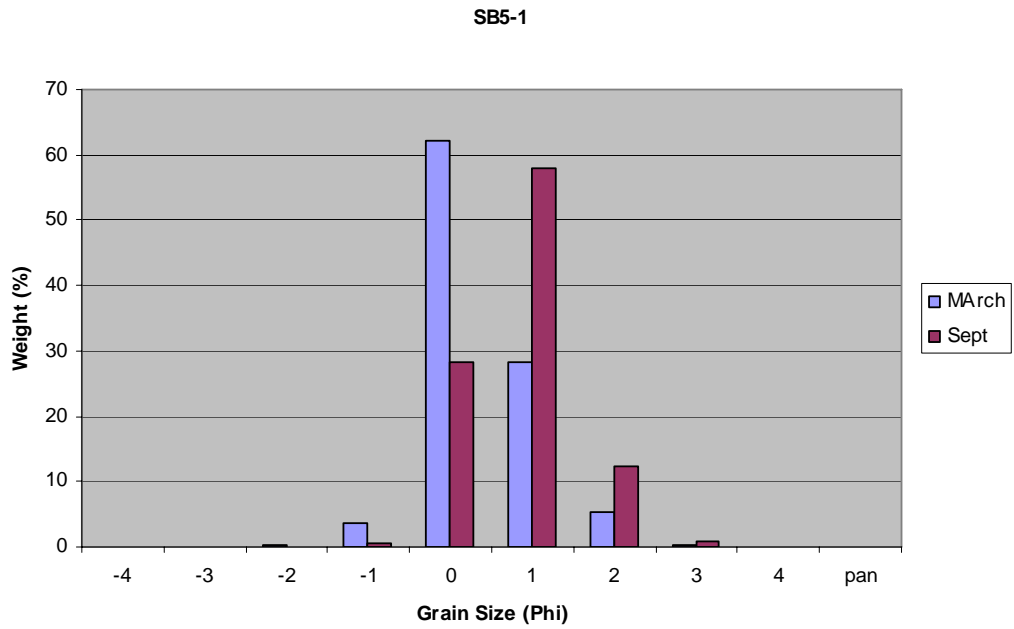
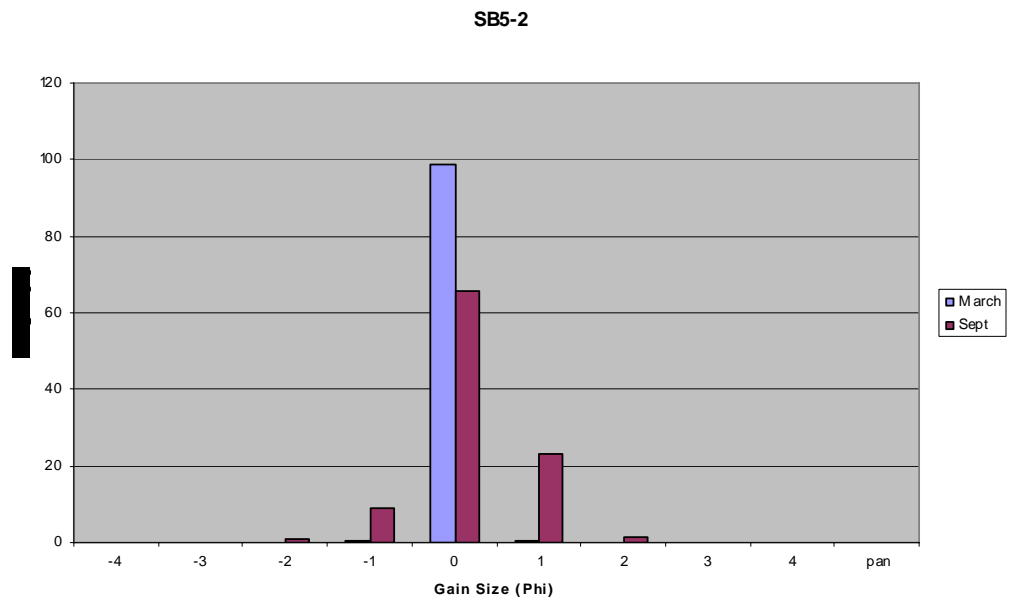


Figure 4.35: Beach profiles for station SB5 during September 2003, classified as a dissipative beach.



**Figure 4.36: Grain size comparison for station SB5-1– Camuy, P.R. dune.**



**Figure 4.37: Grain size comparison for station SB5-2 – Camuy, P.R. swash zone.**

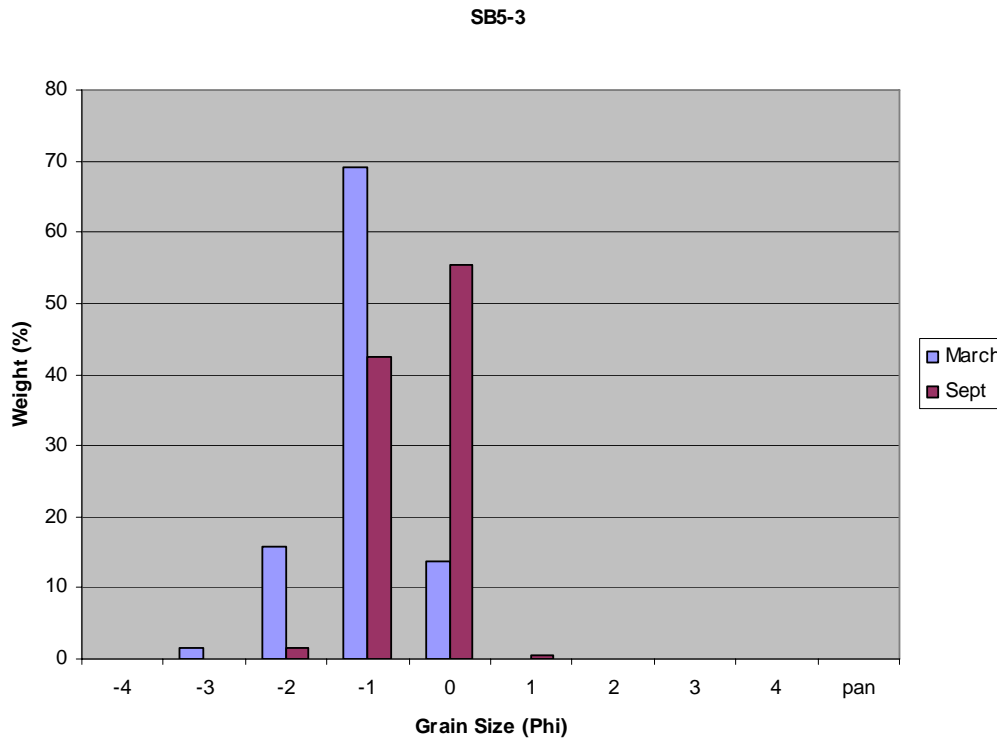


**Figure 4.38: Grain size comparison for station SB5-3 – Camuy, P.R. nearshore.**

The grain size measurements show grain sizes ranging from pebbles to medium sand (Fig. 4.36, 4.37 and 4.38). Distribution was the same for both seasons in the dune. The cumulative curves show that the sediments are well sorted (figure 4.39). This is seen by comparing the steep slopes of the curves in the graph. They all have the same shape, meaning that sand distribution is relatively the same throughout the beach. The grain composition was consistently more than 93% terrigenous (figure 4.40).

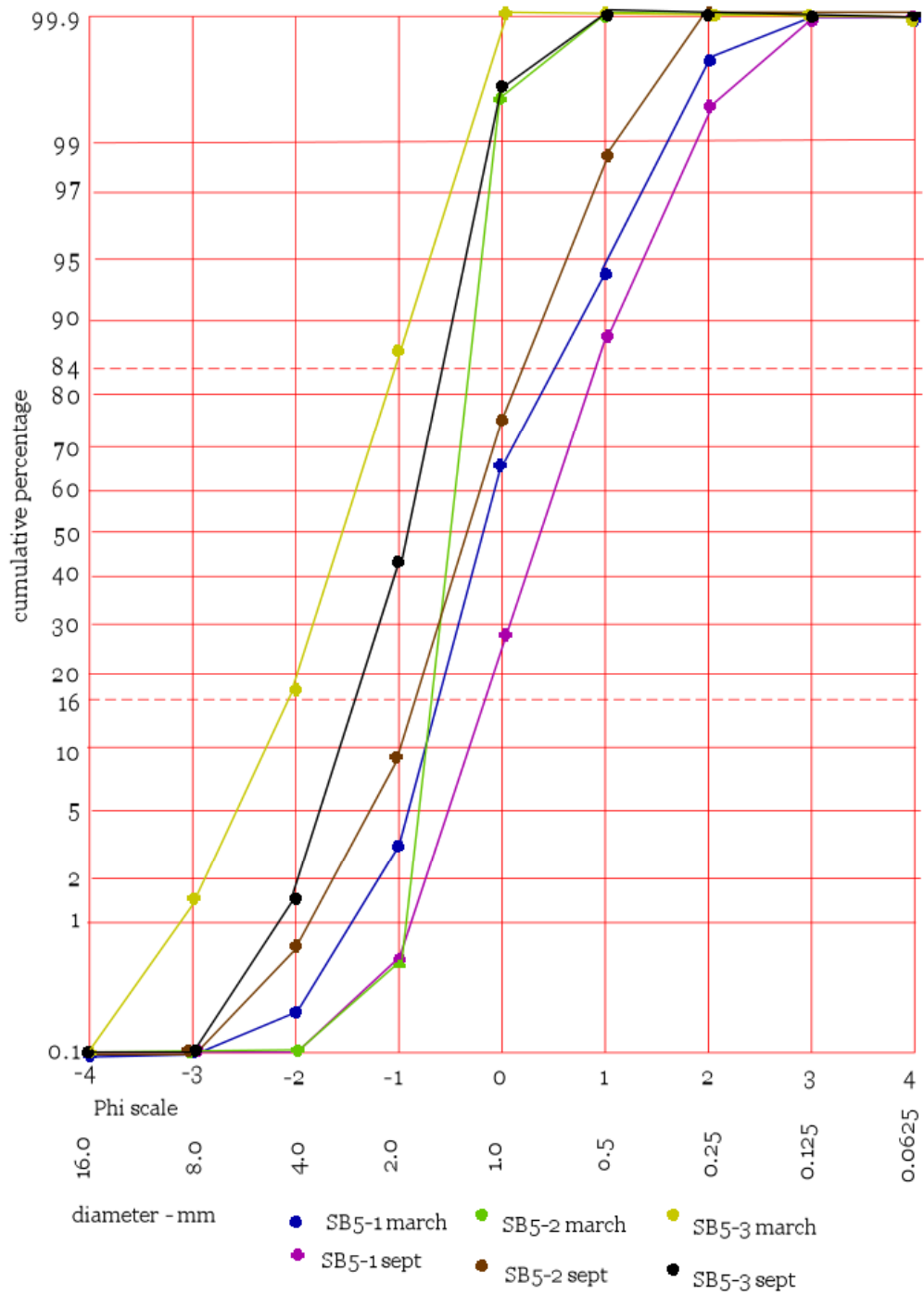


**Figure 4.39: Cumulative Curves for station SB5 (Camuy, P.R.), showing well sorted grain distribution.**

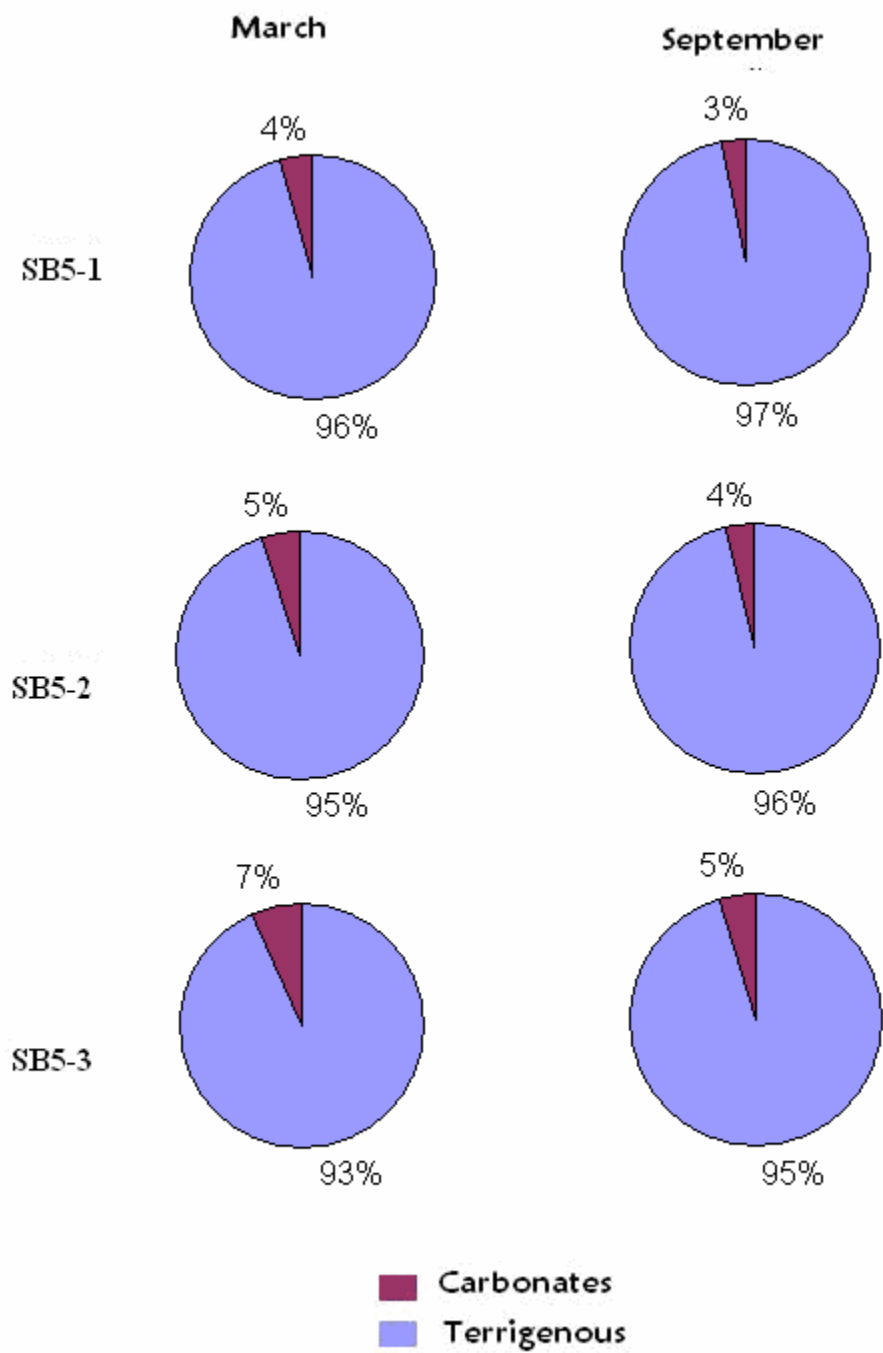
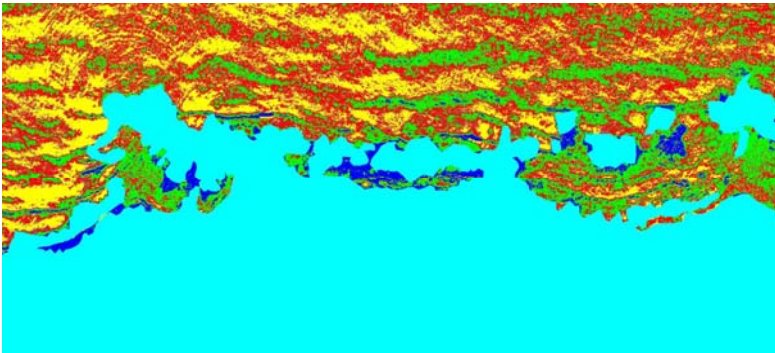


**Figure 4.40: Compositional comparison for station SB5 – Camuy, P.R.**  
 (SB5-1: dune, SB5-2: swash zone and SB5-4: nearshore).



(a)



(b)

**Figure 4.41: IKONOS Satellite Images for station SB5 – Camuy, PR. (a) Pre-processed image with mask (b) Minimum Distance Supervised Classification, and (c) ROI's Legend.**

**Legend:**

-  Class 1: Cays
-  Class 2: Sediment bottom (in between cays)
-  Class 3: Sediment bottom
-  Class 4: Clouds
-  Class 5: Mask
-  Class 6: Sediment bottom (deeper water)
-  Class 7: Deep water

(c)

**Table 6: Radiance Values for supervised classification for station SB5.**

<b>Class Name</b>	<b>Radiance Value (Red Band)</b>	<b>Radiance Value (Green Band)</b>	<b>Radiance Value (Blue Band)</b>
Class 1	0.177028	0.946355	1.101648
Class 2	0.225501	1.074278	1.293956
Class 3	0.704953	1.752407	1.730769
Class 4	0.20946	0.738652	0.949516
Class 5	0	0	0
Class 6	0.218124	0.84124	1.008242
Class 7	0	0	0

In figure 4.41a, the presence of sand bodies is noticeable, but when classifications were attempted (Fig. 4.41b and 4.41c), the classes do not correlate as good as wanted. The radiance values for the satellite image ranged from 1.00 to 1.73 (Table 6). When comparing the original rgb satellite image with the band ratio blue over green image (figure 4.42), no assessment could be made because it gave a result with poor resolution. The water column and waves present interfere noticeably in this image.

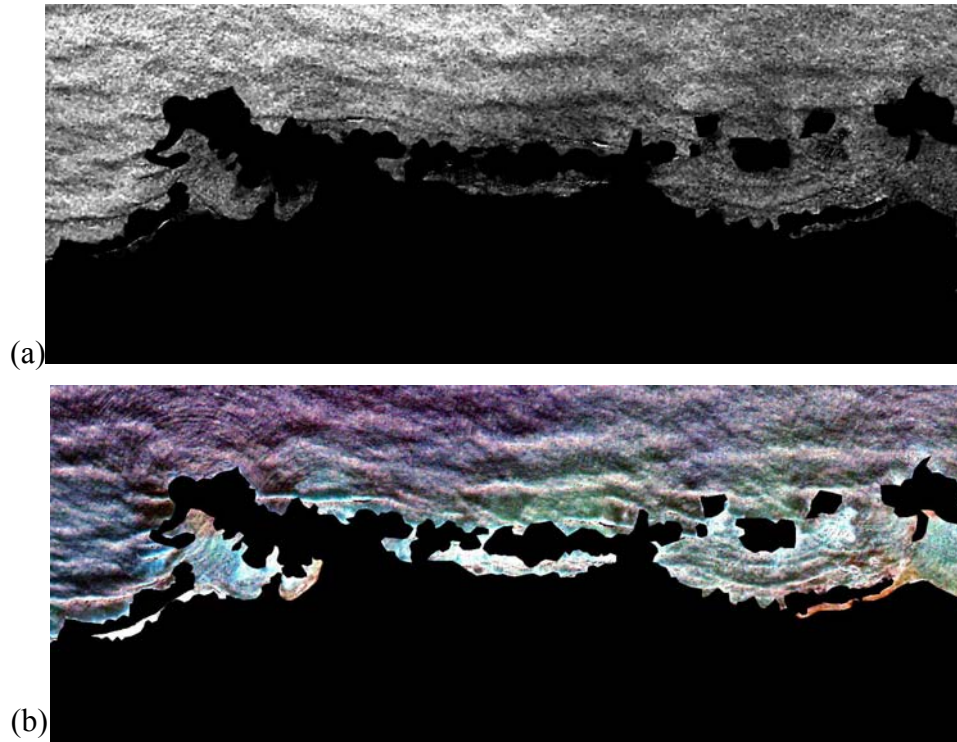


**Figure 4.42: (a) Blue over green band ratio compared to (b) rgb IKONOS satellite image for station SB5.**

## **4.6 Station SB6 – Jobos, Isabela**

In station SB6, the beach profiles show a beach system that varies in classification from reflective to dissipative (Fig. 4.43 and 4.44). It shows berm development in March, but none in September. The water line was higher and it had a steeper beach face in September. Sand deposition is higher in the beach face area in to the west of the system in September. In the nearshore area, sand deposition is higher to the west in September also. Sand movement seems to be to the west of the system in March, but to the right in September in the beach face area. In the nearshore area there seems to be no dominant direction for sand movement March, but is to the west in September.

### Isabela (march)

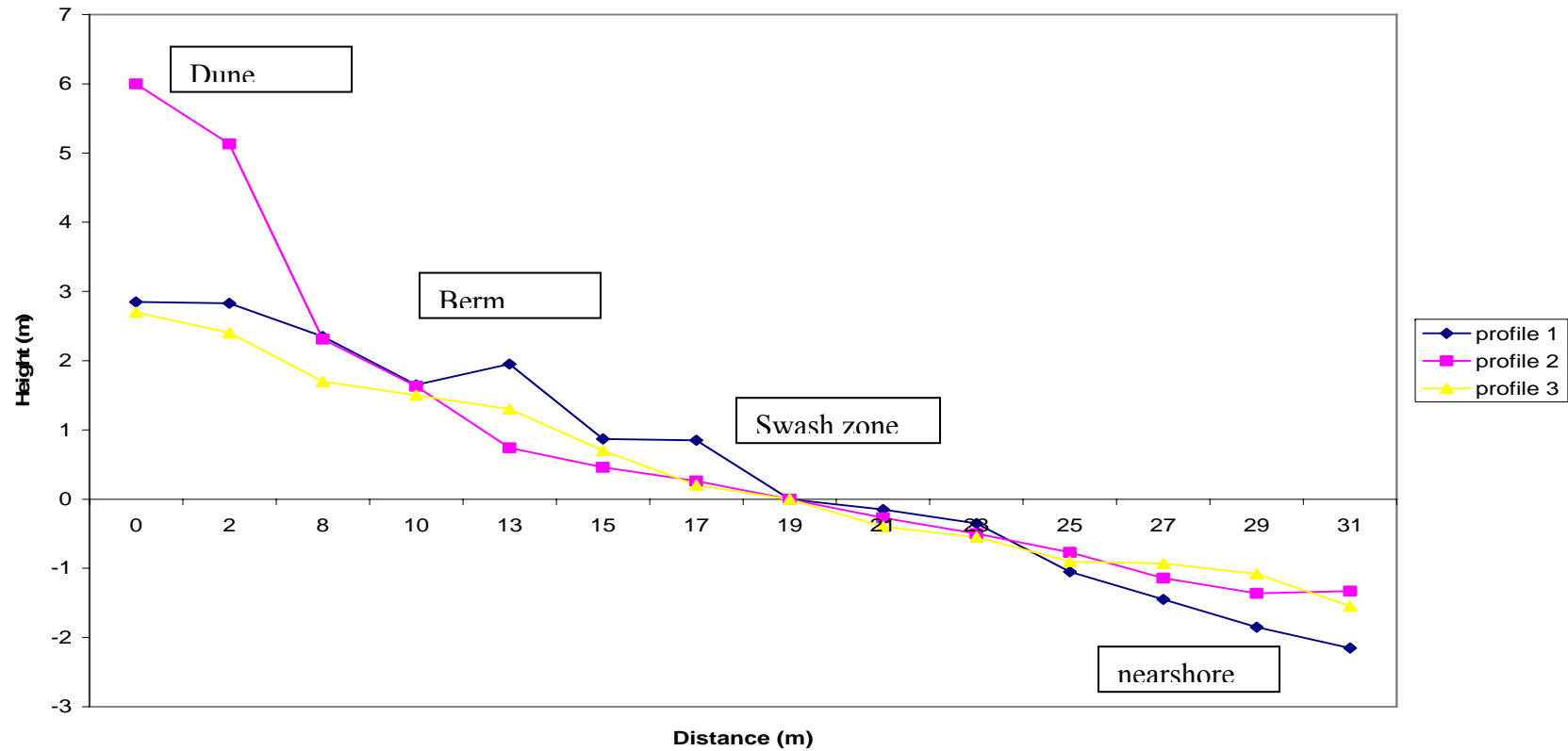
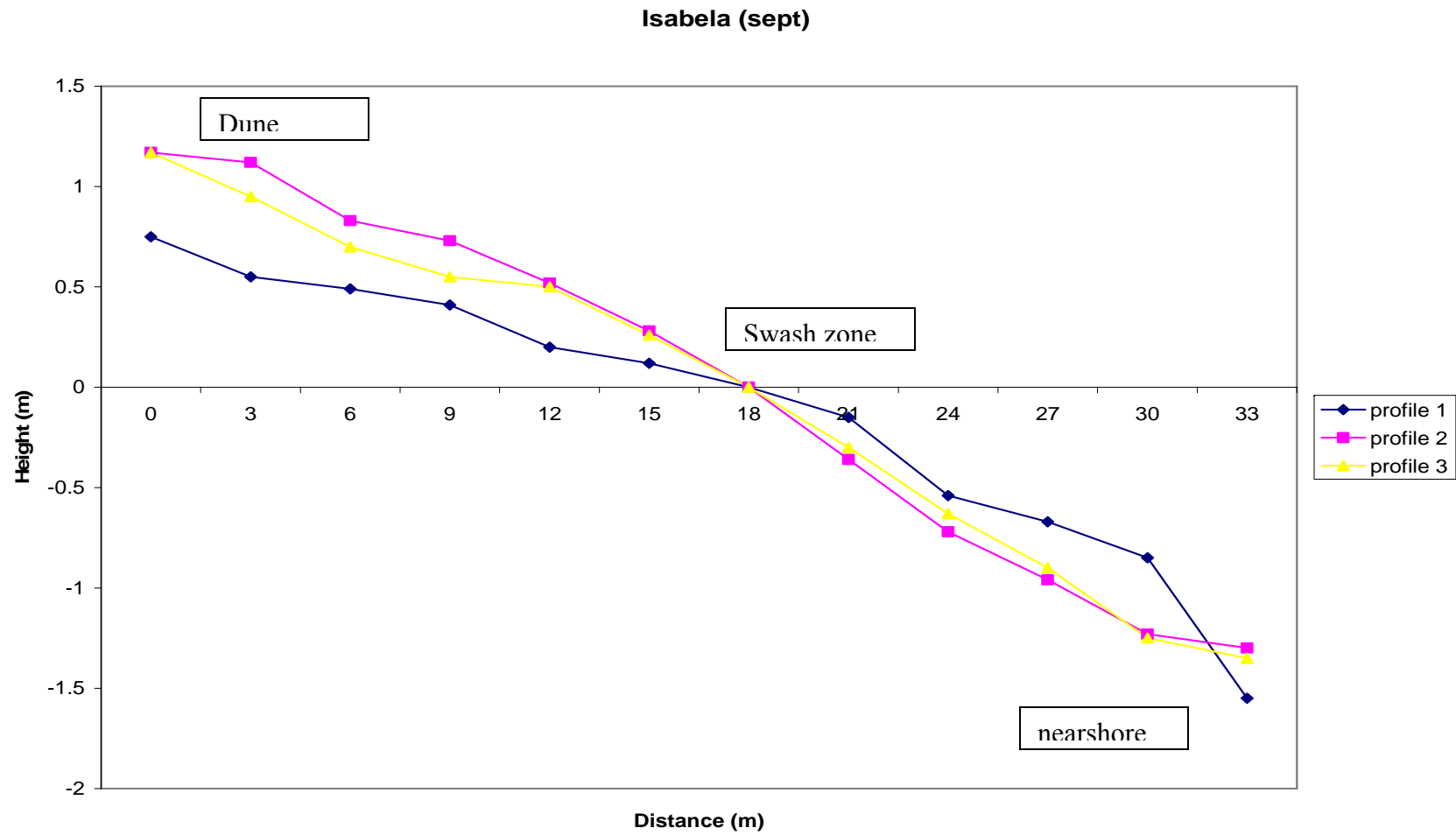
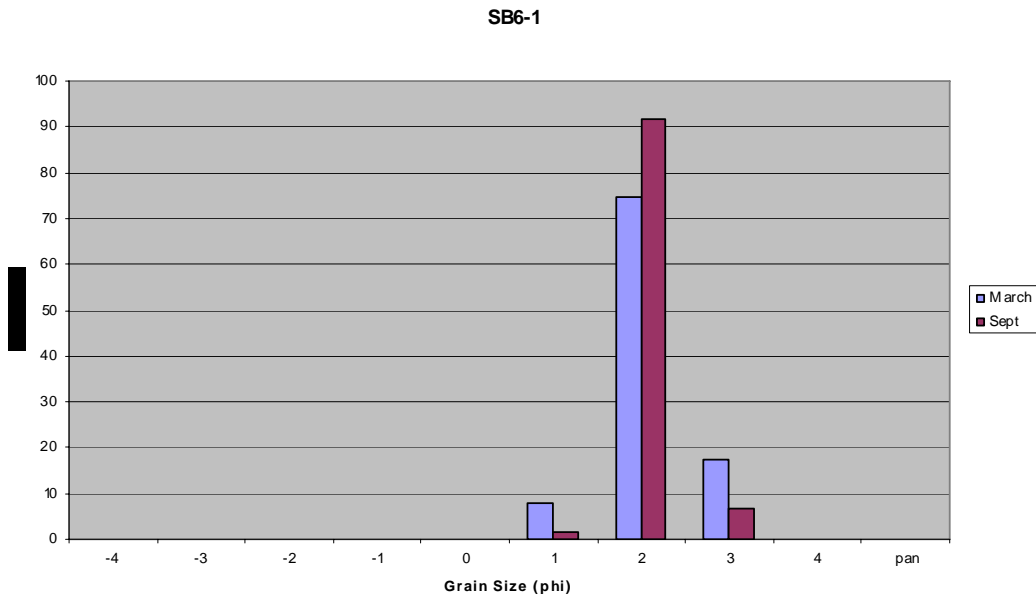


Figure 4.43: Beach profiles for station SB6 for March 2003, classified as a reflective beach.



**Figure 4.44: Beach Profiles for station SB6 during September 2003, classified as a dissipative beach.**



**Figure 4.45: Grain size comparison for station SB6-1 – Jobos (Isabela), P.R. dune.**

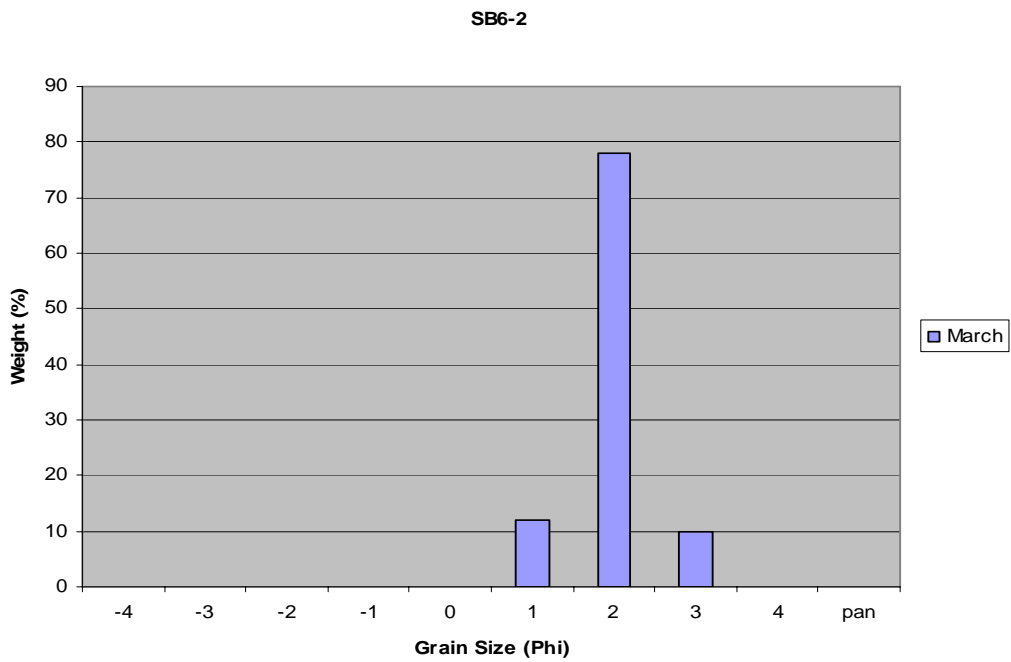


**Figure 4.46: Grain size comparison for station SB6-2 – Jobos (Isabela), P.R. berm.**

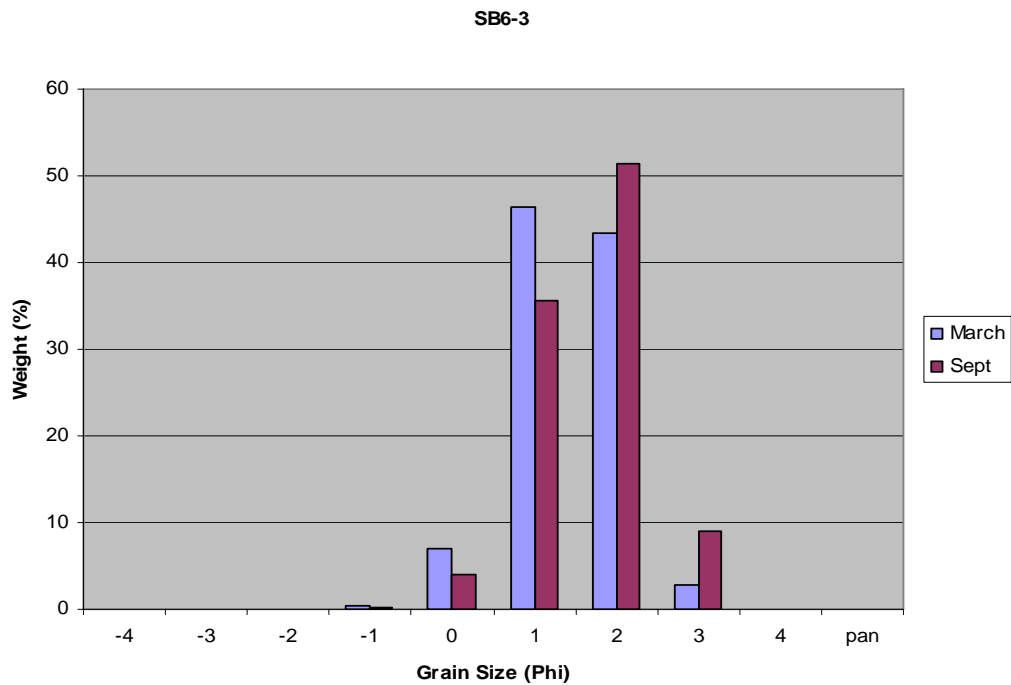


**Figure 4.47: Grain size comparison for station SB6-3 – Jobos (Isabela), P.R. swash zone.**

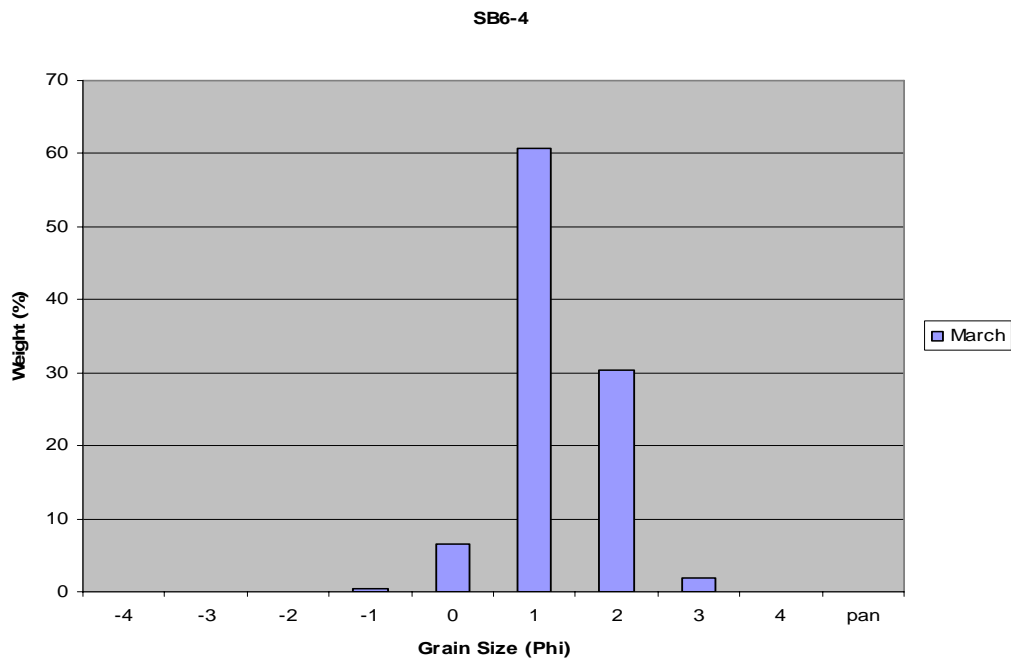


**Figure 4.48: Grain size comparison for station SB6-4 – Jobos (Isabela), P.R. nearshore.**

Sand samples were taken from the sand dune, the berm, the swash zone and in the nearshore. Grain sizes in the dune and the berm range from fine to very fine sand, this suggests low energy in the area (Fig. 4.45 and 4.46). In the swash zone and the nearshore the grain size ranged from coarse to medium sand (Fig. 4.47 and 4.48). No sand sample was collected for the near shore area in September because it was exposed beachrock. The cumulative curves show that the sediments are moderately sorted (figure 4.49). The grain composition showed that terrigenous sediments dominate in both seasons throughout the system (figure 4.50).

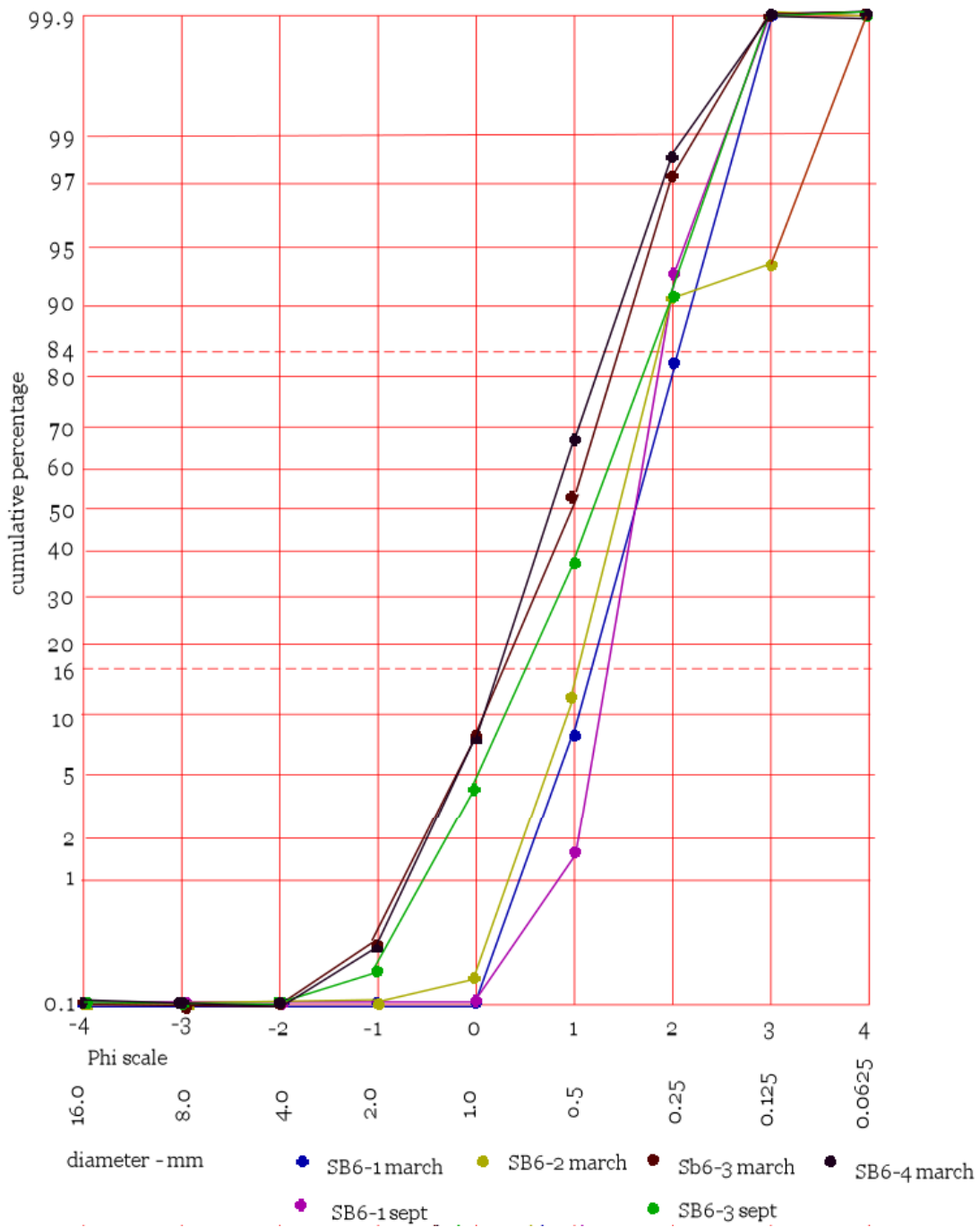


**Figure 4.49: Cumulative Curves for station SB6 (Jobos Isabela, P.R.), showing moderately sorted grain distribution.**

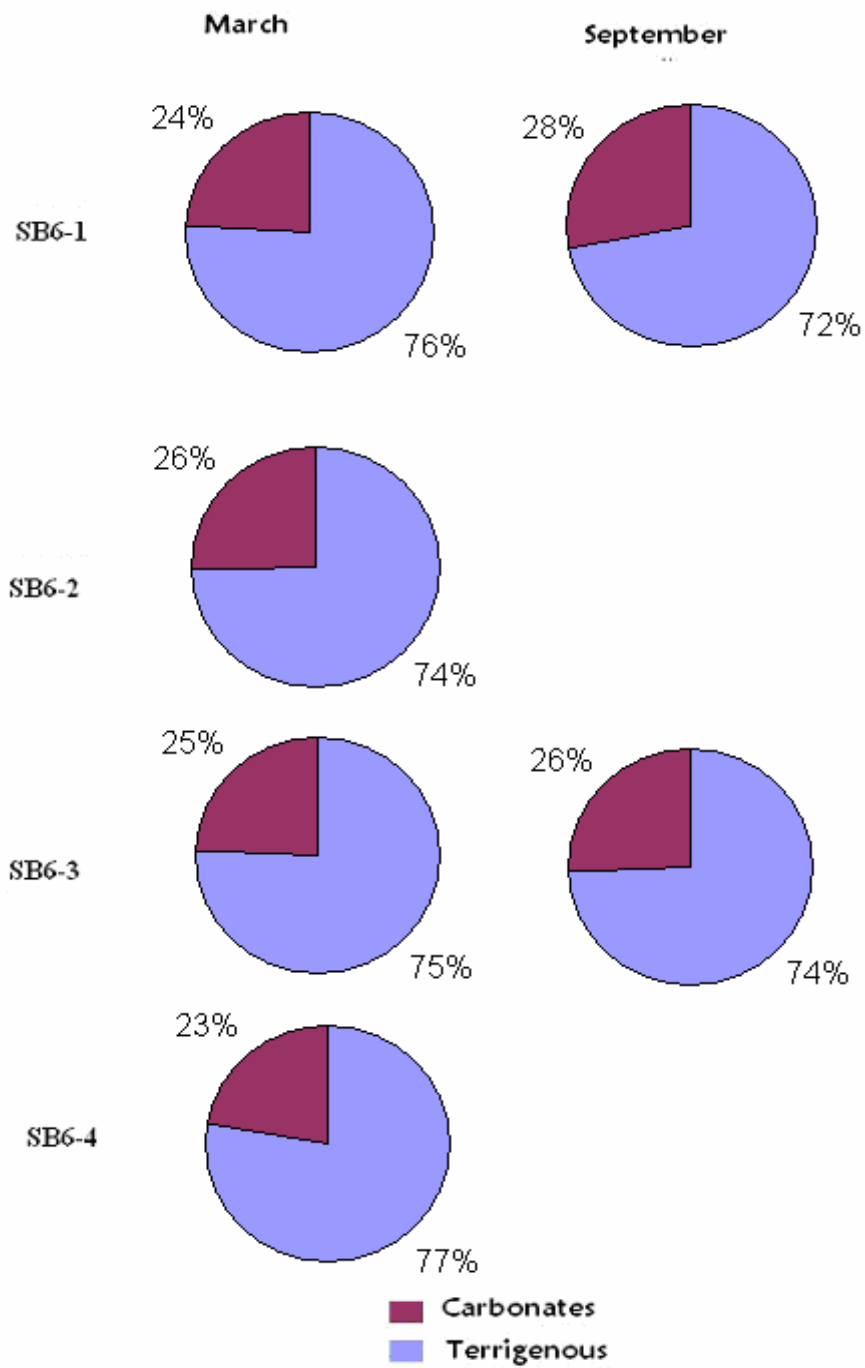
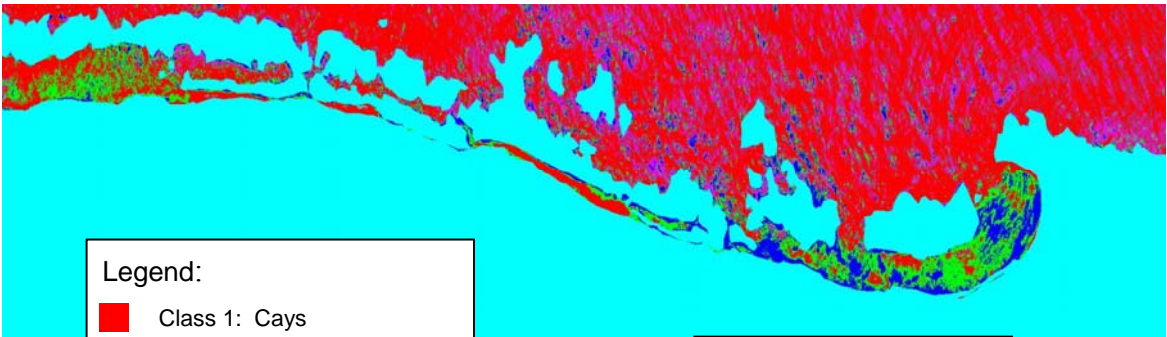
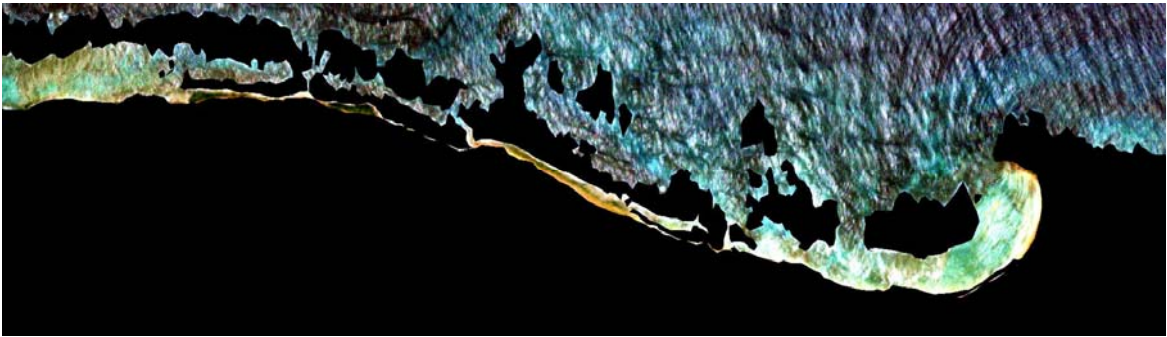


**Figure 4.50: Compositional comparison for station SB6 – Jobos (Isabela), P.R.**

(SB6-1: dune, SB6-2: berm, SB6-3: swash zone and SB6-4: nearshore).



Legend:

- Class 1: Cays
- Class 2: Sediment bottom (in between cays)
- Class 3: Sediment bottom
- Class 4: Clouds
- Class 5: Mask
- Class 6: Sediment bottom (deeper water)
- Class 7: Deep water

(c)

**Figure 4.51: IKONOS Satellite Images for station SB6 – Jobos, Isabela PR. (a) Pre-processed image with mask (b) Minimum Distance Supervised Classification, and (c) ROI's Legend.**

**Table 7: Radiance Values for supervised classification for station SB6.**

<b>Class Name</b>	<b>Radiance Value (Red Band)</b>	<b>Radiance Value (Green Band)</b>	<b>Radiance Value (Blue Band)</b>
Class 1	0.200211	0.643741	0.692308
Class 2	0.238145	0.803301	0.916209
Class 3	0.321391	1.001376	1.129121
Class 4	0	0	0
Class 5	0	0	0
Class 6	0.330875	0.674003	1.010989
Class 7	0.145416	0.594223	0.828297

In figure 4.51a, the presence of sand bodies is noticeable, but when classifications were attempted (Fig. 4.51b and 4.51c), the classes do not correlate as good as wanted. The radiance values for the satellite image ranged from 0.91 to 1.12 (Table 7). When comparing the original rgb satellite image with the band ratio blue over green image (Fig. 4.52), no assessment could be made because it gave a result with poor resolution. The water column and waves present interfere noticeably in this image.

In Barreto 1997 the same beach system was studied. The benchmark used in this study is actually the one created by Barreto. The radiance values reported from the landsat-7 satellite image ranged from 0 to 10.38. The beach was classified as transitional and sediments were classified as well sorted.

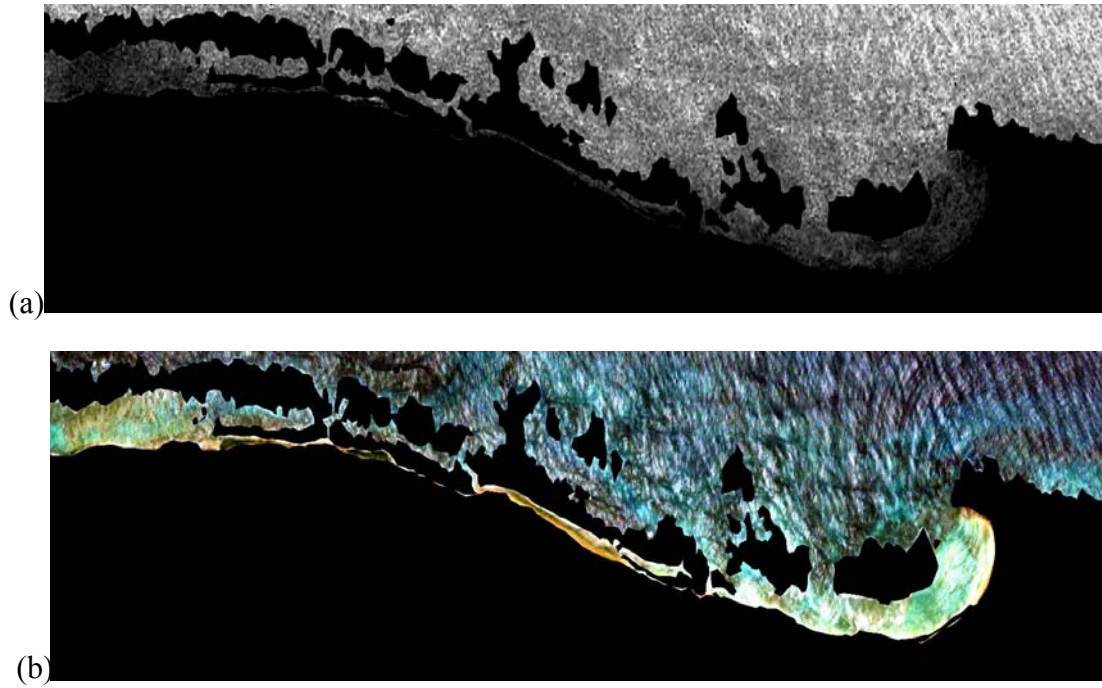


**Figure 4.52: (a) Blue over green band ratio compared to (b) rgb IKONOS satellite image for station SB6.**

## **4.7 Station SB7 – Punta Borinquen, Aguadilla**

In station SB7, the profiles show the beach system varies in classification from reflective to dissipative (Fig. 4.53 and 4.54). It was reflective in March because it had berm development, but dissipative in September because of lack of it. Sand deposition seems higher to the west of the system in March, mostly along the berm area. During September, sand deposition seems to be about the same along all the system. The water line was higher and the beach face slope was steeper in September.

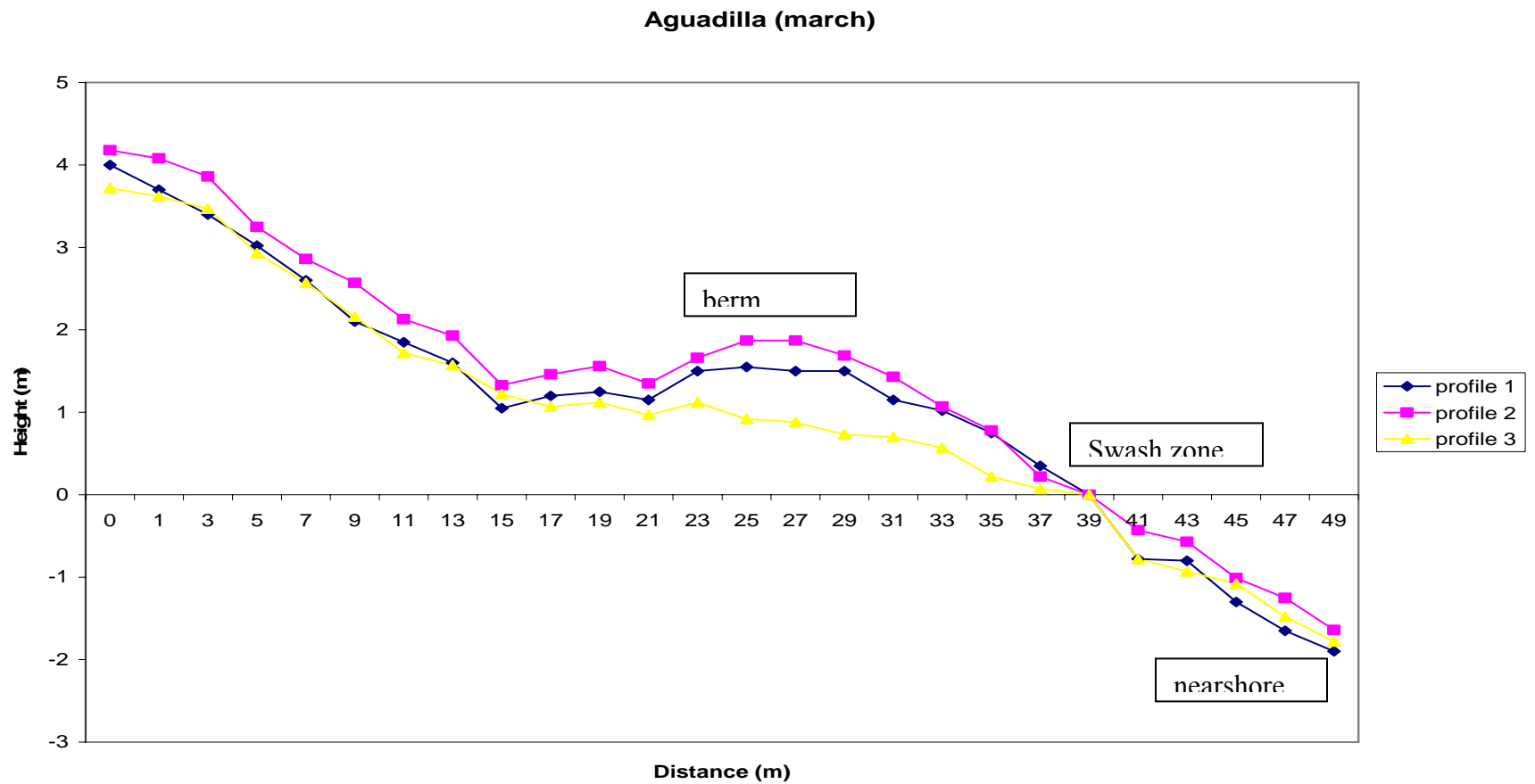


**Figure 4.53: Beach profiles for station SB7 during March 2003, classified as a reflective beach.**

### Aguadilla (sept)

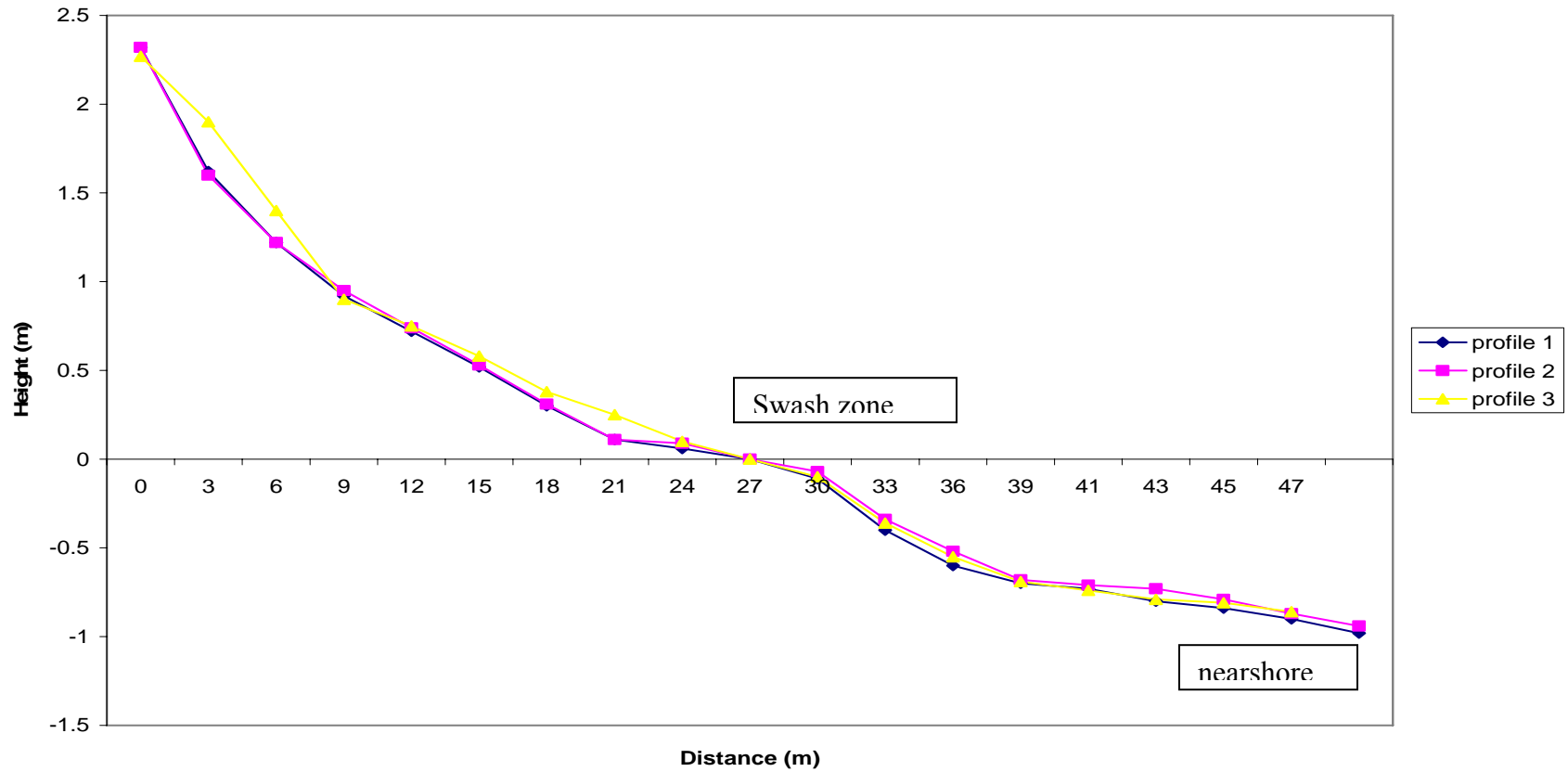
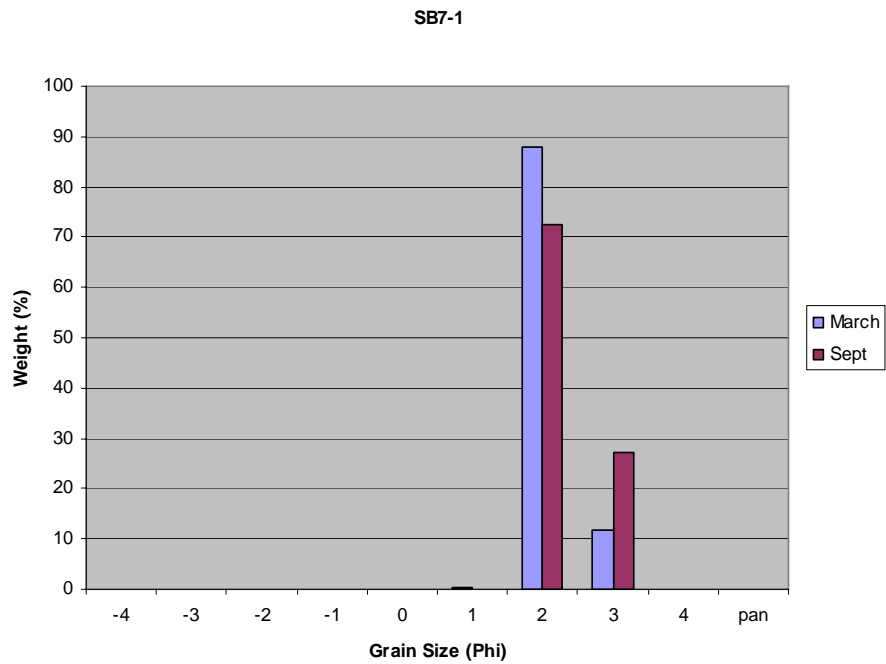
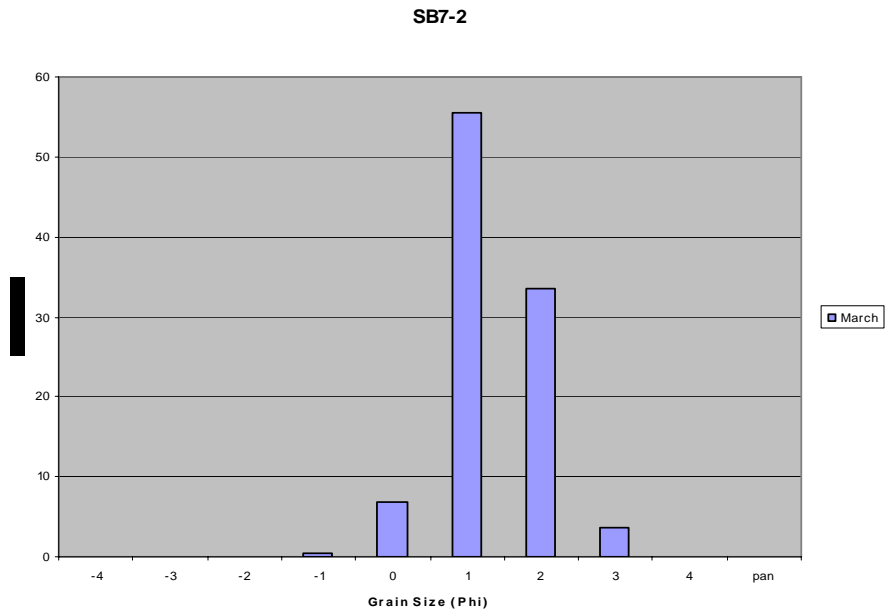


Figure 4.54: Beach profiles for station SB7 during September 2003, classified as a dissipative beach.



**Figure 4.55: Grain size comparison for station SB7-1 – Punta Borinquen (Aguadilla), P.R. dune.**



**Figure 4.56: Grain Size Comparison for station SB7-2 – Punta Borinquen (Aguadilla), P.R. berm.**

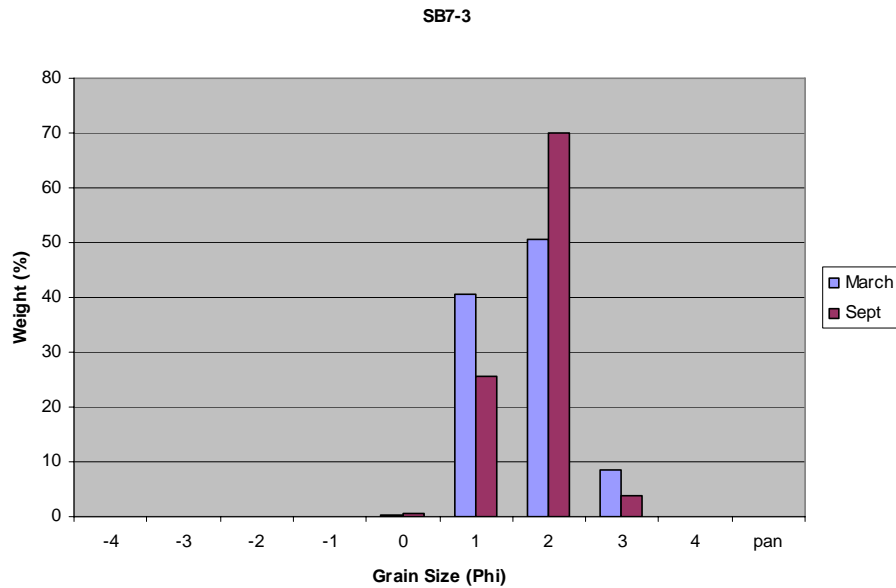


**Figure 4.57: Grain size comparison for station SB7-3 – Punta Borinquen (Aguadilla), P.R. swash zone.**

The granulometry showed there is high wave energy because the grain size ranged from coarse sand to very fine sand (Fig. 4.55, 4.56 and 4.57). The grain size distribution seems to be constant during both seasons. The cumulative curves show that the sediments are well sorted (figure 4.58). The grain composition is dominantly terrigenous throughout the system in both seasons (figure 4.59).

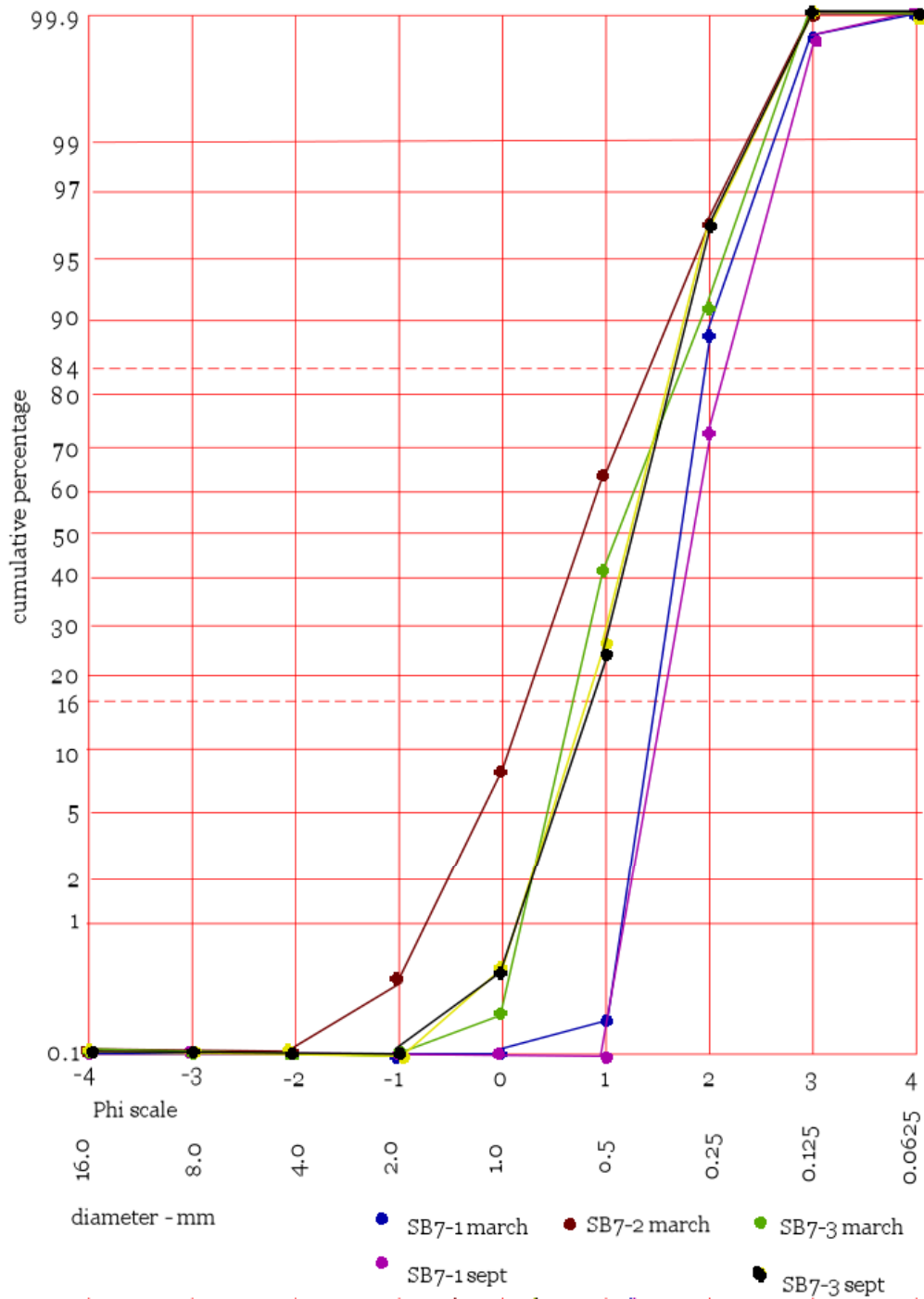


**Figure 4.58: Cumulative Curves for station SB7 (Punta Borinquen Aguadilla, P.R.), showing well sorted grain distribution.**

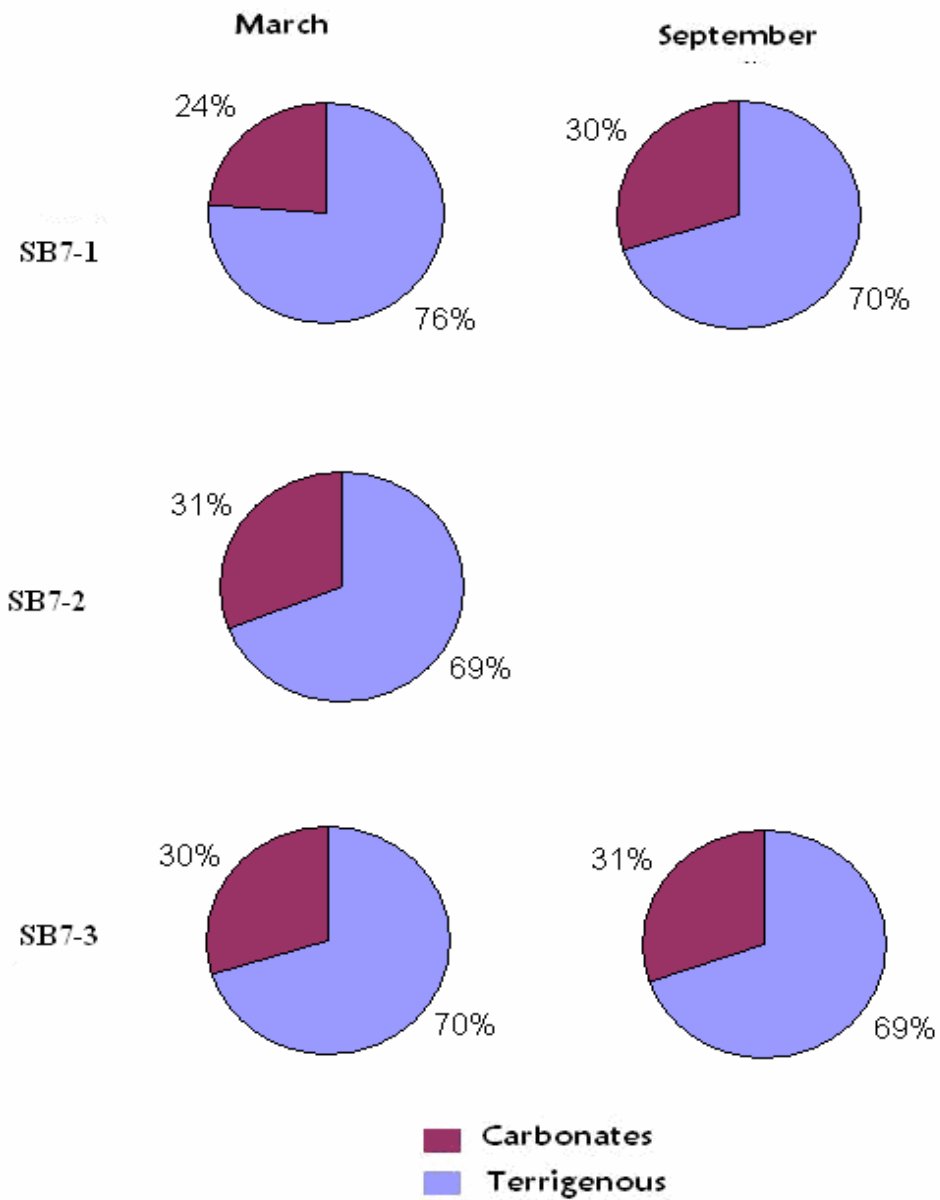


**Figure 4.59: Compositional Comparison for station SB7 – Punta Borinquen (Aguadilla), P.R. (SB7-1: dune, SB7-2: berm, SB7-3: swash zone).**

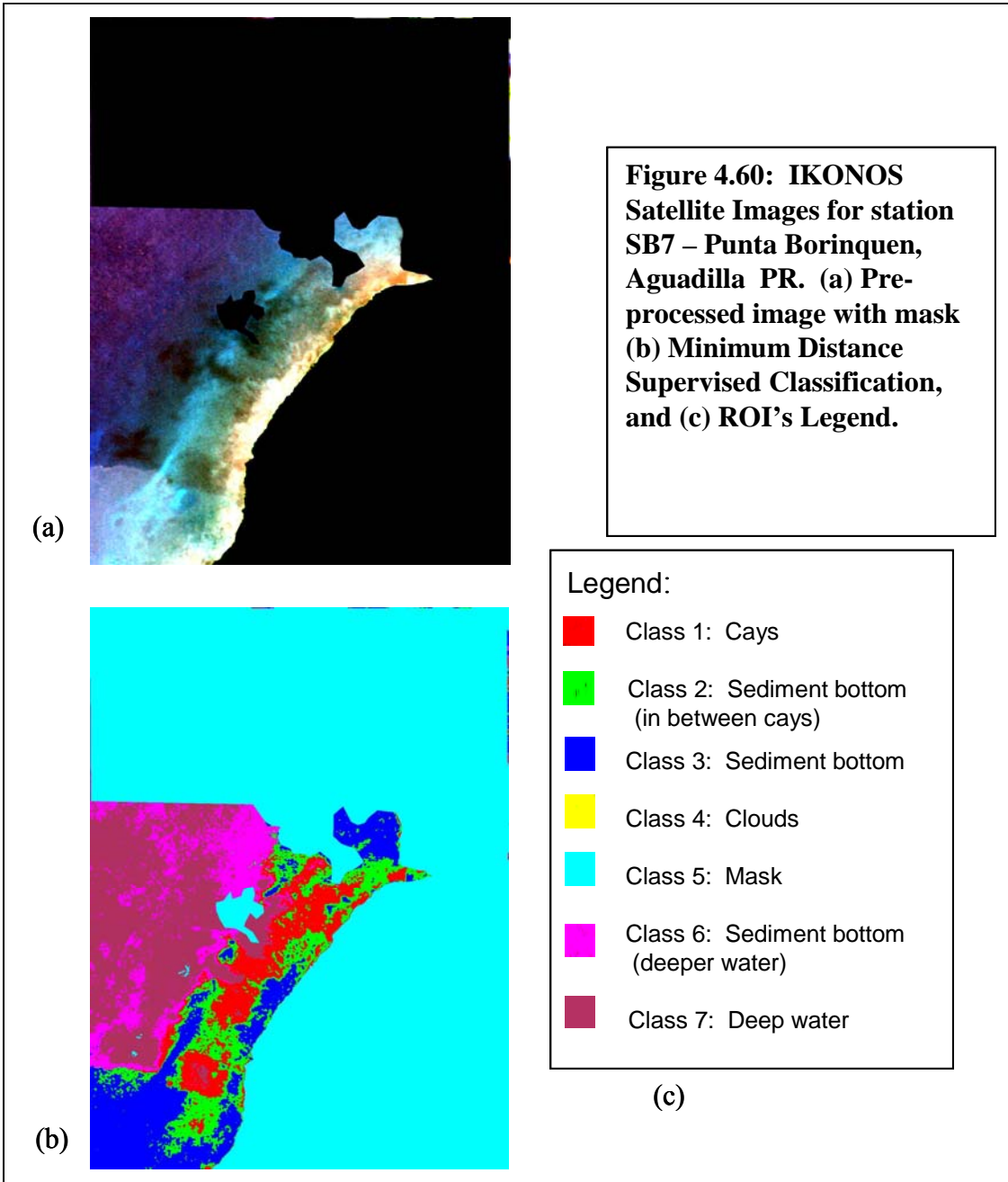


**Table 8: Radiance Values for supervised classification for station SB7**

<b>Class Name</b>	<b>Radiance Value (Red Band)</b>	<b>Radiance Value (Green Band)</b>	<b>Radiance Value (Blue Band)</b>
Class 1	0.037935	0.158184	0.269231
Class 2	0.044257	0.217331	0.331044
Class 3	0.040042	0.246217	0.388736
Class 4	0	0	0
Class 5	0	0	0
Class 6	0.020021	0.110041	0.310440
Class 7	0.010537	0.108666	0.218407

In figure 4.60a, the presence of sand bodies is noticeable, but when classifications were attempted (Fig. 4.60b and 4.60c), the classes do not correlate as good as wanted. The radiance values for the satellite image ranged from 0.31 to 0.38 (Table 8). When comparing the original rgb satellite image with the band ratio blue over green image (Fig. 4.61), no assessment could be made because it gave a result with poor resolution. The water column and waves present interfere noticeably in this image.

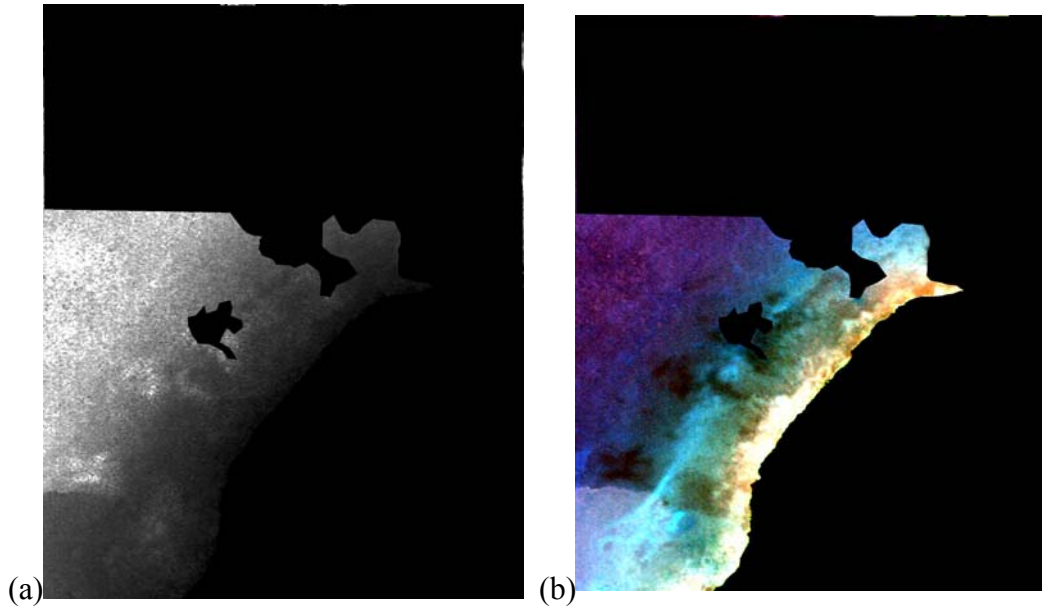


**Figure 4.61: Blue over green band ratio compared to rgb IKONOS satellite image for station SB7.**

## CHAPTER 5: DISCUSSION

### 5.1 Beach Profile Interpretation

Based on Figures 4.1 and 4.2, the Isla de Cabras (SB1) beach system was categorized as a reflective beach system. The beach represents a high energy reflective environment, which includes a berm, a step and a deeper nearshore. The profiles were similar during the measurements taken at different seasons, however the berm was higher in March and the step was more pronounced in September (Fig. 4.1 and 4.2). The Mameyal (SB2) beach system was categorized as dissipative beach. The profiles from figures 4.10 and 4.11 suggest a high wave environment that lacks berm development and has a relatively low slope. The Palmas Altas, Barceloneta (SB3) beach system was categorized as dissipative to reflective beach. It has dissipative characteristics in March but reflective characteristics in September (Fig. 4.18 and 4.19). The beach was classified as reflective during September (Fig. 4.19) because it showed a higher slope, a berm and a pronounced step. It was classified as dissipative during March because it showed a slope that was lower and lacked berm development (Fig. 4.18). The Arecibo (SB4) beach system was categorized as a reflective to dissipative beach system (Fig. 4.27 and 4.28). It showed a high energy environment with a relatively uniform slope. It had no berm development in September, which made it dissipative. The Camuy (SB5) beach system was classified as a dissipative beach. This station showed no berm development with a deeper nearshore in both seasons (Fig. 4.35 and 4.36). The Jobos, Isabela (SB6) beach system classification changed from reflective to

dissipative depending on the season. This station had a well developed berm in March (Fig. 4.43), but not on September (Fig. 4.44). Also, sand dune deposition was more dominant in March. Beach rock exposures in the nearshore were more extensive during September. Barreto (1997) also classified this location as reflective to dissipative beach. The Punta Borinquen, Isabela (SB7) beach system was classified from reflective to dissipative depending on the season. In the March sampling date, there was a well developed berm, which was not present in September (Fig. 4.53 and 4.54). Beach slope was higher in September, where there was a pronounced step and deep nearshore. Sand deposition and/or movement increased to the west in all the beach systems. This can be seen in all the beach profiles developed.

## **5.2 Sediment Texture and Composition Analysis**

In station SB1, grain size distribution ranged from pebbles to very fine sand (Fig. 4.3, 4.4 and 4.5). The berm grain size distribution was fine to very fine sand; the swash zone grain size distribution showed mostly pebbles, and the surf zone grain sizes varied from very coarse to very fine sand. This grain size distribution is unusual in a high energy environment, however, in this case beach morphology may be playing an important role in the sediment distribution. Cumulative curves (Fig. 4.6) show the grain size distribution to be moderately sorted in this beach. In station SB2, grain size distribution was similar at the berm, swash and surf zones (Fig. 4.12 and 4.13). Grain size ranged from very coarse to very fine sand. Sand distribution at station SB2 seems to be controlled probably by the its open morphology and dynamically changing weather conditions. Cumulative curves (Fig. 4.14) show that the

grain size distribution is moderately well sorted, which might be related to the high incidence of waves along this beach. In station SB3, grain size distribution ranged from very coarse to very fine sand (Fig. 4.20, 4.21 and 4.22). The surf zone was totally composed of exposed beach rock. Sand distribution seems to be controlled by high wave energy, but wind transport is also evident since there are sand dunes present. The cumulative curves show moderately well sorted sediments (Fig. 4.23). In station SB4, grain size distribution ranged from coarse to medium sand (Fig. 4.29). This suggests a higher energy present in the area. The surf zone is totally composed of beach rock and high wave energy was observed in this area. Sand distribution seems to be mostly controlled by wave energy. Site SB4 is located to the west of the Arecibo port. This probably influences the grain size distribution due to several coastal man-made structures constructed along the shore in the area. Cumulative curves show moderately sorted sediments (Fig. 4.30). In station SB5, grain size distribution ranges from pebbles to medium sand (Fig. 4.36, 4.37 and 4.38). This is probably related to high wave energy and dynamically changing weather conditions in the area. Cumulative curves show well sorted sediments (Fig. 4.39). In station SB6, grain size distribution varies along the beach profile (Fig. 4.45, 4.46, 4.47 and 4.48). In the dunes and berm, it ranges from fine to very fine sand. This suggests a prevalent low energy in the area, or wind transport. In the swash and surf zones, grain size ranged from coarse to medium sand, which suggests a higher wave energy. The swash zone in this area is composed of exposed beach rock. The lack of sand in the area may have been caused by storm removal or from many years of illegal mining of the dunes. Cumulative curves showed moderately sorted grain composition (Fig. 4.49). In station SB7, the sediment distribution ranged from coarse to very

fine sand (Fig. 4.55, 4.56 and 4.57). High wave energy seems to be the most influential factor, although the presence of sand dunes suggests wind transport. Cumulative curves show well sorted grain size distribution (Fig. 4.58). Sand deposition and movement are probably influenced by climatological (wave energy) factors in all the beach systems. In addition, for most of the systems studied, river discharge is present to the east of the systems. This is evidenced by the terrigenous vs. carbonate ratios in each system, which in turn influences grain size. Also, it can be noted that in the rainy season (September), terrigenous sediment composition is higher in all the systems, indicating more terrigenous input present.

In station SB1, the sediment composition indicated more terrigenous material present during March, with the exception of the swash zone, where carbonates were dominant (Fig. 4.7). In September, carbonates were dominant in the berm and in the surf zone as well (Fig. 4.7). This changes in sediment composition are probably related to the fact that there are no terrigenous inputs (rivers) nearby. In station SB2, sediment composition showed higher terrigenous material at all sampling dates (Fig. 4.15). In station SB3, terrigenous sediments were also dominant over carbonates during both seasons. This might be due to the fact that no marine biogenic structures (reefs) are present in the north coast (Morelock, 1984). In station SB4, the sediment composition showed mostly terrigenous material (Fig. 4.31). This is probably related to discharges from the Rio Grande de Arecibo, which is present nearby. This also raises a question as to why there is so much terrigenous material in this area because the river dam holds up the sediment upstream. It could be possible that what is happening is that the valley is being eroded, thus contributing to this high percentage of terrigenous material present at the beach site. In station SB5, the

sediment composition was always more than 93% terrigenous (Fig. 4.40), suggesting high terrigenous influences. This is also noted in the dark color of the sand. In station SB6, sediment composition showed terrigenous sediments were dominant at all sampling periods (Fig. 4.50). This suggests that the marine environment is not a significant influence in the sand movement and deposition in the area. In station SB7, the sediment composition percentages showed dominant terrigenous sediment over carbonates (Figure 4.59). In six of the seven sites studied, terrigenous sediments were dominant. This is associated to the fact that several major rivers discharge near the sites studied and that littoral transport along the north coast of the island goes from east to west. Also, there are no major marine biogenic sources along the north coast of the island (Morelock 1984). It was also noted that terrigenous sediments were usually dominant during September, which is directly related to higher precipitation due to the rainy season.

### **5.3 Image Analysis**

Multispectral analyses for the IKONOS satellite images did not prove useful for this study. Barreto et al. (1998) recommended the use of a higher spatial resolution when using satellite images for facies studies in the nearshore area. Landsat-7 images were used in her study. For this study, IKONOS images, which have a higher spatial resolution, were used. Unfortunately, the date and time of the image acquisition was not available and the reflectance of the images could not be calculated. Due to the lack of this information, a characterization was tried using radiance values from the blue band, which has proven to be useful in other sediment bottom type studies (Morelock et al, 2002a). In this case, no

correlation was found because values ranged from 0.30 to 1.70, even when, in all the beach systems studied the terrigenous input was dominant. No correlation was detected between radiance values and sediment composition. Another attempt to analyze the images was made using band ratios. Chiques (2005) concluded that the best band ratio for sediment characterization in sand was band 1 (blue) vs. band 2 (green). This was done using IKONOS imagery and GER-1500 spectroradiometer data. Again, lack of spectral field data made this approach useless in this case. In addition, in Chiques (2005) sand characterization was done for coastal areas where sand is aerially exposed and not covered by marine water. There was an attempt to compare imagery data from this study with those in Barreto (1997). Several of the locations in this study were in the same general areas than the ones studied in Barreto (1997), but unfortunately the exact locations of her study were not available in her Ph.D. thesis document. Only one location from her study was used because the benchmark created by Barreto was still recognizable. Radiance values were also reported for that location. These were reported as a range of values with an extreme difference between high and low values. For example, in Jobos, Isabela, the values from the landsat-7 image reported ranged from 0 to 10.38. In this study the IKONOS satellite images showed a range in radiance values from 0 to 1.129121. No comparison was viable because the images and data (classification) used by Barreto (1997) were not available.

## 5.4 North Coast Synthesis

The north coast's dynamically changing environment gives way for different conditions and classifications throughout a geographically close area. Carbonate material is high to the east of the study area (SB1), it decreases and then slightly increases to the west (SB7) (Fig. 5.1). The increase in terrigenous material from Barceloneta to Camuy (SB3 to SB5) might be highly influenced by the discharge of major rivers in the north coast. To the west of the study area, the increase in carbonate material in the areas of Isabela (SB6) and Aguadilla (SB7) is possibly due to the geology of the area, which includes limestones from the Aguada and Aymamón Limestones and some surficial deposits. As seen in figure 5.1, there is a significant decrease in carbonate material between the areas of Mameyal (SB2) and Barceloneta (SB3). There is a possibility that there are underwater canyons in the area and that this sediment is trapped where it becomes unreachable by nearby water currents.

The beach sediments seem to become better sorted to the west of the study area (Fig. 5.1). This might be influenced by the longshore current for the north coast which moves from east to west (Morelock 1984). Wave energy and wind direction in the studied sites are also very important factors to take into consideration because they may have an effect on the variations found among the seven beach sites. In the area where the major rivers discharge in the north coast the sediments were poorly sorted, which was expected due to the proximity of the beach sites to the river mouths and the influence of river dams on the discharge.

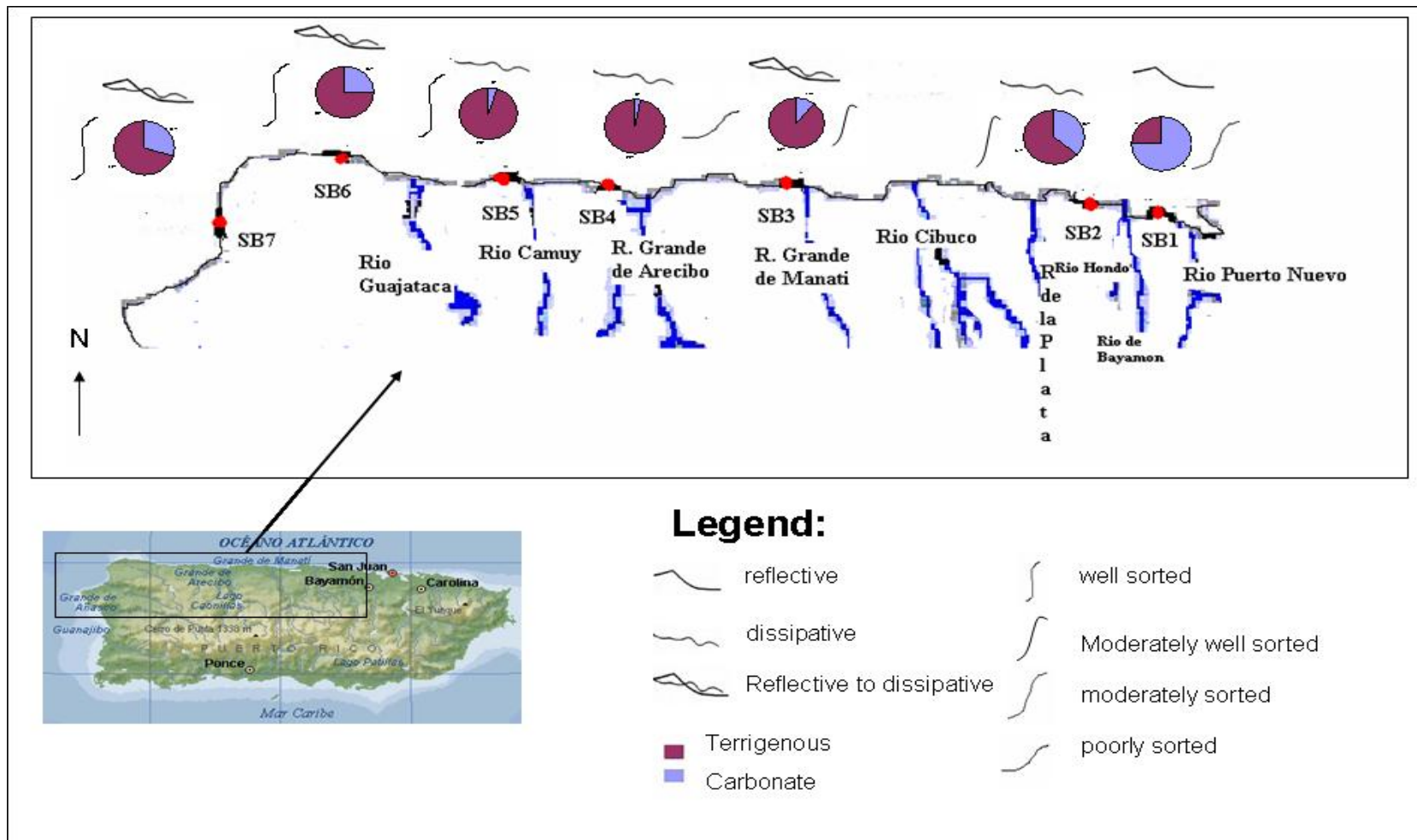


**Figure 5.1: Sediment composition and texture and beach classification variations for the study area in the North Coast of Puerto Rico.**

Isla de Cabras (SB1) was the only beach site that was reflective both sampling periods (Fig. 5.1). This might be influenced by the coast morphology, which is a man-made enclosed bay. Barceloneta (SB3), Isabela (SB6) and Aguadilla (SB7) shifted from reflective to dissipative during both sampling periods (FIG. 5.1). This might be influenced by the changes in wave action between seasons, which tends to be higher during the month of September. Mameyal (SB2), Arecibo (SB4) and Camuy (SB5) were dissipative beaches both sampling periods (FIG. 5.1). This might be influenced by the high wave energy and wind influence in the area. Also, coast morphology might have a role in this classification because these sites were geographically more open coasts than the other sites.

The Isla de Cabras (SB1) study site results show a beach system that varies the most from the other six sites when comparing them all together. This site is a man-made structure constructed with an artificial fill. This in turn might be what influences not only sediment composition and texture variations, but beach classification as well. This might be a good example as to how human impact interferes with the dynamic processes of the beach systems. In Gómez's (2003) study of the effect of man-made structures on the shoreline, he found that the impact depends on the type and dimensions of the structures constructed, littoral drift and the angle of wave approach. Many of these structures are constructed in these systems without making an assessment of how the system works through time, thus possibly aggravating the situation. It has been known that the structures help solve the problem of erosion in areas where these are constructed, but worsen it in other areas because it creates an imbalance in the system.

## CHAPTER 6: CONCLUSIONS

The initial goal of this project was to provide initial insights for a future development of a sediment budget for the whole north coast of Puerto Rico. To accomplish this goal, satellite images, beach profiles and beach sediment texture and composition were described in detail for each studied beach system.

IKONOS satellite images were used because of their availability and their spatial resolution of 1 meter. In previous studies, Landsat-7 images were used and a greater spatial resolution was suggested (Morelock et al, 2002a). For this study, the higher spatial resolution was not enough. It is also important to have greater radiometric resolution. Even more important is to have a better idea the spectral response of the target. It is also a possibility that IKONOS satellite spatial resolution is too high. With a 1 meter resolution too many details are captured and these in turn might interfere with the classifications attempted in these types of studies. For a coast environment like the north coast's and the type of discrimination attempted it would be better to use a satellite with a lower spatial resolution than the IKONOS satellite, but a higher spatial resolution than the Landsat-7 satellite used in prior studies.

Other several methods for image preprocessing were attempted, but not having spectral field data resulted in a failure of assessment. Water column contributions to signal were attempted to be removed by means of the Lyzenga method, but field data was needed for the method to be completed and it was not available. It was also noticed that higher radiance values were possibly be due to sunlight glare. Band ratios were also attempted, but no real assessment could be made because what might seem as sand is more likely to be the sunlight glare component.

In all the beaches studied, the sediment composition varied, as expected depending on the location along the beach profile where the samples were collected. The sand dunes and the berm have grain sizes ranging from fine to very fine sand in most cases. In the swash and nearshore the sediments range from coarse sand to very fine sand in most cases. This is probably the result of the high wave energy combined with weather and oceanographical conditions present along the north coast of Puerto Rico. These variables are unpredictable in most cases.

The sediments in all the beaches studied have a high percentage of terrigenous materials. The towns of Arecibo (Río Grande de Arecibo), Camuy (Río Camuy), Barceloneta and Aguadilla (Río Culebrinas) have rivers that discharge along the north coast shore. River mouths are close to most of the sites studied, and the sediments in their sediments are largely comprised of sand sized rock fragments and resistant minerals that are washed down from the mountains and hills. This sand was often gray to black with little shell fragments. The contributions from the marine environment to the north coast beaches of Puerto Rico are minimal. It is clear that the factors that affect the river sources of sand along the north coast and the factors that transport these river sediments will have a significant impact on the sediment budget.

## CHAPTER 7: RECOMMENDATIONS FOR FUTURE STUDIES

The original methodology plan involved the use of already established benchmarks (e.g. USGS). The beach systems were originally chosen due to proximity to where these were supposed to be, however, these were not found due to vegetation coverage, urban development and human tampering. As an alternative, benchmarks were established for the study using pvc tubes and cement. Luckily, they remained intact during the period of study, but it is likely possible that these are not available anymore due to the same reasons mentioned before. For future studies a better procedure for the establishment of lasting (permanent) benchmarks should be a priority.

When choosing satellite images, it is obvious that for a project like this one image availability and spatial resolution were the deciding factors. This study showed that spatial resolution is not the only important parameter to consider. Radiometric resolution and calibrated reflectance values proved as important, if not more. The collection of field spectral measurements should also be useful because it would serve as a basis for comparison. It is very important to know the specific information needed from the images and the methods that will prove successful when deciding what satellite images to use. As mentioned earlier, satellite images with lower spatial resolution than IKONOS satellite images might prove more useful.

To make a better assessment in future studies there are several recommendations that might prove more useful. These include: conducting monthly samplings; choosing geographical sites that are more close together to one another; the use of bathymetry maps, water current and wind current information. It would also be interesting to conduct these analyses along different

parts of the same beach system to see if there is any change among it. Combining this with an assessment on human impact along the coast would give way to a better understanding and a complete sediment budget of the area. A good idea would be to find a beach system with an erosion problem where a man-made structure is to be built and study all these variables before and after construction to assess as to how the system works and if the structure turns out to be a viable solution.

## REFERENCES

- Barreto, M., 1991, Sediment Budget at Esperanza, Vieques, Puerto Rico (1936-1987), Mayaguez Campus, University of Puerto Rico, unpublished M.S. Thesis, 200p.
- Barreto, M., 1997, Shoreline Changes in Puerto Rico (1936-1993), Mayaguez Campus, University of Puerto Rico, unpublished Ph.D. Thesis, 278p.
- Barreto, M., Morelock, J., and Vásquez, R., 1998 (in progress), Remote sensing as a tool to describe sediment bottom facies in coastal environments.
- Briggs, R. P., 1965, Geologic Map of the Barceloneta Quadrangle, Puerto Rico: U.S.G.S. Quadrangle Map I-421.
- Briggs, R. P., 1968, Geologic Map of the Arecibo Quadrangle, Puerto Rico: U.S.G.S. Quadrangle Map I-551.
- Campbell, J. B., 1996, Introduction to Remote Sensing, 2nd edition: Guilford Press, p. 4-5.
- Chiques, G., 2005, Spectral Characterization of Beach Sediments West of Puerto Rico, Mayaguez Campus, University of Puerto Rico, unpublished M.S. Thesis, 65p.
- Gómez Velásquez, J.F., 2003, Efectos de las Estructuras Construídas por el Hombre Sobre Tramos de Línea de Costa al Norte, Oeste y Sur de Puerto Rico, Mayagüez Campus, University of Puerto Rico, unpublished M.S. Thesis, 150p.
- Krushensky, R. D., and Schellekens, J. H., 2001, Geology of Puerto Rico, in Geology, Geochemistry, Geophysics, Mineral Occurrences and Mineral Resource Assessment for the Commonwealth of Puerto Rico: USGS Open File Report 98-38.
- Monroe, W. H., 1963a, Geologic Map of the Camuy Quadrangle, Puerto Rico: U.S.G.S. Quadrangle Map GQ-197.
- Monroe, W. H., 1963b, Geologic Map of the Vega Alta Quadrangle, Puerto Rico: U.S.G.S. Quadrangle Map GQ-191.

Monroe, W. H., 1967, Geologic Map of the Quebradillas Quadrangle, Puerto Rico: U.S.G.S. Quadrangle Map I-498.

Monroe, W. H., 1969a, Geologic Map of the Aguadilla Quadrangle, Puerto Rico: U.S.G.S. Quadrangle Map I-569.

Monroe, W. H., 1969b, Geologic Map of the Moca and Isabela Quadrangle, Puerto Rico: U.S.G.S. Quadrangle Map I-565.

Monroe, W. H., 1971, Geologic Map of the Manatí Quadrangle, Puerto Rico: U.S.G.S. Quadrangle Map I-671.

Monroe, W. H., 1973, Geologic Map of the Bayamón Quadrangle, Puerto Rico: U.S.G.S. Quadrangle Map I-751.

Morelock, J., 1978, Shoreline of Puerto Rico: San Juan, PR: Coastal Zone Program, Department of Natural Resources, 45p.

Morelock, J., 1984, Coastal Erosion in Puerto Rico. *Shore and Beach* v. 52, p. 18-27.

Morelock, Jack, and J. Trumbull, 1985, Puerto Rico Coastline, *The World's Coastlines*, Ed. Bird, New York: Van Nostrand Reinhold.

Morelock, J., 1987, Beach sand budget for western Puerto Rico. *Coastal Sediments '87* N.C. Kraus, p. 1333-45.

Morelock, J., 2000, Beach System: Geological Oceanography Program webpage [http://geology.uprm.edu/Morelock/GEOLOCN\\_/INDEX.HTM](http://geology.uprm.edu/Morelock/GEOLOCN_/INDEX.HTM).

Morelock, J., Ramírez, W., Barreto, M., Gilbes, F., and R. A. Miller, 2002a (in progress), Use of Satellite Images in Developing a Beach Budget.

Morelock, J., and Maritza Barreto, 2002b (in progress), An Update of Coastal Erosion in Puerto Rico.

Short, Andrew D., 1984, Beach and nearshore facies: southeast Australia. *Marine Geology* v. 60, p. 261-82.

Smith, A. W. Sam, 1990. Slope of the swash zone of an ocean beach, *Shore and Beach* v. 58, no. 3: 26-29.

Space Imaging Inc., 2003: <http://www.spaceimaging.com/products/imagery.html>.

Wright L.D. and A.D. Short, 1983, Morphodynamics of beaches and surf zones in Australia, in Komar, P.D., ed., *CRC Handbook of Coastal Processes and Erosion*: Boca Raton, Florida, CRC Press, p. 35-64.